THEORIES OF ANALYSIS AND MEASUREMENT OF WELDING RESIDUAL
STRESSES AND PWHT.

YUKIO UEDA, K. NAKACHO

OSAKA UNIVERSITY
WELDING RESEARCH INSTITUTE
11-1, MIHOGAOKO,   IBARAKI, OSAKA, 567 JAPAN

Contents

Summary

In this paper, the theories and the methods of thermal elastic-plastic-creep analysis and measurement of residual stresses are described, which have been presented by the authors. Many useful information on elastic-plastic-creep behavior of various joints during and after welding and stress-relief annealing (PWHT) have been obtained by applying these ones. With the several examples, mainly on multi-pass welding of thick plates, the effectiveness and reliability of these theories and methods are shown. Using the results of the theoretical analysis and experimental measurement, characteristics of distribution of multi-pass welding residual stresses, their production mechanisms, influencing factors on them and their relations with cold cracks are discussed synthetically for the thick welded joints.

Key Words

1.   Introduction

1.1 General Introduction

It is well known that welding produces thermal stresses which cause distortion of structures and residual stresses which influence buckling strength, brittle fracture strength, etc. of welded structures. In connection with welding residual stresses, cold cracking is also investigated from various points of view, including mechanical one. For some types of welded structures, stress-relief annealing (PWHT: Post Weld Heat Treatment) is applied in the process of construction.

In recent years, it has become more important to perform more accurate theoretical analysis of transient and resulting residual stresses associated with welding and PWHT for rational design and for critical evaluation of safety. A basic requirement for such work is the capability to analyze thermal elastic-plastic behavior of metals. Of various proposed analytical methods, the finite element method is one of the most powerful tool to deal with nonlinear behavior and arbitrary geometrical configuration. For thermal elastic-plastic analysis, based on the finite element method, the basic theory was formulated by the authors /1,2/ and others. The authors have extended their theory to be applicable to stress-relief annealing of welded joints in thick plate /3-5/.

In parallel with the theoretical analyses, accurate methods of measurement of actual residual stresses are needed and several have been proposed. To measure those in three-dimensions the Sachs method /6/ is accurate in very limited conditions, and the Rosenthal method /7/ is based on an irrational approximation which reduces the accuracy of the result. The authors have developed the general theory of measurement of three-dimensional residual stresses using inherent strains as parameters and the basic procedures based on the finite element method /8/.

In this paper, summarizing these works, the authors will describe the basic theories and procedures, which are based on the finite element method, for theoretical analyses of mechanical behavior of welded joints immediately after welding and during stress-relief annealing and also the measurement of residual stresses.

With several examples, mainly on multi-pass welding of thick plates, the effectiveness of these theories and procedures will be shown. Using the results of these theoretical analysis and experimental measurement, characteristics of distribution of multi-pass welding residual stresses, their production mechanisms, influencing factors on them and their relations with cold cracks are discussed synthetically.

1.2 Outline of the Characteristics of the Problems

In this section the characteristics of the subjects to be dealt with in this paper are outlined.

The phenomenon of welding starts at the instant of providing a concentrated heat source which, in most welds, can be regarded as the weld metal. Heat transfer in the welded joint produces a changing temperature distribution which induces thermal stresses. An important point is that there can be marked changes in the instantaneous mechanical properties as a result of changes in temperature, and it is important to take account of these changes; secondary effects of the coupling of temperature and stress fields can be neglected. Taking this as a basic assumption, the analysis can be divided into two independent analyses: heat conduction and thermal elastic-plastic.

In a one-pass weld the welded joint can be divided into four parts: weld metal (deposit), weld metal (base), heat-affected zone and parent metal, as shown in Fig.1-1(a). Each part is subjected to an individual thermal history and the related changes of the physical properties are indicated in Fig.1-1(b), as are

Fig.1-1   Characteristics of welded joint

① WELD METAL
② WELD METAL
③ HAZ (HEAT-AFFECTED ZONE)
④ PARENT METAL
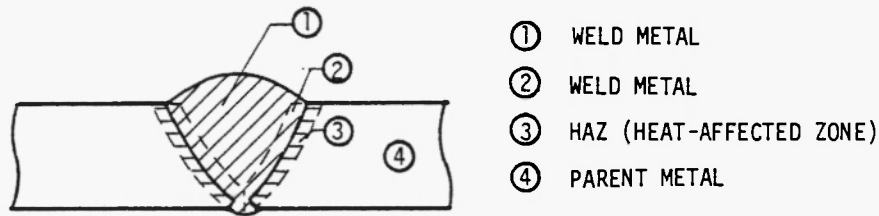
(a)   Four parts subjected to different thermal histories

HEAT CONDUCTION ANALYSIS   TH-EL-PL ANALYSIS
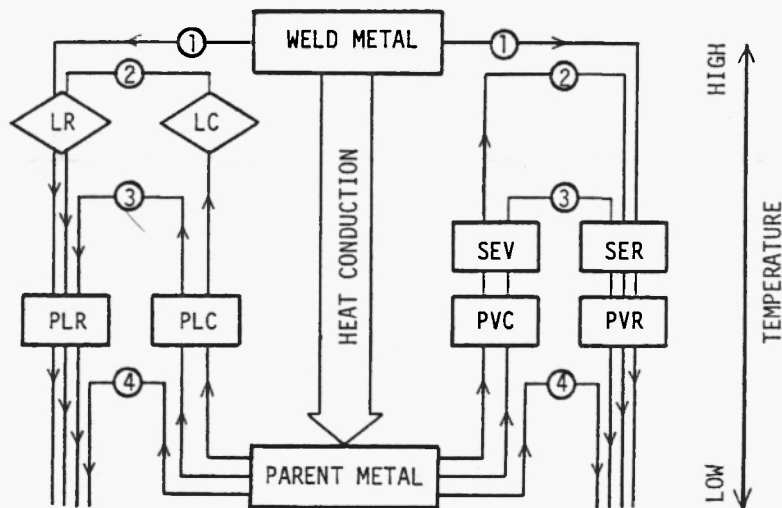
⟨LC⟩ : ABSORPTION OF LATENT HEAT AT MELTING POINT
⟨LR⟩ : RELEASE OF LATENT HEAT AT SOLIDIFYING POINT
|PLC| : ABSORPTION OF LATENT HEAT AT PHASE TRANSFORMATION
|PLR| : RELEASE OF LATENT HEAT AT PHASE TRANSFORMATION
|PVC| : VOLUME SHRINKAGE AT PHASE TRANSFORMATION
|PVR| : VOLUME EXPANSION AT PHASE TRANSFORMATION
|SEV| : YIELD STRESS AND YOUNG'S MODULUS VANISH
|SER| : YIELD STRESS AND YOUNG'S MODULUS RECOVER

(b)   Thermal histories and related changes of physical properties

the corresponding changes of the mechanical properties of the materials.

In multi-pass welds the new weld metal fuses a small region surrounding it and relieves the residual stresses which were already produced. After redistri-

bution of the residual stresses the characteristics of the succeeding phenomena are considered the same as in a one-pass weld, although some part of the joint may be subjected to loading and unloading in the plastic range.

In the usual process of stress-relief annealing for thick joint the rate of heating is kept sufficiently small to prevent thermal stresses by uneven temperature distribution. In this condition the temperature of the object is considered to be uniform at any point. Creep strain rate is influenced by several factors such as temperature and stress, and the appropriate creep law may be different depending upon materials and temperature ranges.

There are two theories for the measurement of residual stresses: the inherent strain method and the section force method. The inherent strain method which the authors have proposed is based on the following idea.

Fundamentally, residual stresses are produced by the source of residual stresses, effective inherent strains (being not necessarily true inherent strains). Conversely, the effective inherent strains can be estimated from the residual stresses which are measured on the surfaces of the object. Once the inherent strains are obtained the entire residual stresses of the object are easily calculated.

On the other hand, the section force method is indifferent to the inherent strain. When the object is sectioned the internal forces on the newly exposed surfaces are relieved. By this relief the existing stresses in the object are consequently relaxed. If the changes in surface strains by the sectioning are measured, the section forces can be estimated by the changes. With repetition of the procedure the original residual stresses will completely relieved. By the summation of the section forces relieved at every step, the original residual stresses can be calculated. This is the section force method.

The former method is based on the relationship between the inherent strains and the response surface strains, and the latter is on the relationship between

the relieved section forces and the relaxed strains. It is very difficult to express these relationships in general analytical expressions. When the finite element method is used they can be represented without any difficulties and these methods can be applied without particular restriction, such as the geometrical configuration.

2.   Thermal Elastic-Plastic-Creep Analysis of Transient and Residual Stresses due to Welding and Stress-Relief Annealing (PWHT)

2.1 Introduction

For better understanding of production mechanism of welding residual stresses and causes of weld cracking, it is necessary to obtain more accurate information on the entire histories of stresses and strains to which the material is subjected during the process of welding. At the instant of welding, a limited portion of the welded joint such as the weld metal and the base metal in its vicinity are heated up to a very high temperature and thereafter cooled down to room temperature. In this way, the thermal cycle proceeds, temperature distribution changes with time and the mechanical properties of metal depend on temperature and plastic history. In order to perform a more reliable analysis, the above mentioned factors should be taken into account.

As stated in the preceding chapter two independent analyses on temperature and stress fields are necessary for the analysis. In both analyses the basic equations are derived in the incremental forms on the assumption that any changes during a small increment of time are linear. Then the accumulation of the solution to the basic equations for each step furnishes the entire histories of temperature, stress, and strain.

Based on the finite element method, the authors had developed methods of

thermal elastic-plastic analysis on this kind of problems with consideration of the effects of changes of the mechanical properties /1/. Furthermore, the authors generalize the theory of thermal elastic-plastic analysis to take into account not only temperature-dependence but also plastic history-dependence of the material properties, introducing a combined rule of isotropic and kinematic workhardening /2/.

The authors have also presented the theory of thermal elastic-plastic-creep analysis to investigate the mechanical behaviors of welded joints during stress-relief annealing by introducing more general and accurate forms for creep strain /3-5/.

Based on these theories, they developed an efficient and accurate method /9-12/ for analysis of multi-pass welding transient and residual stresses. Applying this method, multi-pass welding transient and residual stresses have been obtained, and their production mechanisms, their relations with cold cracks, etc. have been clarified. Transient and residual stresses during PWHT have been also analyzed.

These theories and results will be described in this chapter.

2.2 Theory of Analysis

2.2.1 General forms of constitutive equation and stiffness equation
(1) Constitutive equation (Incremental relation between stress and total strain)

In dealing with nonlinearity of material it is most important to define the stress and strain relationship for derivation of the fundamental equations.

For a small increment of time, dt (which produces an increment of temperature, dT), the relationship between stress increment $\{d\sigma\}$ and total strain increment $\{d\varepsilon\}$ is represented in the following general form, taking account of the effects of temperature upon the elastic, plastic, and creep behavior.

$$\{d\sigma\} = [D]\{d\epsilon\} - \{dC\} \tag{2-1}$$

The explicit forms of the terms $[D]$ and $\{dC\}$ in the above differ according to the condition of stress, that is in the elastic or plastic range with or without creep.

(2) Stiffness equation (Incremental relation between nodal force and nodal displacement)

Applying the finite element method and denoting the stiffness matrix of an element by $[K]$, the relationship between the increment of the nodal force $\{dF\}$ and that of the nodal displacement $\{dw\}$ is written as

$$\{dF\} = [K]\{dw\} - \{dL\} \tag{2-2}$$

In the above equation, $[K]$ is obtained by integration of the term including $[D]$ in Eq.(2-1) and the equivalent nodal force $\{dL\}$ is that including $\{dC\}$ of the same equation. Summing up the stiffness equation (2-2) over the entire object, the stiffness equation for the whole object may be obtained. In usual welding the external forces are not applied. Introducing the boundary conditions into the stiffness equations, the equilibrium equation on the whole object is expressed by

$$\Sigma\{dL\} = \Sigma[K]\{dw\} \tag{2-3}$$

where Σ means the summation for the whole object.

These are the fundamental equations. In each time increment dt, Eq.(2-3) is solved for nodal displacement increment $\{dw\}$. Total strain increment $\{d\epsilon\}$ can be calculated from $\{dw\}$, according to the difinition of the relation between $\{dw\}$ and $\{d\epsilon\}$. Stress increment $\{d\sigma\}$ can be evaluated from Eq.(2-1). In the following sections, explicit expressions of the constitutive equation (2-1) and the stiffness equation (2-2) will be derived.

2.2.2 Constitutive equation (Incremental relation between stress and total

   strain) for thermal elastic-plastic state /2/

In this section, constitutive equations (incremental relation between stress and total strain) with consideration of effects of changes of the material properties will be developed for the elastic range and plastic range respectively, introducing a combined rule of isotropic and kinematic workhardening.

The mechanical properties of material generally change when temperature changes or its plastic deformation progresses. Especially in the process of welding, the magnitudes of changes of the material properties are very large because the welded joint is heated up to a very high temperature and thereafter cooled down to room temperature generally with large stresses and plastic strains. Accordingly, when termal stresses, strains or deformations produced by welding are analyzed, it is necessary to consider such temperature-dependence and plastic history-dependence of the material properties.

(1) Constitutive equation in elastic range

In this section, it it assumed that creep strain is not produced in the material, and the total increment of thermal strain including transformation strain is denoted by $\{d\varepsilon^T\}$, which will be called simply thermal strain increment hereafter. Such thermal strain increment can be expressed by instantaneous linear expansion coefficient $\{\alpha\}$ and temperature increment dT as

$$\{d\varepsilon^T\} = \{\alpha\}\, dT \tag{2-4}$$

The above instantaneous linear expansion coefficient $\{\alpha\}$ is usually a coefficient which indicates the magnitude of expansion or shrinkage due to temperature changes at every instant. By this coefficient, expansion or shrinkage due to both temperature change and transformation can be expressed when the material is in the temperature range of the transformation. Then, in the elastic range, total strain increment $\{d\varepsilon\}$ is represented as the summation of thermal strain

increment $\{d\epsilon^T\}$ and elastic strain increment $\{d\epsilon^e\}$ which are produced to satisfy the conditions of compatibility, that is,

$$\{d\epsilon\} = \{d\epsilon^e\} + \{d\epsilon^T\} \tag{2-5}$$

Elastic strains $\{\epsilon^e\}$ have always the relation to stresses $\{\sigma\}$ as

$$\{\sigma\} = [D^e]\{\epsilon^e\} \tag{2-6}$$

where

$$\{\sigma\} = \{\sigma_x\ \sigma_y\ \sigma_z\ \tau_{yz}\ \tau_{zx}\ \tau_{xy}\}^T,$$

$$\{\epsilon^e\} = \{\epsilon^e_x\ \epsilon^e_y\ \epsilon^e_z\ \gamma^e_{yz}\ \gamma^e_{zx}\ \gamma^e_{xy}\}^T,$$

$$[D^e] = \frac{E(1-\nu)}{(1+\nu)(1-2\nu)}\begin{bmatrix} 1 & \frac{\nu}{1-\nu} & \frac{\nu}{1-\nu} & 0 & 0 & 0 \\ & 1 & \frac{\nu}{1-\nu} & 0 & 0 & 0 \\ & & 1 & 0 & 0 & 0 \\ & & & \frac{1-2\nu}{2(1-\nu)} & 0 & 0 \\ & \text{Sym.} & & & \frac{1-2\nu}{2(1-\nu)} & 0 \\ & & & & & \frac{1-2\nu}{2(1-\nu)} \end{bmatrix}$$: elasticity matrix or elastic stress-strain matrix

E : Young's modulus, ν : Poisson's ratio

When the stresses $\{\sigma\}$, elastic strains $\{\epsilon^e\}$ and elasticity matrix $[D^e]$ change into $\{\sigma+d\sigma\}$, $\{\epsilon^e+d\epsilon^e\}$ and $[D^e]+d[D^e]$ respectively due to the subsequent temperature change, they must satisfy the same equation as Eq.(2-6), that is,

$$\{\sigma+d\sigma\} = ([D^e] + d[D^e])\{\epsilon^e + d\epsilon^e\} \tag{2-7}$$

In the case where the elasticity matrix $[D^e]$ (containing the material properties) is a function of only temperature, an increment of elasticity matrix $[D^e]$, $d[D^e]$, in the above equation can be represented as

$$d[D^e] = \frac{d[D^e]}{dT}dT \tag{2-8}$$

Introduction of Eq.(2-8) into Eq.(2-7) and substraction of Eq.(2-6) from Eq.(2-7) provide the relationship between stress increment and elastic strain increment as

$$\{d\sigma\} = [D^e_d]\{d\epsilon^e\} + \frac{d[D^e]}{dT}dT\{\epsilon^e\} \tag{2-9}$$

where

$$[D^e_d] = [D^e] + \frac{d[D^e]}{dT}dT$$

It should be noted that as temperature history and temperature-dependence of elasticity matrix $[D^e]$ are known in advance, the second term $(d[D^e]/dT)dT$ in the above matrix $[D^e_d]$ can be obtained directly as a change of $[D^e]$ by dT . This

procedure does not produce nonlinear term with respect to unknown quantities but improves the accuracy of analyses. In the right side of the above Eq.(2-9), the first term indicates a part of stress increment due to an increase of elastic strain, and the second term does the rest of stress increment due to change of temperature.

Elimination of elastic strain increment $\{d\varepsilon^e\}$ from Eq.(2-9) by using Eq. (2-5) and introduction of Eq.(2-4) for thermal strain increment furnish the incremental relationship between stress and total strain, that is, constitutive equation as

$$\{d\sigma\} = [D_d^e]\{d\varepsilon\} - [D_d^e]\left(\{\alpha\} - [D_d^e]^{-1}\frac{d[D^e]}{dT}\{\varepsilon^e\}\right) dT \tag{2-10}$$

(2) Constitutive equation in plastic range

(i) Yield criterion, workhardening rule and yield surface

When a set of stresses produced at a point reaches certain magnitudes, the material yields and shows complex plastic behavior for the subsequent loading. In a certain combination of stresses, a condition which defines the limit of elasticity of the material is called yield criterion. In the space (stress space) of which co-ordinate axes are stress components, the yield criterion can be shown by a closed curved surface (yield surface). Generally the shape, size and position of the yield surface change with progress of plastic deformation of the material. That is, the yield criterion changes, being subjected to plastic work. The law for such changes of the yield criterion is called workhardening rule or strain- hardening rule. Hitherto, various workhardening rules have been proposed. Isotropic workhardening rule /13/ assumes that the size of the yield surface changes with increase of plastic work but the position and shape do not change (see Fig.2-1(a)). This implies that the initial yield surface expands uniformly during the susequent plastic flow. In kinematic workhardening rule /14/, it is assumed that the yield surface does not change its initial size and

Fig.2-1   Schematic illustration of workhardening rules
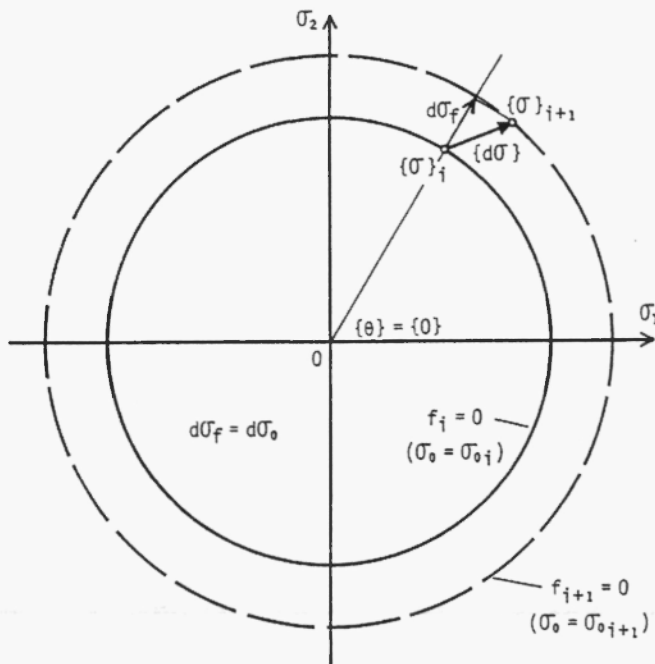
$f = 0$: yield surface (in this example, circle)

$\{\theta\}$: vector which indicates center of yield surface

σ_0 : a measure of size of yield surface
(in this example, radius of yield surface)

$\{\sigma\}$: stresses on yield surface

$i, i+1$: loading step

(suffix f indicates normal component of each increment)

(a)   Isotropic workhardening rule
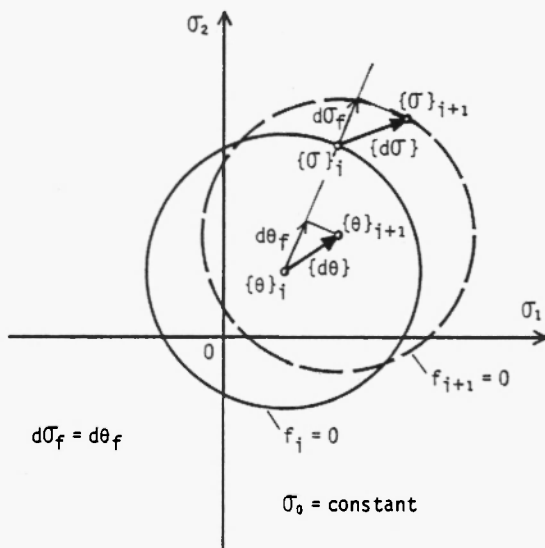
(b)   Kinematic workhardening rule
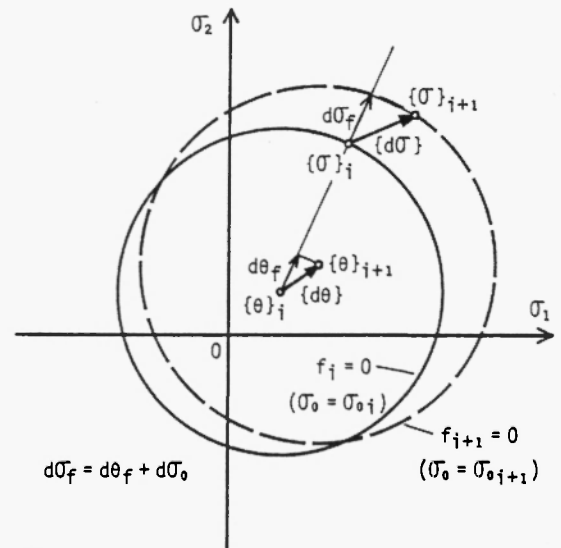
(c)   Combined workhardening rule

shape but moves in the stress space like a rigid body (see Fig.2-1(b)). With the aid of this rule, the Bauschinger effect can be easily represented within a certain degree of accuracy. Furthermore, in order to represent plastic behavior more accurately, many complex workhardening rules have been proposed. In this study, the isotropic and kinematic workhardening rules will be combined and it is assumed that the size and position of the yield surface can be changed but its initial shape does not (see Fig.2-1(c)). Generally, such combined yield surface may be expressed by the following equation.

$$f(\sigma_{ij} - \theta_{ij}, \ \sigma_0) = 0 \tag{2-11}$$

where $\{\theta\}$: translation vector which indicates the position of the center of

yield surface in the stress space

σ_0 : a measure of the size of the yield surface

The above function f which defines the yield surface (the yield criterion) is called yield function.

For the initial yielding or in case of the isotropic hardening, θ_{ij} is zero and σ_0 is a scaler function of the yield stress, and the yield function may be expressed in a form as

$$f(\sigma_{ij}, \ \sigma_0) = 0 \tag{2-11}'$$

Next, to describe changes of the size and position of the yield surface shown by Eq.(2-11), the following hypotheses are furnished. First, the size of the yield surface (σ_0) is assumed to be a function of the quantity ε_ℓ^p of plastic strain and temperature T. Here,

$$\varepsilon_\ell^p = \int d\varepsilon_\ell^p \tag{2-12}$$

where $d\varepsilon_\ell^p$: the length of the vector of the plastic strain increment (see Eq.(2-17)

Secondly concerning translation of the yield surface, it is assumed that, as a general rule, the yield surface can move only when the plastic deformation in-

creases. It should be noted that temperature change can not be the direct cause to move the yield surface. Such translation increment $\{d\theta\}$ is proportional to the magnitude $d\varepsilon_{\ell}^{n}$ of plastic strain increment $\{d\varepsilon^{p}\}$. The above hypotheses can be expressed as follows.

$$\sigma_0 = \sigma_0 \ (\varepsilon_{\ell}^{p}, \ T) \qquad\qquad (2\text{-}13)$$

$$d\sigma_0 = \frac{\partial \sigma_0}{\partial \varepsilon_{\ell}^{p}} d\varepsilon_{\ell}^{p} + \frac{\partial \sigma_0}{\partial T} dT$$

$$\{d\theta\} = k \, d\varepsilon_{\ell}^{p} \, \{n_{\theta}\} \qquad\qquad (2\text{-}14)$$

where k : translation coefficient

$\{n_{\theta}\}$: unit vector which indicates the direction of translation increment of the yield surface

In case of kinematic workhardening rule, σ_0 is constant if temperature does not change, but σ_0 should be assumed to depend on temperature in treating of thermal stress.

In general cases, an explicit form of Eq.(2-13) should be determined based on the results of experiment. In this paper, the direction of translation increment of the yield surface is selective, that is, its direction can be determined to represent well the behavior of the material. For example, when the Ziegler rule /15/ is adopted, unit vector $\{n_{\theta}\}$ in Eq.(2-14) is expressed as

$$\{n_{\theta}\} = \frac{\{\sigma - \theta\}}{|\{\sigma - \theta\}|} \qquad\qquad (2\text{-}15)$$

where

$$|\{\sigma - \theta\}| = (\{\sigma - \theta\}^{T} \{\sigma - \theta\})^{1/2}$$

(ii) Plastic strain increment and workhardening modulus

The following condition must be satisfied when the material is under loading in the plastic range,

$$df = 0 \qquad\qquad (2\text{-}16)$$

Assuming that the material behaves according to the incremental strain theory of plasticity (plastic flow theory) in the plastic range and introducing

the yield function (f of Eq.(2-11)) as a plastic potential, plastic strain increment $\{d\epsilon^p\}$ is defined as

$$\{d\epsilon^p\} = d\epsilon^p_\ell \{n\} \tag{2-17}$$

where $d\epsilon^p_\ell$: magnitude of plastic strain increment $\{d\epsilon^p\}$ (that is, the length of

the vector $\{d\epsilon^p\}$)

$$\{n\} = \{\frac{\partial f}{\partial(\sigma-\theta)}\} / f'_\ell \qquad : \text{unit vector outward normal to the yield surface}$$

at the stress point

$$f'_\ell = |\{\frac{\partial f}{\partial(\sigma-\theta)}\}| = ((\{\frac{\partial f}{\partial(\sigma-\theta)}\}^T \{\frac{\partial f}{\partial(\sigma-\theta)}\}))^{1/2}$$

The above expression implies that the direction of plastic strain increment $\{d\epsilon^p\}$ is shown by a vector outward normal to the yield surface at the stress point (see Fig.2-2). When a yield function is expressed by the deviatric stresses and is independent of hydrostatic stress, plastic strain increment given by Eq.(2-17) satisfies the condition of incompressibility of the material automatically.

Next, a relationship between plastic strain increment $\{d\epsilon^p\}$ and stress increment $\{d\sigma\}$ will be derived.
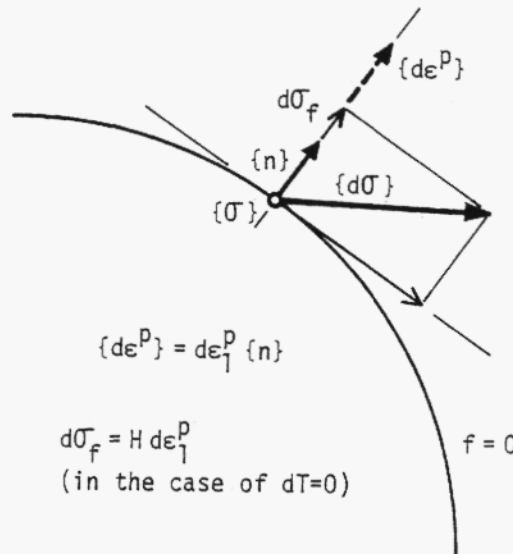
Fig.2-2 Relation between stress increment $\{d\sigma\}$ and plastic strain increment $\{d\epsilon^p\}$ (in the case of dT=0)

First, the case where temperature does not change like usual plastic problem will be discussed. As the yield surface is defined by Eq.(2-11) and the changes of its size and position are calculated by Eqs. (2-13) and (2-14) respectively, Eq.(2-16) may be rewritten in the explicit form as

$$0 = df = \{-\frac{\partial f}{\partial(\sigma - \theta)}\}^T \{d(\sigma - \theta)\} + \frac{\partial f}{\partial \sigma_0} d\sigma_0 = f'_{\sigma} d\sigma_f - f'_{\ell} k\, n_{\theta f}\, d\varepsilon^p_{\ell} + \frac{\partial f}{\partial \sigma_0}\frac{\partial \sigma_0}{\partial \varepsilon^p_{\ell}} d\varepsilon^p_{\ell} \qquad (2\text{-}18)$$

where
$$d\sigma_f = \{n\}^T \{d\sigma\}, \quad n_{\theta f} = \{n\}^T \{n_{\theta}\}$$

Rearrangement of the above expression for $d\sigma_f$ and $d\varepsilon^p_{\ell}$ may produce

$$d\sigma_f = (k\, n_{\theta f} - f'^{-1}_{\ell}\frac{\partial f}{\partial \sigma_0}\frac{\partial \sigma_0}{\partial \varepsilon^p_{\ell}})\, d\varepsilon^p_{\ell} \qquad (2\text{-}19)$$

The above equation represents that the magnitude $d\varepsilon^p_{\ell}$ of plastic strain increment $\{d\varepsilon^p\}$ is proportional to the normal component $d\sigma_f$ of stress increment $\{d\sigma\}$ to the yield surface (see Fig.2-2). Accordingly, even for the same magnitude of stress increment $\{d\sigma\}$, the magnitude of plastic strain increment $\{d\varepsilon^p\}$ is not necessarily the same, depending upon the direction of $\{d\sigma\}$. That is, nearer is the direction of $\{d\sigma\}$ to normal to the yield surface, larger is the magnitude $d\varepsilon^p_{\ell}$ of plastic strain increment $\{d\varepsilon^p\}$. Therefore, in this meaning, the normal component $d\sigma_f$ of stress increment $\{d\sigma\}$ should be called effective stress increment. For further development of plastic deformation in the case of usual metals, it is necessary to increase the stresses if the temperature does not change. This phenomenon is caused by hardening of the material due to plastic work or plastic deformation and is called workhardening or strain-hardening. As seen from Eq.(2-19) which represents the relationship between $d\sigma_f$ and the magnitude $d\varepsilon^p_{\ell}$ of plastic strain increment $\{d\varepsilon^p\}$ produced by $\{d\sigma\}$, the above-mentioned effective stress increment $d\sigma_f$ is the effective one to progress the plastic deformation.

Here, Eq.(2-19) may be rewritten as

$$d\sigma_f = H\, d\varepsilon^p_{\ell} \qquad (2\text{-}20)$$

where $\quad H = k\, n_{\theta f} - f_\ell^{!-1} \dfrac{\partial f}{\partial \sigma_0} \dfrac{\partial \sigma_0}{\partial \varepsilon_\ell^p}$ (2-21)

In the above Eqs.(2-20) and (2-21), H is called workhardening modulus or strain-hardening modulus.

Next, temperature change is taken into account. As the temperature change affects the mechanical properties, such as modulus of elasticity and yield stress, the size of the yield surface changes not only by the plastic deformation but also by temperature as assumed by Eq.(2-13). Therefore, the relationship between stress increment $\{d\sigma\}$ and plastic strain increment $\{d\varepsilon^p\}$ is influenced by the temperature change. With consideration of this effect, Eq.(2-20) may be rewritten in the following form, from Eqs.(2-16), (2-11), (2-13), (2-14) and (2-21).

$$d\sigma_f = H\, d\varepsilon_\ell^p - f_\ell^{!-1} \dfrac{\partial f}{\partial \sigma_0} \dfrac{\partial \sigma_0}{\partial T}\, dT$$ (2-22)

This represents the relation among stress, plastic strain and temperature increments.

Again, Eq.(2-22) is solved for $d\varepsilon_\ell^p$ as

$$d\varepsilon_\ell^p = \frac{1}{H}\left(d\sigma_f + f_\ell^{!-1} \frac{\partial f}{\partial \sigma_0} \frac{\partial \sigma_0}{\partial T}\, dT\right)$$ (2-23)

To keep the material being under loading in the plastic range, $d\varepsilon_\ell^p$ should be positive. Then, this equation requires that the effective stress increment $d\sigma_f$ must exceed the increment $\quad -f_\ell^{-1}(\partial f/\partial\sigma_0)(\partial\sigma_0/\partial T)dT\quad$ due to expansion or shrinkage of the yield surface by temperature change in order to increase plastic deformation. This may be interpreted that when the yield surface expands by temperature change, the stress needs to increase beyond the expansion by the temperature change in order to keep loading in the plastic range.

(iii) Constitutive equation

In the plastic range, total strain increment $\{d\varepsilon\}$ is expressed by the summation of components as

$$\{d\varepsilon\} = \{d\varepsilon^e\} + \{d\varepsilon^p\} + \{d\varepsilon^T\}$$ (2-24)

Next, the relationship between the magnitude $d\varepsilon_\ell^p$ of plastic strain incre-ment $\{d\varepsilon^p\}$ and total strain increment $\{d\varepsilon\}$ will be obtained. Equation (2-16) for the condition of loading in the plastic range may be reformed by introduction of Eqs.(2-11), (2-13), (2-14) and (2-21).

$$0 = df = \{\frac{\partial f}{\partial(\sigma - \theta)}\}^T \{d(\sigma - \theta)\} + \frac{\partial f}{\partial \sigma_0} d\sigma_0$$

$$= f_\ell' \{n\}^T \{d\sigma\} - f_\ell' k\, n_{\theta f}\, d\varepsilon_\ell^p + \frac{\partial f}{\partial \sigma_0}\frac{\partial \sigma_0}{\partial \varepsilon_\ell^p} d\varepsilon_\ell^p + \frac{\partial f}{\partial \sigma_0}\frac{\partial \sigma_0}{\partial T} dT$$

$$= f_\ell' \{n\}^T \{d\sigma\} - f_\ell' H\, d\varepsilon_\ell^p + \frac{\partial f}{\partial \sigma_0}\frac{\partial \sigma_0}{\partial T} dT \tag{2-25}$$

where
$$f_\ell' = |\{\frac{\partial f}{\partial(\sigma - \theta)}\}| = (\{\frac{\partial f}{\partial(\sigma - \theta)}\}^T \{\frac{\partial f}{\partial(\sigma - \theta)}\})^{1/2}, \quad \{n\} = \frac{\{\frac{\partial f}{\partial(\sigma - \theta)}\}}{f_\ell'}, \quad n_{\theta f} = \{n\}^T \{n_\theta\}$$

The above equation will be further transformed according to the following procedure.

1) To subsitute Eq.(2-9) into stress increment $\{d\sigma\}$ in the first term of the right side and express in terms of elastic strain increment $\{d\varepsilon^e\}$ etc..

2) To replace elastic strain increment $\{d\varepsilon^e\}$ with total strain increment $\{d\varepsilon\}$ etc., using Eq.(2-24).

3) To express thermal strain increment $\{d\varepsilon^T\}$ by Eq.(2-4) and plastic strain increment $\{d\varepsilon^p\}$ by Eq.(2-17).

As a result of this manipulation, Eq.(2-25) is transformed into a function of only total strain increment $\{d\varepsilon\}$ and the magnitude $d\varepsilon_\ell^p$ of plastic strain increment $\{d\varepsilon^p\}$ as unknowns. Rearrangement of the equation provides the relationship between $\{d\varepsilon\}$ and $d\varepsilon_\ell^p$ as

$$d\varepsilon_\ell^p = \left[\{n\}^T [D_d^e]\{d\varepsilon\} - \left\{ \{n\}^T[D_d^e]\left(\{\alpha\} \right.\right.\right.$$
$$\left.\left.\left. - [D_d^e]^{-1}\frac{d[D^e]}{dT}\{\varepsilon^e\}\right) - f_\ell'^{-1}\frac{\partial f}{\partial \sigma_0}\frac{\partial \sigma_0}{\partial T} \right\} dT \right] \Big/ S$$

$$\tag{2-26}$$

where $S = \{n\}^T [D_d^e]\{n\} + H$

With these information, the incremental relationship between stress and total strain, that is, constitutive equation will be derived. Based on Eq.(2-9)

which represents the relationship between stress increment $\{d\sigma\}$ and elastic strain increment $\{d\varepsilon^e\}$, the right side of Eq.(2-9) will be transformed as follows.

1) To replace elastic strain increment $\{d\varepsilon^e\}$ with total strain increment $\{d\varepsilon\}$ etc., using Eq.(2-24).

2) To express thermal strain increment $\{d\varepsilon^T\}$ by Eq.(2-4) and plastic strain increment $\{d\varepsilon^p\}$ by Eq.(2-17). Further, replace the magnitude $d\varepsilon_\ell^p$ of $\{d\varepsilon^p\}$ by $\{d\varepsilon\}$ etc., using Eq.(2-26).

As a result of the above calculation, only total strain increment $\{d\varepsilon\}$ remains as unknown on the right side of Eq.(2-9), and Eq.(2-9) becomes the incremental equation representing the relationship between stress increment $\{d\sigma\}$ and total strain increment $\{d\varepsilon\}$. Rearrangement of the right side and division of the expression into terms relating to total strain increment $\{d\varepsilon\}$ and the other terms (including temperature increment dT) furnish the following constitutive equation.

$$\{d\sigma\}=[D_d^p]\,\{d\varepsilon\}-\left\{[D_d^p]\left(\{\alpha\}-[D_d^e]^{-1}\,\frac{d[D^e]}{dT}\{\varepsilon^e\}\right)+[D_d^e]\{n\}f_\ell'^{-1}\frac{\partial f}{\partial\sigma_0}\frac{\partial\sigma_0}{\partial T}\Big/S\right\}dT \qquad (2-27)$$

where $\qquad [D_d^p] = [D_d^e] - [D_d^e]\{n\}\{n\}^T[D_d^e]\big/S$

Here, it is recognized that the above constitutive equation, Eq.(2-27) is in the same form as Eq.(2-1), like Eq.(2-10).

Equation (2-27) is applied when the material is under loading in the plastic range by the subsequent loading. Then, the scalar $d\varepsilon_\ell^p$, the magnitude of the plastic strain increment expressed by Eq.(2-26), is assumed to be positive. In contrast with this, if unloading occurs from the plastic range, $d\varepsilon_\ell^p$ becomes negative and the behavior of the material is elastic . Therefore, Eq.(2-10), the constitutive equation in the elastic range, should be used for the analysis of the subsequent step of loading in place of Eq.(2-27). In summary,

$$d\varepsilon_\ell^p > 0 \; : \; \text{loading}$$
$$d\varepsilon_\ell^p = 0 \; : \; \text{neutral loading} \qquad\qquad (2-28)$$
$$d\varepsilon_\ell^p < 0 \; : \; \text{unloading}$$

In order to proceed the analysis at the new increment of loading, the resulting new size and position of the yield surface by the previous increment should be obtained. It is assumed that the size (σ_0) of the yield surface is the function of the quantity ε_ℓ^p of plastic strain and temperature T as shown in Eq.(2-13). In connection with this, an explicit form of Eq.(2-13) should have been determined in advance based on experimental results. The position vector of the yield surface, {θ} , after each increment is known by summing up all translation increments {dθ} obtained at the preceding steps of loading. For calculation of {dθ} , the translation coefficient k in Eq.(2-14) must be determined and this can be done with the aid of Eq.(2-21) as the workhardening modulus H has been determined in advance based on experimental results[*)].

In the above description, the combined workhardening rule was used. However, in the case where only the isotropic workhardening rule or kinematic one is assumed, the equations shown in this section may be simplified. That is, if only the isotropic workhardening rule is used, the equations may be rewritten by replacing {θ} , {σ-θ} , k with {0} , {σ} , 0. For example, Eq.(2-21) for workhardening modulus becomes as follows.

$$ H = \frac{d\sigma_f}{d\varepsilon_\ell^p} - f'^{-1} \frac{\partial f}{\partial \sigma_0} \frac{\partial \sigma_0}{\partial \varepsilon_\ell^p} \qquad\qquad (2\text{-}21)' $$

---

*)   One of the methods to obtain the workhardening modulus H is to conduct usual uniaxial tensile tests at the temperature range in which the material is supposed to be heated up (Each test is conducted in a constant temperature). Then, the workhardening modulus H may be obtained as a function of the quantity ε_ℓ^p of plastic strain and temperature T, from the resulting stress-plastic strain diagrams (see Eq.(2-20)).

2.2.3 Constitutive equation (Incremental relation between stress and total

　　　strain) for thermal elastic-plastic-creep state /3-5/

　　Though the interaction between plasticity and creep have been investigated, the existing various theories are still under discussion. Then, it is assumed in this study that plasticity and creep are independent phenomena and there is no interaction between them so that plastic strain and creep strain are defined separately.

　　Under the assumption, the thermal elastic-plastic-creep theory is developed by introducing more general forms of workhardening rule and creep law respectively, according to the following procedure.

1)　To express creep constitutive equations at multi-axial stress state in a
　　general form.

2)　To introduce the above creep constitutive equation into the theory of
　　thermal elastic-plastic analysis represented in the previous section.

(1)　Creep strain at multi-axial stress state

　　Creep behavior of metal is usually influenced by stress, temperature and changes of its metallurgical structure. In this section, such creep behavior at multi-axial stress state will be expressed in such a general form of equation as to introduce it into the thermal elastic-plastic theory shown in section 2.2.2.

(i)　Creep constitutive equation in uni-axial stress state (Creep hardening rule)
　　/16/

　　Creep constitutive equation of metal is usually expressed in a differential form for creep strain rate $\dot{\varepsilon}^c$ which is regarded as a state function of stress σ , temperature T and suitable internal variables s_i (i=1, 2, ..., n) which represent changes of its metallurgical structure as follows.

$$\dot{\varepsilon}^c = p\,(\,\sigma, s_1, s_2, \cdots, s_n, T\,) \qquad\qquad (2\text{-}29)$$

$$\dot{s}_i = q_i\,(\,\sigma, s_1, s_2, \cdots, s_n, T) \quad (i = 1, 2, \cdots, n) \qquad\qquad (2\text{-}30)$$

　　As it is considered that change of creep strain rate represents the harden-

ing of the material, which increases with deformation, the theory which rules change of creep strain rate due to change of the metallurgical structure is called creep hardening rule. Based on this rule, unsteady-state creep constitutive equation can be formulated. Creep hardening rule is classified according to the kind of physical quantities adopted as variables in Eq.(2-29).

One of such variables is creep strain ϵ^C , which is one of simple measures. In this case, the constitutive equation of creep strain rate is expressed as

$$\dot{\epsilon}^c = p\,(\sigma, \epsilon^c, T) \qquad\qquad (2\text{-}31)$$

As the above equation assumes that the hardening of the material is controlled by creep strain, this rule is called strain-hardening rule. Many detailed examinations indicated that strain-hardening rule is considered superior to most of other classical creep hardening rules. Thus, this rule is adopted in many unsteady-state creep analyses.

(ii) Creep constitutive equation in multi-axial stress state

As stress state in actual engineering creep problems is multi-axial, it is necessary to expand the uni-axial creep constitutive equation for multi-axial stress state. This expansion can be conducted by the same way as for the plastic constitutive equation, employing similar hypotheses introduced in plasticity. They are:

1)   no change of volume due to creep deformation

2)   no influence of hydrostatic stress on creep deformation

Validity of the above hypotheses for metals is confirmed experimentally.

In similar to plastic strain increment, creep strain rate is expressed as a vector $\{\dot{\epsilon}^C\}$ in a multi-axial state, and the direction and magnitude of the creep strain rate $\{\dot{\epsilon}^C\}$ should be determined. Here, the direction and magnitude of creep strain rate $\{\dot{\epsilon}^C\}$ are assumed to be treated separately. For the direction, as usual, it is assumed that the flow law (creep flow law) holds like the case of

plastic deformation and the creep strain rate $\{\dot{\varepsilon}^C\}$ is expressed as follows.

$$\{\dot{\varepsilon}^c\} = \Lambda \left\{ \frac{\partial g}{\partial (\sigma - \theta_c)} \right\} \tag{2-32}$$

In the above equation, Λ is a positive scalar coefficient, and g is a scalar function which depends on the histories of stresses, temperature, etc. and is called the creep potential. Like the yield surface, g=0 represents a closed curved surface (the creep potential surface) in the stress space, which contains the current stress point, and $\{\theta_c\}$ is a vector which indicates the position of center of the creep potential surface (see Fig.2-3). The creep strain rate $\{\dot{\varepsilon}^C\}$ is expressed as a vector outward normal to the creep potential surface at the current stress point.

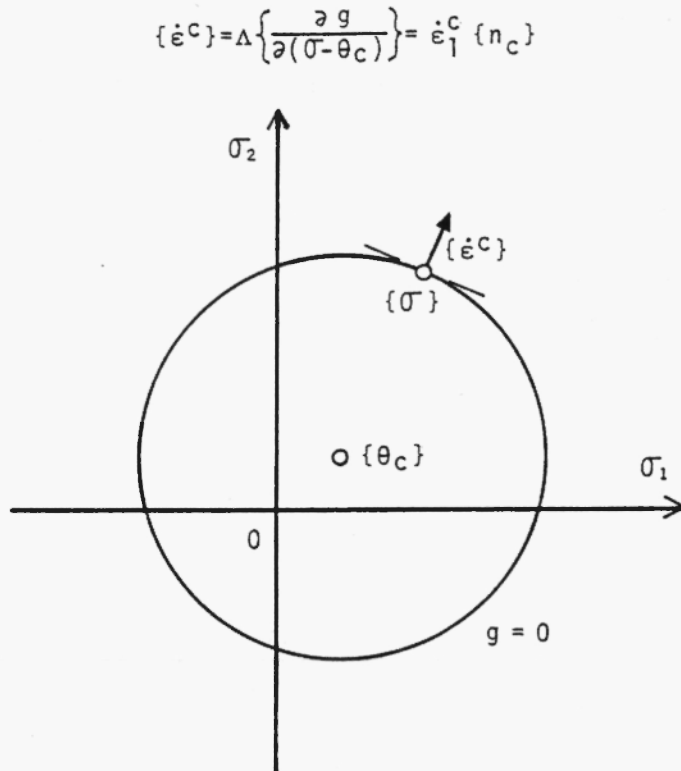Here, Eq.(2-32) will be rewritten in the same form as Eq.(2-17) for plastic

$$\{\dot{\varepsilon}^C\} = \Lambda \left\{ \frac{\partial g}{\partial (\sigma - \theta_c)} \right\} = \dot{\varepsilon}_1^C \{n_c\}$$

Fig.2-3 Schematic illustration of relation between creep potential surface g=0 and creep strain rate $\{\dot{\varepsilon}^C\}$

strain increment, adopting a creep potential surface which may move in the stress space.

$$\{\dot{\varepsilon}^c\} = \dot{\varepsilon}^c_{\ell} \{n_c\} \qquad (2\text{-}33)$$

where $\dot{\varepsilon}^C_{\ell}$: the magnitude of the creep strain rate $\{\dot{\varepsilon}^C\}$ (that is, the length of the vector $\{\dot{\varepsilon}^C\}$)

$$\{n_c\} = \left\{\frac{\partial g}{\partial(\sigma - \theta_c)}\right\} \Big/ g'_{\ell} \quad . \text{ the unit vector outward normal to the creep potential surface at the current stress point}$$

$$g'_{\underset{\sim}{\ell}} = \left| \left\{\frac{\partial g}{\partial(\sigma - \theta_c)}\right\} \right| = \left(\left\{\frac{\partial g}{\partial(\sigma - \theta_c)}\right\}^T \left\{\frac{\partial g}{\partial(\sigma - \theta_c)}\right\} \right)^{\frac{1}{2}}$$

In the above equation, the magnitude $\dot{\varepsilon}^C_{\ell}$ of creep strain rate $\{\dot{\varepsilon}^C\}$ is expressed by the creep hardening rule (uni-axial creep constitutive equation) explained briefly in the previous section (i).

The characteristics of the creep potential surface depend on the creep characteristics of the metal, like the creep hardening rule. For the shape of the surface, von Mises type and Tresca type, for example, can be adopted, which are widely used for the yield surface. For translation of the creep potential surface in the stress space, Bailey's theory /17/ and Orowan's theory /18/, etc. may be applied to rule the translation rate $\{\dot{\theta}_c\}$ of center of the creep potential surface.

(iii) Creep strain increment

By introduction of the creep strain increment into the thermal elastic-plastic theory shown in section 2.2.2, thermal elastic-plastic-creep theory can be developed. A creep strain increment can be obtained by integrating the creep strain rate with respect to time. The creep strain rate is usually a function of stresses, temperature, internal variables and their histories. So, there are two

procedures for the above integration. One is to integrate the creep strain rate, regarding it as constant in each time increment. Another is to integrate the rate with consideration of the changes of variables during each time increment.

First, the creep strain increment will be obtained by the former method which is less accurate than the latter, but the method is simple and can be applied for all types of creep theories (creep strain rates). That is, the creep strain increment $\{d\varepsilon^C\}$ between t_i and t_{i+1} is calculated by multiplying the creep strain rate $\{\dot{\varepsilon}^C\}$ at time t_i , by the time increment $dt = t_{i+1} - t_i$.

$$\{d\epsilon^c\} = \{\dot{\epsilon}^c\}\, dt \qquad\qquad\qquad (2\text{-}34)$$

In the case where the creep strain increment is expressed as Eq.(2-34), it can be calculated immediately as the product of two known quantities. Therefore, even if the creep effect is taken into account in the thermal elastic-plastic theory, the theory including the creep effect does not become more complex than the thermal elastic-plastic one. If it is necessary to obtain more accurate creep strain increment, the integration must be performed for a smaller time ·increment.

When the second procedure is applied, the integration is conducted with consideration of the change of the creep strain rate during each time increment. In this case, the method of the integration and the form of the creep strain increment derived for such accurate integration are usually different in each cases. The authors have derived the creep strain increments with consideration of the changes of the variables (stresses, creep constants) as accurately as possible for some comparatively simple creep theories, that is, isotropic time-hardening theory, isotropic strain-hardening theory, isotropic power-hardening theory and isotropic exponential-hardening theory /3,4/.

The process of the integration will be demonstrated in the following.

First, the creep potential surface is assumed to have the following features.

1)   Its center coincides with the origin of the stress space.

2)   Its shape is similar to that of Mises' yield surface.

3)   Its size is determined so that the stress point is always on it.

Next, assuming that the magnitude of creep strain rate is represented by the time-hardening rule, creep strain increment is obtained by integrating the following expression for a short time increment.

$$\{\dot{\varepsilon}^C\} = \sqrt{\frac{3}{2}} \, m \, A \, \sigma^{\gamma} \, t^{m-1} \{n_c\} = \sqrt{\frac{3}{2}} \, a \, \bar{\sigma}^{\gamma} \, t^d \{n_c\} \tag{2-35}$$

where $\bar{\sigma}$: equivalent stress, t: time,   m, A, γ : creep constants

   $a = m A$, $d = m-1$

For integration of the above creep strain rate, it is assumed that creep constant a, the equivalent stress $\bar{\sigma}$ and the normal unit vector $\{n_c\}$ to the creep surface change linearly and creep constants d and γ are constant during a short time increment dt.

Based on these assumptions, creep strain increment can be calculated according to the time-hardening law as follows.

$$\{d\varepsilon^C\} = \{d\hat{\varepsilon}^C\} + [C_C] \{d\sigma\} \tag{2-36}$$

where
$$\{d\hat{\varepsilon}^C\} = \sqrt{\frac{3}{2}} \, \bar{\sigma}^{\gamma} \, (K_1 \, a + K_2 \, da) \{n_c\} ,$$

$$[C_C] = \frac{3}{2} \bar{\sigma}^{\gamma-1} (K_2 \, a + K_3 \, da) \{(\gamma - 1) \{n_c\} \{n_c\}^{\top} + [C_{cc}]\} ,$$

$$K_1 = \frac{(t+dt)^{d+1} - t^{d+1}}{d+1} , \quad K_2 = \frac{(t+dt)^{d+1}}{d+1} - \frac{(t+dt)^{d+2} - t^{d+2}}{(d+1)\,(d+2)\,dt} ,$$

$$K_3 = \frac{(t+dt)^{d+1}}{d+1} - \frac{2(t+dt)^{d+2}}{(d+1)\,(d+2)\,dt} + \frac{2\{(t+dt)^{d+3} - t^{d+3}\}}{(d+1)\,(d+2)\,(d+3)\,dt^2} ,$$

$$[C_{cc}] = \begin{bmatrix} 2/3 & -1/3 & -1/3 & 0 & 0 & 0 \\ & 2/3 & -1/3 & 0 & 0 & 0 \\ & & 2/3 & 0 & 0 & 0 \\ & \text{Sym.} & & 2 & 0 & 0 \\ & & & & 2 & 0 \\ & & & & & 2 \end{bmatrix}$$

da : increment of a due to change dT of temperature during change dt of

time

The equation can be also used for evaluation of creep strain increment according to the strain-hardening law or the power law only by modifying the time t in the equation (see t_{eq} etc. in Appendix). The reference for the equivalent time t_{eq} is IIW Document or Trans. of JWRI shown in Ref.4.

(2) Constitutive equations for thermal elastic-plastic-creep state

(i) Thermal elastic-creep constitutive equation

In the case where the current stress point is inside the yield surface, that is, the material is in the elastic range, accompanying temperature changes and creep strains, the total strain increment $\{d\epsilon\}$ is represented as the summation of the thermal strain increment $\{d\epsilon^T\}$, elastic strain increment $\{d\epsilon^e\}$ and creep strain increment $\{d\epsilon^C\}$.

$$\{d\epsilon\} = \{d\epsilon^T\} + \{d\epsilon^e\} + \{d\epsilon^c\} \tag{2-37}$$

The constitutive equation (incremental relation between stress and total strain) for this state will be obtained by using Eq.(2-9) and transforming it in the almost same way as in section 2.2.2.

After the transformations, rearrangement of the equation provides the following thermal elastic-creep constitutive equation,

(a) In the case where Eq.(2-34) is adopted for creep strain increment

$$\{d\sigma\} = [D_c^e] \{d\epsilon\} - [D_d^e] \left\{ \left(\{\alpha\} \right. \right.$$
$$\left. - [D_d^e]^{-1} \frac{d[D^e]}{dT} \{\epsilon^e\} \right) dT + \{\dot{\epsilon}^c\} dt \right\} \tag{2-38}$$

This equation is the same as for thermal elastic state shown in Eq.(2-10) except that the term, $-[D_d^e]\{\dot{\epsilon}^C\}dt$, is supplemented on the right side.

(b) In the case where Eq.(2-36) is adopted for creep strain increment

$$\{d\sigma\} = [\widehat{D_d^e}] \{d\epsilon\} - [\widehat{D_d^e}] \left\{ \left(\{\alpha\} - [D_d^e]^{-1} \frac{d[D^e]}{dT} \{\epsilon^e\} \right) dT + \{\widehat{d\epsilon^C}\} \right\} \tag{2-39}$$

where $\quad [\widehat{D_d^e}] = ([D_d^e]^{-1} + [C_c])^{-1}$

(ii) Thermal elastic-plastic-creep constitutive equation

In the plastic range, the total strain increment $\{d\epsilon\}$ is expressed by the summation of the components as

$$\{d\epsilon\} = \{d\epsilon^T\} + \{d\epsilon^e\} + \{d\epsilon^p\} + \{d\epsilon^c\} \tag{2-40}$$

The constitutive equation for this state is obtained in the almost same way as in section 2.2.2.

The relationships between $\{d\epsilon\}$ and $d\epsilon_\ell^p$, and constitutive equations are expressed as follows.

(a) In the case where Eq.(2-34) is adopted for creep strain increment

$$d\epsilon_\ell^p = \left[\{n\}^T [D_d^e] \{d\epsilon\} - \left[\left\{ \{n\}^T [D_d^e] \left(\{\alpha\} - [D_d^e]^{-1} \frac{d[D^e]}{dT} \{\epsilon^e\} \right) \right. \right. \right.$$
$$\left. \left. \left. - f_\ell'^{-1} \frac{\partial f}{\partial \sigma_0} \frac{\partial \sigma_0}{\partial T} \right\} dT + \{n\}^T [D_d^e] \{\dot{\epsilon}^c\} dt \right] \right] \Big/ S \tag{2-41}$$

where $\quad S = \{n\}^T [D_d^e] \{n\} + H$

$$\{d\sigma\} = [D_d^p] \{d\epsilon\} - \left[\left\{ [D_d^p] \left(\{\alpha\} - [D_d^e]^{-1} \frac{d[D^e]}{dT} \{\epsilon^e\} \right) + [D_d^e] \{n\} f_\ell'^{-1} \right. \right.$$
$$\left. \left. \times \frac{\partial f}{\partial \sigma_0} \frac{\partial \sigma_0}{\partial T} \Big/ S \right\} dT + [D_d^p] \{\epsilon^c\} dt \right] \tag{2-42}$$

where $\quad [D_d^p] = [D_d^e] - [D_d^e] \{n\} \{n\}^T [D_d^e] \Big/ S$

(b) In the case where Eq.(2-36) is adopted for creep strain increment

$$d\epsilon_\ell^p = \left[\{n\}^T [\widehat{D_d^e}] \{d\epsilon\} - \left[\left\{ \{n\}^T [\widehat{D_d^e}] \left(\{\alpha\} - [D_d^e]^{-1} \frac{d[D^e]}{dT} \{\epsilon^e\} \right) \right. \right. \right.$$
$$\left. \left. \left. - f_\ell'^{-1} \frac{\partial f}{\partial \sigma_0} \frac{\partial \sigma_0}{\partial T} \right\} dT + \{n\}^T [\widehat{D_d^e}] \{\widehat{d\epsilon^C}\} \right] \right] \Big/ \widehat{S} \tag{2-43}$$

where $\quad \widehat{S} = \{n\}^T [\widehat{D_d^e}] \{n\} + H$

$$\{d\sigma\} = [\widehat{D_d^p}] \{d\epsilon\} - \left[\left\{ [\widehat{D_d^p}] \left(\{\alpha\} - [D_d^e]^{-1} \frac{d[D^e]}{dT} \{\epsilon^e\} \right) + [\widehat{D_d^e}] \{n\} f_\ell'^{-1} \right. \right.$$
$$\left. \left. \times \frac{\partial f}{\partial \sigma_0} \frac{\partial \sigma_0}{\partial T} \Big/ \widehat{S} \right\} dT + [\widehat{D_d^p}] \{\widehat{d\epsilon^C}\} \right] \tag{2-44}$$

where
$$[\widehat{D_d^p}] = [\widehat{D_d^e}] - [\widehat{D_d^e}] \{n\} \{n\}^T [\widehat{D_d^e}] \Big/ \widehat{S}$$

2.2.4 Summary of constitutive equations /19/

Constitutive equations used for possible cases related to welding and PWHT are summarized in Table A-1 (Appendix)[*]. In the table, the corresponding phenomenon indicated by each row becomes more complex from the left to the right, such as thermal elastic, thermal elastic-plastic, etc.. At the lower row on each column, the more influential factors are taken into account in the constitutive equation. Once a problem is specified, the type of the problem is defined and the degree of temperature dependency of the material properties can be furnished. With this information an appropriate constitutive equation to the analysis of the problem can be chosen from Table A-1. For analysis of welding, it is necessary to use the constitutive equation (6) for Thermal Elastic-Plastic State – II with more accurate consideration of temperature dependent properties of the material since the temperature range in which the material undergoes is very wide from room temperature to the melting point and thus changes of the material properties are very large. For analysis of stress-relief annealing, it is necessary to use the constitutive equation (11) for Thermal Elastic-Plastic-Creep State – IV or (16) for Thermal Elastic-Plastic-Creep State – VIII including creep strain.

All constitutive equations in Table A-1 can be represented in the same following simple form.

$$\{d\sigma\} = [D]\{d\varepsilon\} - \{dC\} \tag{2-45}$$

This equation shows that an increment of stress can be expressed as the sum of two terms. The first term is due to an increment of total strain and the second term is due to the production of thermal strain and creep strain, and changes of the material properties by temperature changes. Usually, changes in the temperature distribution and the material properties at an arbitrary temperature are

---

[*] It should be noted that in Table A-1 which had been shown in Ref.19, some notations are different from those already represented in this chapter.

known before the thermal stress analysis is conducted. At the same time, with information on the stress history, the second term in Eq.(2-45) can be also calculated before Eq.(2-45) is used for the next step of the analysis.

In this section, the constitutive equations for thermal elastic, thermal elastic-plastic and thermal elastic-plastic-creep states are developed with consideration of various effects of temperature changes. They can be expressed in a simple form as Eq.(2-45). It is a routine procedure as shown in next section to derive the fundamental equations (stiffness equation) for each state based on the finite element method, introducing these constitutive equations.

2.2.5 Basic equations for thermal elastic-plastic-creep analysis by finite element method (Stiffness equation)

The basic concept of the finite element method, expressed simply, is to regard a structure as an assembly of simple structural elements interconnected at a finite number of nodal points, where the equilibrium and compatibility conditions are satisfied. Accordingly, the structure under consideration should be divided into a finite number of elements at the beginning of the analysis such as triangular finite elements for plane stress or strain problems, or tetrahedral finite elements for three-dimensional stress problems.

Considering one of typical finite elements in the continuum concerned basic equations in the finite element method will be derived in the following.

(1) Incremental relation between total strain and displacement in an element

The displacements $\{s\}$ of an arbitrary point in an element will be defined as a function of the nodal displacements $\{w\}$.

$$\{s\} = [N]\{w\} = [N_i \; N_j \; \ldots] \{w_i \; w_j \; \ldots\}^T \tag{2-46}$$

where $[N]$: displacement function (the components of $[N]$ are generally a function of co-ordinates)

Table A-1 Constitutive equations for thermal elastic-plastic creep analysis

Temperature	Temperature Dependency of Properties		Thermal Elastic State	Thermal Elastic-Plastic State	Thermal Elastic-Plastic Creep State (I)
	El-Pl	Creep			
Constant			**(1) Elastic State** $\{d\sigma\}=[D^e]\{d\varepsilon\}$ $\{d\varepsilon\}=\{d\varepsilon^e\}$	**(4) Elastic-Plastic State** $\{d\sigma\}=[D^P]\{d\varepsilon\}$ $\{d\varepsilon\}=\{d\varepsilon^e\}+\{d\varepsilon^P\}$ $\{d\varepsilon^P\}=\{A\}^T\{d\varepsilon\}\{n\}$ $\{d\theta\}=k\|\{d\varepsilon^P\}\|\{n_\theta\}$	**(7) Elastic-Plastic Creep State - I** $\{d\sigma\}=[D^P]\{d\varepsilon\}-[D^P]\{d\varepsilon^c\}$ $\{d\varepsilon\}=\{d\varepsilon^e\}+\{d\varepsilon^P\}+\{d\varepsilon^c\}$ $\{d\varepsilon^P\}=\{A\}^T(\{d\varepsilon\}-\{d\varepsilon^c\})\{n\}$ $\{d\varepsilon^c\}=\{\dot\varepsilon_I^c\}dt$ $\{d\theta\}=k\|\{d\varepsilon^P\}\|\{n_\theta\}$
Changing	Neglected	Neglected	**(2) Thermal Elastic State - I** $\{d\sigma\}=[D^e]\{d\varepsilon\}-[D^e]\{d\varepsilon^T\}$ $\{d\varepsilon\}=\{d\varepsilon^e\}+\{d\varepsilon^T\}$ $\{d\varepsilon^T\}=\{\alpha\}dT$	**(5) Thermal Elastic-Plastic State - I** $\{d\sigma\}=[D^P]\{d\varepsilon\}-[D^P]\{d\varepsilon^T\}$ $\{d\varepsilon\}=\{d\varepsilon^e\}+\{d\varepsilon^P\}+\{d\varepsilon^T\}$ $\{d\varepsilon^P\}=\{A\}^T(\{d\varepsilon\}-\{d\varepsilon^T\})\{n\}$ $\{d\varepsilon^T\}=\{\alpha\}dT$ $\{d\theta\}=k\|\{d\varepsilon^P\}\|\{n_\theta\}$	**(8) Thermal El-Pl Creep State - I** $\{d\sigma\}=[D^P]\{d\varepsilon\}-[D^P](\{d\varepsilon^c\}+\{d\varepsilon^T\})$ $\{d\varepsilon\}=\{d\varepsilon^e\}+\{d\varepsilon^P\}+\{d\varepsilon^c\}+\{d\varepsilon^T\}$ $\{d\varepsilon^P\}=\{A\}^T(\{d\varepsilon\}-\{d\varepsilon^c\}-\{d\varepsilon^T\})\{n\}$ $\{d\varepsilon^c\}=\{\dot\varepsilon_I^c\}dt$ $\{d\varepsilon^T\}=\{\alpha\}dT$ $\{d\theta\}=k\|\{d\varepsilon^P\}\|\{n_\theta\}$
	Neglected	Included			**(9) Thermal El-Pl Creep State - II** $\{d\sigma\}=[D^P]\{d\varepsilon\}-[D^P](\{d\varepsilon^c\}+\{d\varepsilon^T\})$ $\{d\varepsilon\}=\{d\varepsilon^e\}+\{d\varepsilon^P\}+\{d\varepsilon^c\}+\{d\varepsilon^T\}$ $\{d\varepsilon^P\}=\{A\}^T(\{d\varepsilon\}-\{d\varepsilon^c\}-\{d\varepsilon^T\})\{n\}$ $\{d\varepsilon^c\}=\{\dot\varepsilon_{IT}^c\}dt$ $\{d\varepsilon^T\}=\{\alpha\}dT$ $\{d\theta\}=k\|\{d\varepsilon^P\}\|\{n_\theta\}$
	Included	Neglected	**(3) Thermal Elastic State - II** $\{d\sigma\}=[D_I^e]\{d\varepsilon\}-[D_I^e]\{d\varepsilon^T\}+\{dP_T^e\}$ $\{d\varepsilon\}=\{d\varepsilon^e\}+\{d\varepsilon^T\}$ $\{d\varepsilon^T\}=\{\alpha\}dT$	**(6) Thermal Elastic-Plastic State - II** $\{d\sigma\}=[D_I^P]\{d\varepsilon\}-[D_I^P]\{d\varepsilon^T\}+\{dP_T^P\}$ $\{d\varepsilon\}=\{d\varepsilon^e\}+\{d\varepsilon^P\}+\{d\varepsilon^T\}$ $\{d\varepsilon^P\}=[\{A_T\}^T(\{d\varepsilon\}-\{d\varepsilon^T\})+dP_T^{P1}]\{n\}$ $\{d\varepsilon^T\}=\{\alpha\}dT$ $\{d\theta\}=k\|\{d\varepsilon^P\}\|\{n_\theta\}$	**(10) Thermal El-Pl Creep State - III** $\{d\sigma\}=[D_I^P]\{d\varepsilon\}-[D_I^P](\{d\varepsilon^c\}+\{d\varepsilon^T\})+\{dP_T^P\}$ $\{d\varepsilon\}=\{d\varepsilon^e\}+\{d\varepsilon^P\}+\{d\varepsilon^c\}+\{d\varepsilon^T\}$ $\{d\varepsilon^P\}=[\{A_T\}^T(\{d\varepsilon\}-\{d\varepsilon^c\}-\{d\varepsilon^T\})+dP_T^{P1}]\{n\}$ $\{d\varepsilon^c\}=\{\dot\varepsilon_I^c\}dt$ $\{d\varepsilon^T\}=\{\alpha\}dT$ $\{d\theta\}=k\|\{d\varepsilon^P\}\|\{n_\theta\}$
	Included	Included	**Remarks** * : For constitutive equations of Thermal Elastic-Plastic Creep State (II), creep strain increment is obtained by integrating creep strain rate with consideration of its change during the time increment		**(11) Thermal El-Pl Creep State - IV** $\{d\sigma\}=[D_I^P]\{d\varepsilon\}-[D_I^P](\{d\varepsilon^c\}+\{d\varepsilon^T\})+\{dP_I^P\}$ $\{d\varepsilon\}=\{d\varepsilon^e\}+\{d\varepsilon^P\}+\{d\varepsilon^c\}+\{d\varepsilon^T\}$ $\{d\varepsilon^P\}=[\{A_T\}^T(\{d\varepsilon\}-\{d\varepsilon^c\}-\{d\varepsilon^T\})+dP_T^{P1}]\{n\}$ $\{d\varepsilon^c\}=\{\dot\varepsilon_{IT}^c\}dt$ $\{d\varepsilon^T\}=\{\alpha\}dT$ $\{d\theta\}=k\|\{d\varepsilon^P\}\|\{n_\theta\}$

Thermal Elastic Creep State : The constitutive equation for thermal elastic creep state can be derived by making the workhardening modulus H infinite in each equation of Thermal Elastic—Plastic Creep State (I) and (II).

Notations

$\{d\sigma\}$: Stress increment

$\{d\varepsilon\}$: Total strain increment

$\{d\varepsilon^e\}$: Elastic strain increment

$\{d\varepsilon^P\} = d\varepsilon_1^P\{n\}$: Plastic strain increment

$\{d\varepsilon^C\}$: Creep strain increment

$\{d\varepsilon^T\} = \{\alpha\}dT$: Thermal strain increment

$\{d\theta\} = kd\varepsilon_1^P\{n_\theta\}$: Translation increment

$\{\varepsilon^e\} = [D^e]^{-1}\{\sigma\}$: Elastic strain

$d\sigma_f = \{n\}^T\{d\sigma\}$

$d\theta_f = \{n\}^T\{d\theta\}$

$d\varepsilon_1^P = |\{d\varepsilon^P\}| = (\{d\varepsilon^P\}^T\{d\varepsilon^P\})^{\frac{1}{2}}$

$\varepsilon_1^P = \int d\varepsilon_1^P$

$(d\varepsilon^C)^2 = \frac{2}{9}[(d\varepsilon_x^C - d\varepsilon_y^C)^2 + (d\varepsilon_y^C - d\varepsilon_z^C)^2 + (d\varepsilon_z^C - d\varepsilon_x^C)^2 + \frac{1}{3}(d\gamma_{zx}^{C2} + d\gamma_{xy}^{C2} + d\gamma_{yz}^{C2})]$

$\bar{\varepsilon}^C = \int d\bar{\varepsilon}^C$

$\{\alpha\}$: Instantaneous linear expansion coefficient

T, dT : Temperature, temperature increment

dt : Time increment

$f(\sigma_{ij} - \theta_{ij}, \sigma_0)$: Yield function (f=0 represents the yield surface)

$\{\theta\}$: Translation vector which indicates the position of center of the yield surface in the stress space

$\sigma_0 = \sigma_0(\varepsilon_1^P, T)$: A measure of the size of the yield surface

$f_1' = |\{\frac{\partial f}{\partial(\sigma - \theta)}\}| = (\{\frac{\partial f}{\partial(\sigma - \theta)}\}^T\{\frac{\partial f}{\partial(\sigma - \theta)}\})^{\frac{1}{2}}$

$\{n\} = \{\frac{\partial f}{\partial(\sigma - \theta)}\}/f_1'$

$H = (d\sigma_f + f_1'^{-1}\frac{\partial f}{\partial \sigma_0}\frac{\partial \sigma_0}{\partial T}dT)/d\varepsilon_1^P$: Workhardening modulus

$k = (H + f_1'^{-1}\frac{\partial f}{\partial \sigma_0}\frac{\partial \sigma_0}{\partial \varepsilon_1^P})/n_{\theta f}$

$n_{\theta f} = \{n\}^T\{n_\theta\}$

$\{n_\theta\}$: Unit vector which indicates the direction of translation increment of the yield surface

$[D^e]$: Elastic stress-strain matrix

$[D_T^e] = [D^e] + \frac{d[D^e]}{dT}dT$

$[\hat{D}^e] = ([D^e]^{-1} + [C_S])^{-1}$

$[\hat{D}_{T1}^e] = ([D^e]^{-1} + [C_{ST}])^{-1}$

$[\hat{D}_{T2}^e] = ([D_T^e]^{-1} + [C_S])^{-1}$

$[\hat{D}_T^e] = ([D_T^e]^{-1} + [C_{ST}])^{-1}$

$[D^P] = [D^e] - [D^e]\{n\}\{n\}^T[D^e]/(\{n\}^T[D^e]\{n\} + H)$
　　: Plastic stress-strain matrix

$[D_T^P] = [D_T^e] - [D_T^e]\{n\}\{n\}^T[D_T^e]/(\{n\}^T[D_T^e]\{n\} + H)$

$[\hat{D}^P] = [\hat{D}^e] - [\hat{D}^e]\{n\}\{n\}^T[\hat{D}^e]/(\{n\}^T[\hat{D}^e]\{n\} + H)$

$[\hat{D}_{T1}^P] = [\hat{D}_{T1}^e] - [\hat{D}_{T1}^e]\{n\}\{n\}^T[\hat{D}_{T1}^e]/(\{n\}^T[\hat{D}_{T1}^e]\{n\} + H)$

$[\hat{D}_{T2}^P] = [\hat{D}_{T2}^e] - [\hat{D}_{T2}^e]\{n\}\{n\}^T[\hat{D}_{T2}^e]/(\{n\}^T[\hat{D}_{T2}^e]\{n\} + H)$

$[\hat{D}_T^P] = [\hat{D}_T^e] - [\hat{D}_T^e]\{n\}\{n\}^T[\hat{D}_T^e]/(\{n\}^T[\hat{D}_T^e]\{n\} + H)$

$\{A\}^T = \{n\}^T[D^e]/(\{n\}^T[D^e]\{n\} + H)$

$\{A_T\}^T = \{n\}^T[D_T^e]/(\{n\}^T[D_T^e]\{n\} + H)$

$\{\hat{A}\}^T = \{n\}^T[\hat{D}^e]/(\{n\}^T[\hat{D}^e]\{n\} + H)$

$\{\hat{A}_{T1}\}^T = \{n\}^T[\hat{D}_{T1}^e]/(\{n\}^T[\hat{D}_{T1}^e]\{n\} + H)$

$\{\hat{A}_{T2}\}^T = \{n\}^T[\hat{D}_{T2}^e]/(\{n\}^T[\hat{D}_{T2}^e]\{n\} + H)$

$\{\hat{A}_T\}^T = \{n\}^T[\hat{D}_T^e]/(\{n\}^T[\hat{D}_T^e]\{n\} + H)$

Thermal Elastic-Plastic Creep State (II)*

---

(12) Elastic-Plastic Creep State – II

$\{d\sigma\} = [\hat{D}^P]\{d\varepsilon\} - [\hat{D}^P]\{d\hat{\varepsilon}^C\}$

$\{d\varepsilon\} = \{d\varepsilon^e\} + \{d\varepsilon^P\} + \{d\varepsilon^C\}$

$\{d\varepsilon^P\} = \{\hat{A}\}^T(\{d\varepsilon\} - \{d\hat{\varepsilon}^C\})\{n\}$

$\{d\varepsilon^C\} = \{d\hat{\varepsilon}^C\} + [C_S]\{d\sigma\}$

$\{d\theta\} = k|\{d\varepsilon^P\}|\{n_\theta\}$

---

(13) Thermal El-Pl Creep State – V

$\{d\sigma\} = [\hat{D}^P]\{d\varepsilon\} - [\hat{D}^P](\{d\hat{\varepsilon}^C\} + \{d\varepsilon^T\})$

$\{d\varepsilon\} = \{d\varepsilon^e\} + \{d\varepsilon^P\} + \{d\varepsilon^C\} + \{d\varepsilon^T\}$

$\{d\varepsilon^P\} = \{\hat{A}\}^T(\{d\varepsilon\} - \{d\hat{\varepsilon}^C\} - \{d\varepsilon^T\})\{n\}$

$\{d\varepsilon^C\} = \{d\hat{\varepsilon}^C\} + [C_S]\{d\sigma\}$

$\{d\varepsilon^T\} = \{\alpha\}dT$

$\{d\theta\} = k|\{d\varepsilon^P\}|\{n_\theta\}$

---

(14) Thermal El-Pl Creep State – VI

$\{d\sigma\} = [\hat{D}_{T1}^P]\{d\varepsilon\} - [\hat{D}_{T1}^P](\{d\hat{\varepsilon}_T^C\} + \{d\varepsilon^T\})$

$\{d\varepsilon\} = \{d\varepsilon^e\} + \{d\varepsilon^P\} + \{d\varepsilon^C\} + \{d\varepsilon^T\}$

$\{d\varepsilon^P\} = \{\hat{A}_{T1}\}^T(\{d\varepsilon\} - \{d\hat{\varepsilon}_T^C\} - \{d\varepsilon^T\})\{n\}$

$\{d\varepsilon^C\} = \{d\hat{\varepsilon}_T^C\} + [C_{ST}]\{d\sigma\}$

$\{d\varepsilon^T\} = \{\alpha\}dT$

$\{d\theta\} = k|\{d\varepsilon^P\}|\{n_\theta\}$

---

(15) Thermal El-Pl Creep State – VII

$\{d\sigma\} = [\hat{D}_{T2}^P]\{d\varepsilon\} - [\hat{D}_{T2}^P](\{d\hat{\varepsilon}^C\} + \{d\varepsilon^T\}) + \{d\hat{P}_{T2}^P\}$

$\{d\varepsilon\} = \{d\varepsilon^e\} + \{d\varepsilon^P\} + \{d\varepsilon^C\} + \{d\varepsilon^T\}$

$\{d\varepsilon^P\} = [\{\hat{A}_{T2}\}^T(\{d\varepsilon\} - \{d\hat{\varepsilon}^C\} - \{d\varepsilon^T\}) + d\hat{P}_{T2}^{P1}]\{n\}$

$\{d\varepsilon^C\} = \{d\hat{\varepsilon}^C\} + [C_S]\{d\sigma\}$

$\{d\varepsilon^T\} = \{\alpha\}dT$

$\{d\theta\} = k|\{d\varepsilon^P\}|\{n_\theta\}$

---

(16) Thermal El-Pl Creep State – VIII

$\{d\sigma\} = [\hat{D}_T^P]\{d\varepsilon\} - [\hat{D}_T^P](\{d\hat{\varepsilon}_T^C\} + \{d\varepsilon^T\}) + \{d\hat{P}_T^P\}$

$\{d\varepsilon\} = \{d\varepsilon^e\} + \{d\varepsilon^P\} + \{d\varepsilon^C\} + \{d\varepsilon^T\}$

$\{d\varepsilon^P\} = [\{\hat{A}_T\}^T(\{d\varepsilon\} - \{d\hat{\varepsilon}_T^C\} - \{d\varepsilon^T\}) + d\hat{P}_T^{P1}]\{n\}$

$\{d\varepsilon^C\} = \{d\hat{\varepsilon}_T^C\} + [C_{ST}]\{d\sigma\}$

$\{d\varepsilon^T\} = \{\alpha\}dT$

$\{d\theta\} = k|\{d\varepsilon^P\}|\{n_\theta\}$

Notations (Continued)

$$\{dP_T^e\} = \frac{d[D^e]}{dT} dT\{\varepsilon^e\}$$

$$\{dP_T^p\} = [[D_T^p][D_T^e]^{-1}\frac{d[D^e]}{dT}\{\varepsilon^e\} - [D_T^e]\{n\}f_1'^{-1}\frac{\partial f}{\partial \sigma_0}\frac{\partial \sigma_0}{\partial T}/(\{n\}^T[D_T^e]\{n\}+H)]dT$$

$$\{d\hat{P}_{T2}^p\} = [[\hat{D}_{T2}^p][D_T^e]^{-1}\frac{d[D^e]}{dT}\{\varepsilon^e\} - [\hat{D}_{T2}^e]\{n\}f_1'^{-1}\frac{\partial f}{\partial \sigma_0}\frac{\partial \sigma_0}{\partial T}/(\{n\}^T[\hat{D}_{T2}^e]\{n\}+H)]dT$$

$$\{d\hat{P}_T^p\} = [[\hat{D}_T^p][D_T^e]^{-1}\frac{d[D^e]}{dT}\{\varepsilon^e\} - [\hat{D}_T^e]\{n\}f_1'^{-1}\frac{\partial f}{\partial \sigma_0}\frac{\partial \sigma_0}{\partial T}/(\{n\}^T[\hat{D}_T^e]\{n\}+H)]dT$$

$$dP_T^{p1} = [(\{n\}^T\frac{d[D^e]}{dT}\{\varepsilon^e\} + f_1'^{-1}\frac{\partial f}{\partial \sigma_0}\frac{\partial \sigma_0}{\partial T})/(\{n\}^T[D_T^e]\{n\}+H)]dT$$

$$d\hat{P}_{T2}^{p1} = [(\{n\}^T[\hat{D}_{T2}^e][D_T^e]^{-1}\frac{d[D^e]}{dT}\{\varepsilon^e\} + f_1'^{-1}\frac{\partial f}{\partial \sigma_0}\frac{\partial \sigma_0}{\partial T})/(\{n\}^T[\hat{D}_{T2}^e]\{n\}+H)]dT$$

$$d\hat{P}_T^{p1} = [(\{n\}^T[\hat{D}_T^e][D_T^e]^{-1}\frac{d[D^e]}{dT}\{\varepsilon^e\} + f_1'^{-1}\frac{\partial f}{\partial \sigma_0}\frac{\partial \sigma_0}{\partial T})/(\{n\}^T[\hat{D}_T^e]\{n\}+H)]dT$$

$\{\dot{\varepsilon}^c\} = \dot{\varepsilon}_1^c\{n_c\}$: Creep strain rate

$\dot{\varepsilon}_1^c$: Magnitude of creep strain rate

$\{n_c\} = \{\frac{\partial f_c}{\partial \sigma}\}/f_{c1}'$: Unit vector which indicates the direction of creep strain rate

f_c : Creep potential

In Thermal Elastic-Plastic Creep State (II), it is assumed that

$$f_c = f_c(\sigma_{ij}, \sigma_{0c}) = \bar{\sigma}^2 - \sigma_{0c}^2$$

$\bar{\sigma}^2 = \frac{1}{2}[(\sigma_x-\sigma_y)^2+(\sigma_y-\sigma_z)^2+(\sigma_z-\sigma_x)^2+6(\tau_{yz}^2+\tau_{zx}^2+\tau_{xy}^2)]$: Equivalent stress from the origin of the stress space

σ_{0c} : A measure of the size of the creep surface ($f_c = 0$)

$$f_{c1}' = |\{\frac{\partial f_c}{\partial \sigma}\}| = (\{\frac{\partial f_c}{\partial \sigma}\}^T\{\frac{\partial f_c}{\partial \sigma}\})^{\frac{1}{2}}$$

$\{\dot{\varepsilon}_1^c\}$: Creep strain rate which is determined from stress state etc. before each increment, for a constant temperature

$\{\dot{\varepsilon}_{1T}^c\}$: Creep strain rate which is determined from temperature, stress state etc. before each increment

$$\{d\hat{\varepsilon}^c\} = \sqrt{\frac{3}{2}}\bar{\sigma}^\gamma G_1 a\{n_c\}$$

$$\{d\hat{\varepsilon}_T^c\} = \sqrt{\frac{3}{2}}\bar{\sigma}^\gamma(G_1 a + G_2 da)\{n_c\}$$

$$[C_S] = \frac{3}{2}\bar{\sigma}^{\gamma-1}G_2 a[(\gamma-1)\{n_c\}\{n_c\}^T + [C_{SJ}]]$$

$$[C_{ST}] = \frac{3}{2}\bar{\sigma}^{\gamma-1}(G_2 a + G_3 da)[(\gamma-1)\{n_c\}\{n_c\}^T + [C_{SJ}]]$$

$$[C_{SJ}] = \begin{bmatrix} \frac{2}{3} & -\frac{1}{3} & -\frac{1}{3} & 0 & 0 & 0 \\ -\frac{1}{3} & \frac{2}{3} & -\frac{1}{3} & 0 & 0 & 0 \\ -\frac{1}{3} & -\frac{1}{3} & \frac{2}{3} & 0 & 0 & 0 \\ 0 & 0 & 0 & 2 & 0 & 0 \\ 0 & 0 & 0 & 0 & 2 & 0 \\ 0 & 0 & 0 & 0 & 0 & 2 \end{bmatrix}$$

$$G_1 = \frac{1}{d+1}[(t_{eq}+dt)^{d+1} - t_{eq}^{d+1}]$$

$$G_2 = \frac{1}{d+1}(t_{eq}+dt)^{d+1} - \frac{1}{(d+1)(d+2)dt}[(t_{eq}+dt)^{d+2} - t_{eq}^{d+2}]$$

$$G_3 = \frac{1}{d+1}(t_{eq}+dt)^{d+1} - \frac{2}{(d+1)(d+2)dt}(t_{eq}+dt)^{d+2} + \frac{2}{(d+1)(d+2)(d+3)(dt)^2}[(t_{eq}+dt)^{d+3} - t_{eq}^{d+3}]$$

a, d, γ : Creep constants (see Eq. (1))

da : Change of creep constant a with temperature change dT during time increment dt

t_{eq} : Equivalent time

In the case where a material obeys the time hardening rule
$$t_{eq} = t$$

In the case where a material obeys the strain hardening rule* or the power rule**
$$t_{eq} = [\varepsilon^c/(A\bar{\sigma}^\gamma)]^{\frac{1}{m}}$$

* $\{\dot{\varepsilon}^c\} = \sqrt{\frac{3}{2}}mA^{\frac{1}{m}}\bar{\sigma}^{\frac{\gamma}{m}}(\varepsilon^c)^{-\frac{1}{m}}\{n_c\}$ ($m=d+1$, $A=a/m$)

** $\{\dot{\varepsilon}^c\} = \sqrt{\frac{3}{2}}A\bar{\sigma}^\gamma\{n_c\}$ ($m=1$, $A=a$)

{w} : nodal displacements

suffix i, j, ... : nodal numbers

Introducing the co-ordinates of any point within the element into the displacement function [N], the displacements of the point can be expressed as functions of the nodal displacements by Eq.(2-46).

The total strains {ε} in the element are obtained as functions of the nodal displacements as a result of appropriate differentiation of Eq.(2-46) (that is, the differentiation of [N]) with respect to the co-ordinates,

$$\{\epsilon\} = [B]\{w\} \tag{2-47}$$

In the case of infinitesimal displacement problem, the above matrix [B] can be regarded as a constant matrix. Then, the above equation may be expressed in the form of increment as

$$\{d\epsilon\} = [B]\{dw\} \tag{2-48}$$

(2) Constitutive equation

When temperature of the element changes during an increment of time, dt, the constitutive equation may be generally expressed in the following form as shown in Eq.(2-45).

$$\{d\sigma\} = [D]\{d\epsilon\}-\{dC\} \tag{2-49}$$

(3) Stiffness equation (Incremental relation between nodal force and nodal displacement)

From the basic equations which have been already shown, the incremental relationship between nodal forces and nodal displacements, that is, stiffness equation will be derived by applying the principle of virtual displacement.

Here, the nodal forces {F} of an element are defined, which are statically in equilibrium with the stresses acting on the boundary of the element, etc..

$$\{F\} = \{F_i \ F_j \dots\}^T \tag{2-50}$$

Each of the forces $\{F_i\}$ must contain the same number of components as the corresponding nodal displacements $\{w_i\}$.

142

Imposing arbitrary virtual nodal displacements $\{w^*\}$ to the element, the external work δW_e done by the nodal forces $\{F\}$ during that displacement is

$$\delta W_e = \{w*\}^T \{F\} \qquad (2\text{-}51)$$

Similarly, the internal work δW_i per unit volume done by the stresses $\{\sigma\}$ is

$$\delta W_i = \{\epsilon*\}^T \{\sigma\} \qquad (2\text{-}52)$$

$\{\epsilon^*\}$ in the above equation are virtual strains due to virtual nodal displacements $\{w^*\}$, and they have the relation of Eq.(2-47). Thus, expressing the internal work δW_i with virtual nodal displacements $\{w^*\}$, Eq.(2-52) becomes

$$\delta W_i = \{w*\}^r [B]^T \{\sigma\} \qquad (2\text{-}53)$$

Equating the external work by Eq.(2-51) with the total internal work obtained by integrating Eq.(2-53) over the volume of the element, the following equation is obtained.

$$\{w*\}^T \{F\} = \{w*\}^T \int [B]^T \{\sigma\} \, d(\text{vol}) \qquad (2\text{-}54)$$

As this relation is valid for any value of the virtual displacements, the multipliers must be equal to each other. Therefore,

$$\{F\} = \int [B]^T \{\sigma\} \, d(\text{vol}) \qquad (2\text{-}55)$$

In the case where matrix $[B]$ can be regarded as constant matrix, the above equation may be expressed in the form of increment as

$$\{dF\} = \int [B]^T \{d\sigma\} \, d(\text{vol}) \qquad (2\text{-}56)$$

Substitution of Eqs.(2-49) and (2-48) into Eq.(2-56) provides stiffness equation for time increment dt, that is,

$$\{dF\} = [K] \{dw\} - \{dL\} \qquad (2\text{-}57)$$

where $[K] = \int [B]^T [D] [B] \, d(\text{vol})$: stiffness matrix of the element

$\{dL\} = \int [B]^T \{dC\} \, d(\text{vol})$: equivalent nodal force increment

Stiffness equation for the whole structure is obtained as the summation of stiffness equation, Eq.(2-57), for all elements at each node.

$$\Sigma \{dF\} = \Sigma [K] \{dw\} - \Sigma \{dL\} \qquad (2\text{-}58)$$

Once the above Eq.(2-58) is solved for nodal displacement increment $\{dw\}$,

satisfying the specified boundary conditions, total strain increment $\{d\varepsilon\}$ and stress increment $\{d\sigma\}$ of each element can be evaluated from Eqs.(2-48) and (2-49).

2.3 Results of Analysis and Discussion

By using the theories derived in the above, the authors have analyzed transient and residual stresses produced in various types of welded joints, especially multi-pass welded joints of thick plates, and the production mechanisms of such stresses, the relations with cold cracks, etc. have been investigated.

In this section, using the results of multi-pass welded joints, characteristics of residual stress distributions due to multi-pass welding and stress-relief annealing, influencing factors on them and their relations with cold cracks are discussed sythetically. A simple joint model under simple welding condition (SM 50 butt welded joint of 50mm thickness plane plate) is chosen as an example (first example) to describe the characteristics of distributions of residual stresses. In the theoretical analyses treated in this section, temperature or temperature-history dependence of mechanical properties of materials are considered, and as workhardening rule isotropic one is assumed (In the study shown in section 2.3.4, kinematic and combined workhardening rules are also applied to analysis and the effects of the type of workhardening rule adopted is discussed in Ref.20).

2.3.1 Multi-pass butt welded joint of thick plane plate (SM 50, plate thickness: 50mm) /12/

As shown in Fig.2-4, narrow gap butt welding was applied to SM 50 steel plate of 50mm thickness being accumulated 20-layers (20-passes). It was considered that the distribution pattern of residual stresses depends on the restraint condition of a joint, and two extreme restraint conditions were assumed (see Fig.
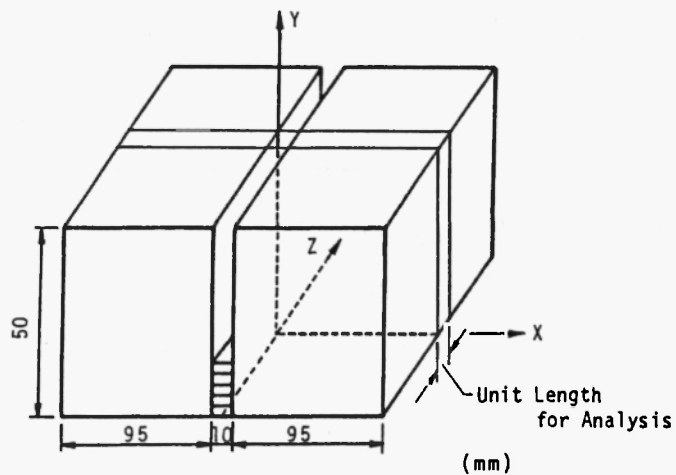
Fig.2-4   Specimen for analysis

2-5); a condition under which longitudinal bending deformation and angular distortion occur freely (restraint condition A) and one under which both deforma-

Fig.2-5   Restraint conditions of the specimen
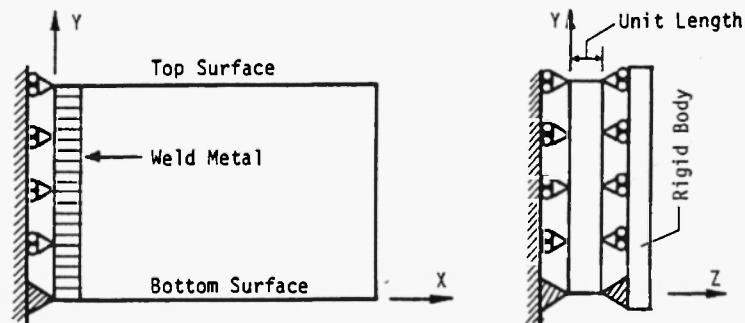
(a)   Restraint condition A
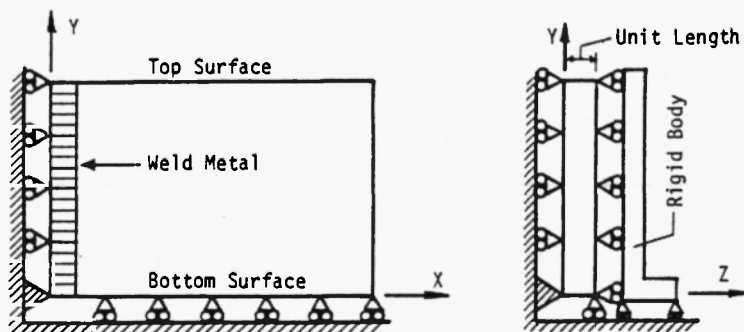
(b)   Restraint condition B

tions are restricted (restraint condition B). These restraint conditions are the two extreme ones in actual butt joints. If the model is sufficiently long and welding velocity is sufficiently fast, it might be rational to regard that the XY-plane of model is allowed to move, remaining as a plane. Making this as an assumption, three-dimensional stress state was realized in thermal elastic-plastic analysis. The mechanical properties of the material used in the analysis is shown in Fig.2-6.

Distributions of residual stresses in the middle cross section of the weld zone and on the top surface of the specimen are shown in Fig.2-7. σ_X indicates
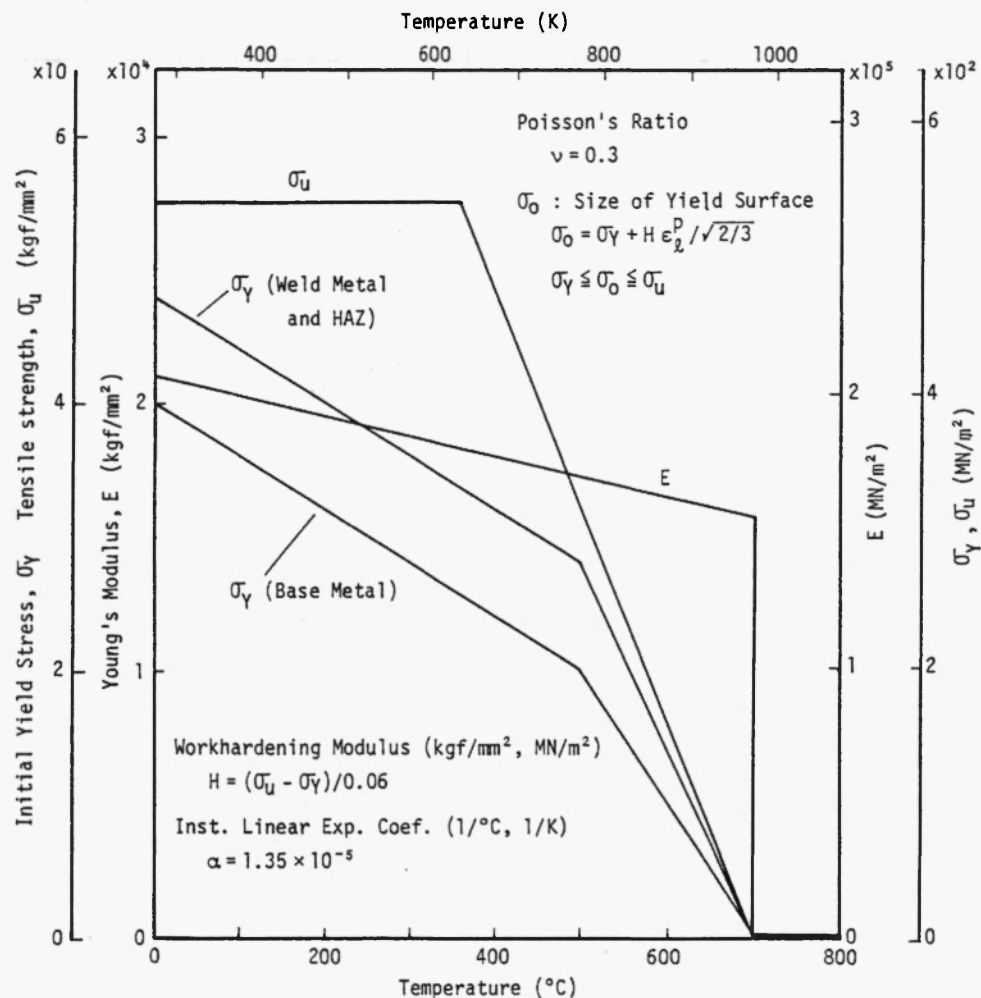
Fig.2-6   Mechanical properties used in thermal stress analysis

Fig.2-7   Calculated welding residual stresses
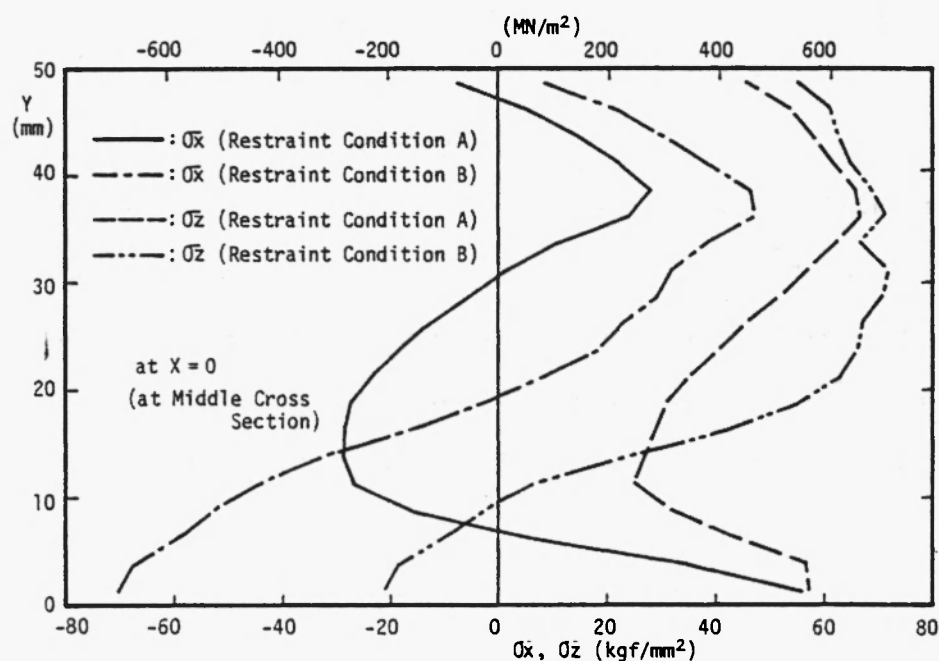
(a)   At the middle cross section
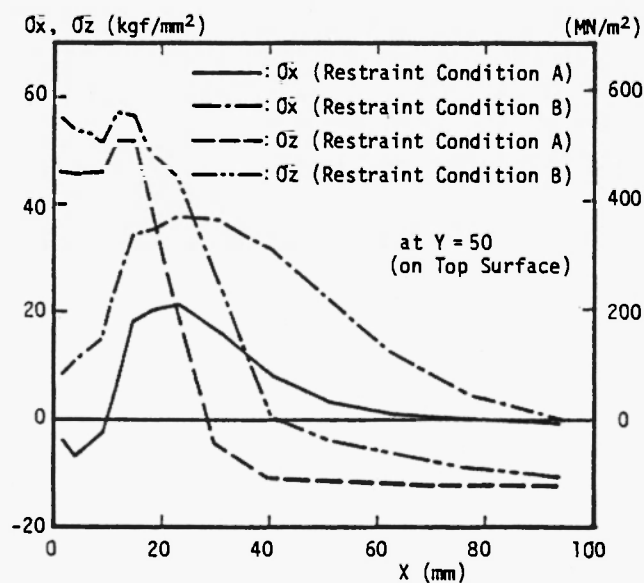
(b)   On the top surface

stresses in the plate width direction and σ_z those along the weld line.   In
case of restraint condition A in which longitudinal bending deformation and
angular distortion occur freely, residual stresses near the bottom surface of the

weld zone become largely tensile both along the weld line and in the plate width direction.   In case of restraint condition B in which the above-mentioned deformations are restrained, these stresses are converted to compressive ones. Accordingly, root crack may occur when the degree of restraint is small.

On the other hand, the effect of restraint condition on the distribution was relatively small for the top surface, i.e., in the vicinity of the finishing bead.   The reason is that as the plate thickness increases, the above-mentioned deformations are more restrained internally when the welding near the finishing bead is applied, because the weld metal already laid recovers its rigidity.   The distribution of residual stresses near the finishing bead may be characterized by that the maximum tensile stresses appear not on the finishing bead but several layers below (see Refs.10 and 4 for this reason).   This is remarkable in plate width direction.   Large tensile residual stresses in this vicinity may cause underbead crack, longitudinal crack and transverse crack.

2.3.2   Cylinder-head welded joint of a pressure vessel of very thick plate
        (2 1/4Cr-1Mo steel, plate thickness: 100, 150mm) /9,10,4/

Welding residual stresses produced in a cylinder-head joint (U-groove) of a pressure vessel (Fig.2-8(a)) made of very thick 2 1/4Cr-1Mo steel plate were estimated.   For analysis and experiment, double U-groove joint models (Fig. 2-8 (b)) of 200 and 300mm plate thickness which are twice as thick as the original were prepared, since it was considered that longitudinal bending deformation and angular distortion hardly occur due to the high degree of internal structural restraint for the actual joint.   Each pass of welding was applied to these models alternately on each side of the grooves.   In the experiment, submerged arc welding was applied.   The numbers of passes were 87 for Model M-200 of 200mm plate thickness and 167 for Model M-300 of 300mm plate thickness.   The plane (XY-plane in Fig.2-8(b)) stress state for unit weld length was assumed in the

Fig.2-8   Cylinder-head welded joint of a pressure vessel and its research model
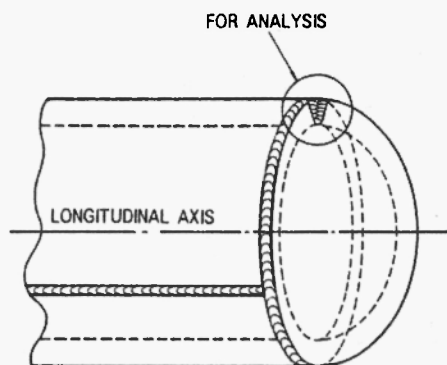
(a)   Cylinder-head welded joint
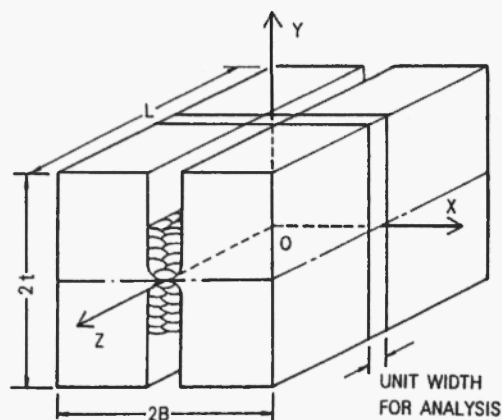
(b)   Idealized research model

analysis, but plane deformation may be appropriate. Particular attention was not given since this analysis was performed at the early stage of this kind of work. The result analyzed in plane stress state is approximate to one in plane deformation The relation between these results will be described in section 3.2.3. The mechanical properties used in the analysis are idealized as illustrated in Fig. 2-9, which change according to the thermal history of the material undergone.

Shown in Fig.2-10 are the transverse welding transient and residual stresses σ_x on the top surface and in the middle cross section of Model M-300 obtained by both theoretical analysis and experiment. ·If attention is paid to residual

Fig. 2-9   Mechanical properties used in thermal stress analysis

T_0: HIGHEST TEMP. UNDERGONE BEFORE
T_N: HIGHEST TEMP. DURING THE CURRENT THERMAL CYCLE

(a)   Case I   ($T_0 < 750°C$ & $T_N < 750°C$)

(b)   Case II   ($T_0 \geqq 750°C$ & $T_N < 750°C$)

(c)   Case III   ($T_0 < 750°C$ & $T_N \geqq 750°C$)

(d)   Case IV   ($T_n \geqq 750°C$ & $T_N \geqq 750°C$)
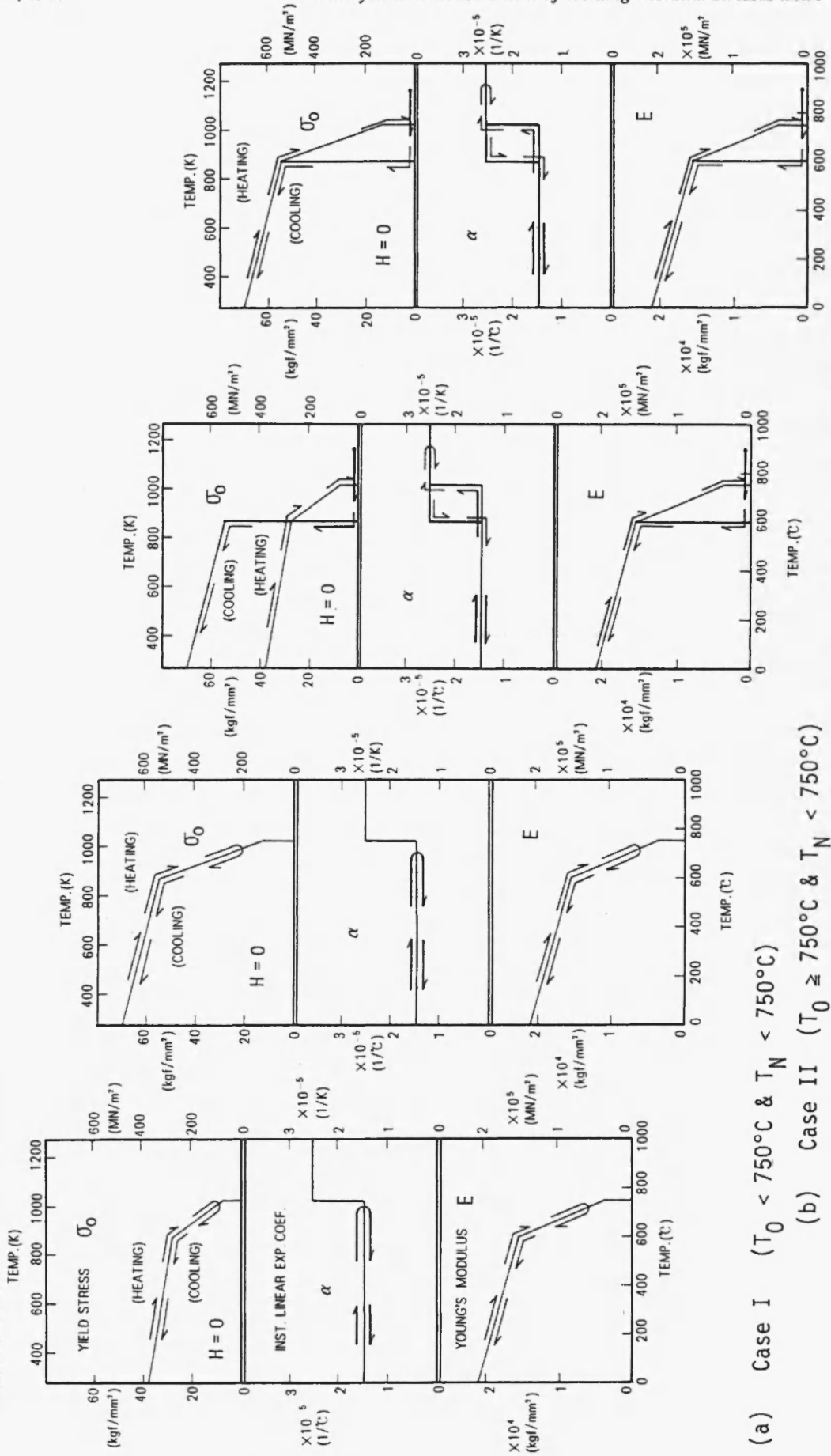
Fig.2-10   Transverse welding transient and residual stresses
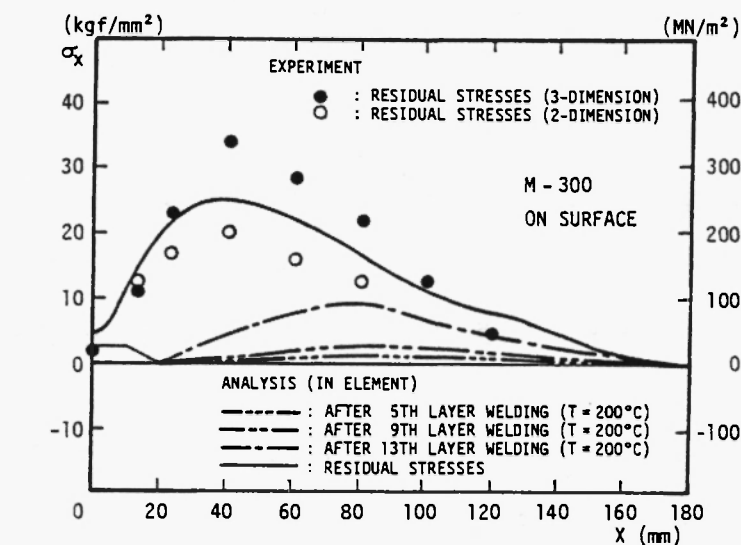
(a)   On the top surface
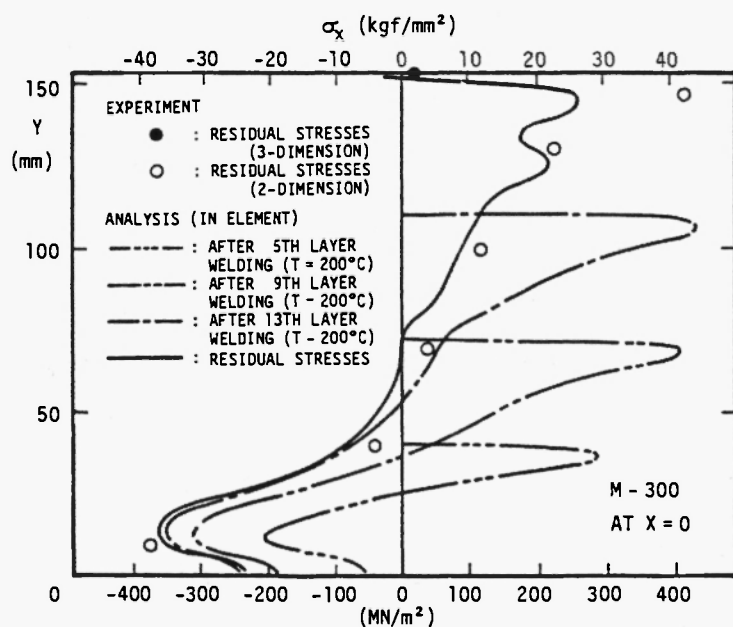
(b)   At the middle cross section

stresses, it is seen that their distributions are subjected to the effect of restraint. Like the case of a butt joint of a plane plate under restraint condition B of the previous example, compressive stresses remain in the middle of the plate thickness direction (corresponds to the inner surface of an actual

joint), the initially welded portion, and tensile stresses are produced near the top surface, of which maximum value appears just under the finishing bead. If embrittlement due to diffusive hydrogen accompanies, underbead crack may occur and expand to the surface.

Transient stresses produced when the groove is welded halfway and cooled to the interpass temperature (200°C) are also shown in Fig.2-10. The pattern of these distributions shows fundamentally the same characteristics as of the afore-mentioned residual stresses.

Next, residual stresses in M-200 and M-300 produced by welding and decreased by annealing were analyzed. The creep property of 2 1/4 Cr-1Mo steel was deter-mined by experiments. The results indicate that the material obeys strain-hardening law below 575°C and power hardening law above 575°C /4/. Figure 2-11 shows the results of residual stresses in M-200 after annealing by the theoreti-cal analyses and experiments. They are stresses in the x-direction, σ_x , on the top surface and in the middle cross-section for four specimens of M-200 which are provided with the same welding condition, but subjected to four different annealing conditions as shown in Table 2-1.

The magnitudes of the residual stresses on the top surface of the specimen

Table 2-1 Conditions of stress-relief annealing

Name of SR condition	Name of specimen	Heating and cooling rate (°C/hr.)	Heating temp. (°C)	Holding time (hr.)
SR - 1	MSR-200-1 MSR-300-1	30	600	0
SR - 2	MSR-200-2 MSR-300-2	30	650	0
SR - 3	MSR-200-3 MSR-300-3	100	650	0 *
SR - 4	MSR-200-4 MSR-300-4	30	650	4

* : To let the model reach the annealing temperature of 650°C, additional one hour is needed.

Fig.2-11 Transverse residual stresses after annealing

σ_x (MN/m²)

EXPERIMENT
(2-DIMENSION)
● : AS WELDED
○ : MSR-200-1 (600℃, 30℃/hr.)
⊙ : MSR-200-2 (650℃, 30℃/hr.)
◐ : MSR-200-3 (650℃, 100℃/hr.)
◑ : MSR-200-4 (350℃×4hr., 30℃/hr.)

Y (mm)

AT X=0

ANALYSIS
(IN ELEMENT)
—— : AS WELDED
—··— : MSR-200-1
—·— : MSR-200-2
——— : MSR-200-3
---- : MSR-200-4

Y (mm)

σ_x (kgf/mm²)

AT X=0

σ_x (kgf/mm²)

(MN/m²)

EXPERIMENT (3-DIMENSION)
● : AS WELDED
○ : MSR-200-1 (600℃, 30℃/hr.)
⊙ : MSR-200-2 (650℃, 30℃/hr.)
◐ : MSR-200-3 (650℃, 100℃/hr.)
◑ : MSR-200-4 (650℃×4hr., 30℃/hr.)

ON SURFACE

σ_x (kgf/mm²)

(MN/m²)

ANALYSIS (IN ELEMENT)
—— : AS WELDED
—··— : MSR-200-1
—·— : MSR-200-2
——— : MSR-200-3
---- : MSR-200-4

ON SURFACE

X (mm)

(a) On the top surface
(b) At the middle cross section

153

obtained by theoretical analysis indicate a tendency according to the conditions of the annealing as follows;

$$0(MSR-200-1) > 0(MSR-200-2) \cong 0(MSR-200-3) > 0(MSR-200-4)$$

The same tendency is also observed in the measured values. Concerning the absolute value of stress, the theoretical values are somewhat smaller than the experimental ones. This is attributed to the fact that the theoretical values are obtained by the analysis in the plane stress state, while the experimental values are measured in the three-dimensional stress state, similar to those due to welding.

In contrant with this, the calculated stresses on the cross section of the specimen are well correlated with the experimental ones (The measured values are the stresses remaining in the sliced plate perpendicular to weld line. The stress state is plane stress state and the relation of the residual stresses to original residual stresses in three-dimensional stress state will be discussed in section 3.2.3) under all annealing conditions.

Good coincidence of these results including the welding residual stresses confirms validity of the method adopted for this study.

2.3.3 Multi-pass corner welded joint of thick plane plate (SM 50, plate thickness: 40mm) /21-24/

In order to investigate and prevent lamellar tearing and root crack of a multi-pass corner joint from a dynamical view point, welding residual stresses produced in such a joint have been analyzed for different cases. CJC (Corner Joint weld Cracking) test model shown in Fig.2-12 was used for the analysis of a corner joint. Changing the external restraint, theoretical analyses were performed for the cases when bending restraint intensity is large (K_B = 10^6 kgf·mm/mm·rad) and when it is the least (K_B = 0). The same plane stress state as section 2.3.2 was assumed in the analysis. The mechanical properties are the same as shown in Fig.2-6.

Fig.2-12   Corner joint weld cracking test (CJC-test) apparatus
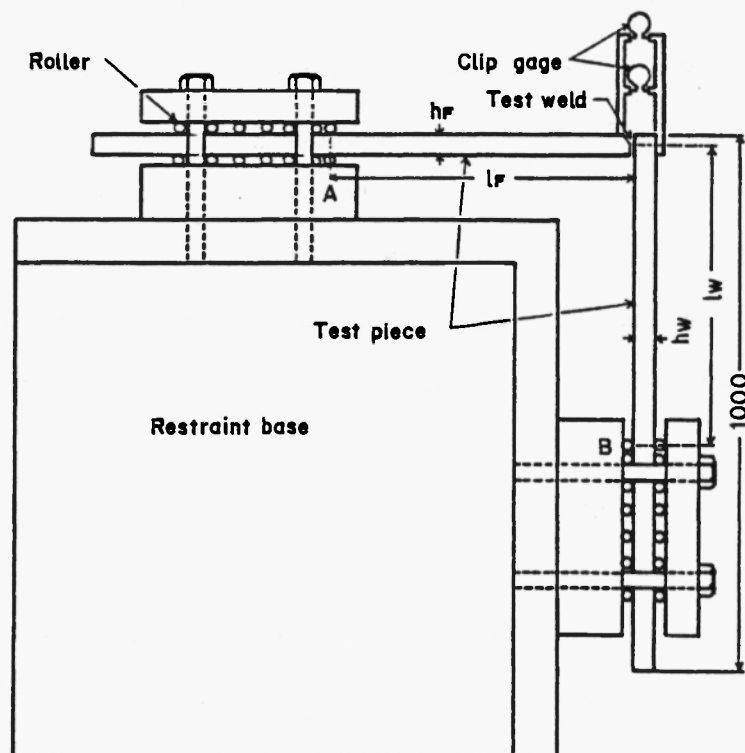
Fig.2-13   Transverse welding residual stresses
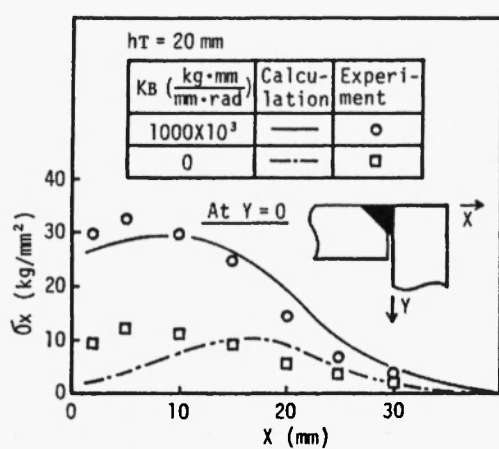
(a)   On the top surface (at Y=0)
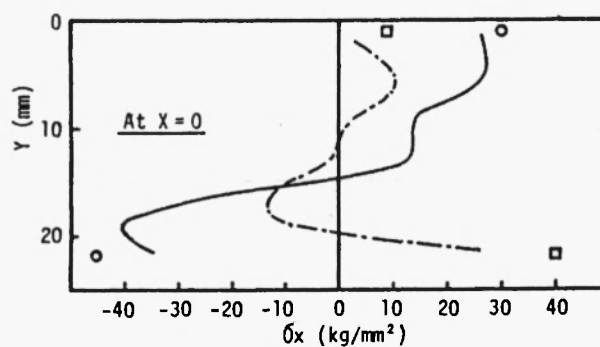
(b)   At the cross section (at X=0)

Shown in Fig.2-13 are the distributions of welding residual stresses σ_x (perpendicular to the weld line) in the section of the weld zone and on the top surface of the vertical plate. These distributions change in a similar manner to those in the butt joint of the first example according to the change of restraint to angular distortion (corresponds to bending restraint here). When bending restraint is large, tensile residual stresses on the top surface of the vertical plate become larger and may cause lamellar tearing. When bending restraint is small, large tensile stresses are produced at the root of the groove and may cause root crack.

With the purpose to prevent initiation of lamellar tearing by decreasing tensile stresses on the top surface of the vertical plate even when bending restraint is large, residual stresses were analyzed on four types of groove (Fig.2-14). Residual stress distributions near the top surface of the vertical plate are shown in Fig.2-15. Tensile residual stresses of types P and C are smaller than those of type M.

Fig.2-14   Shapes of Grooves
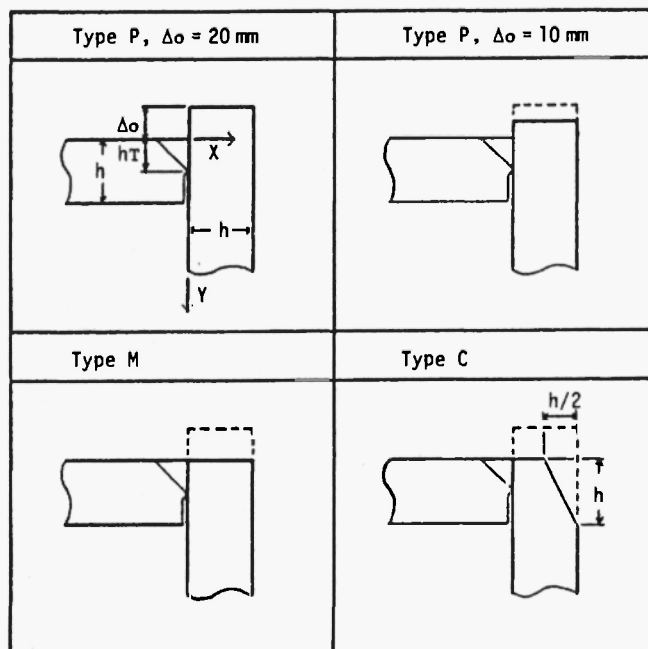
h = 40 mm, hT = 20 mm, Angle of vee : 45°
KB = 1000X10³ kg·mm/mm·rad (1 = 56 mm)

Fig.2-15　　Calculated transverse welding residual stresses on the top surface
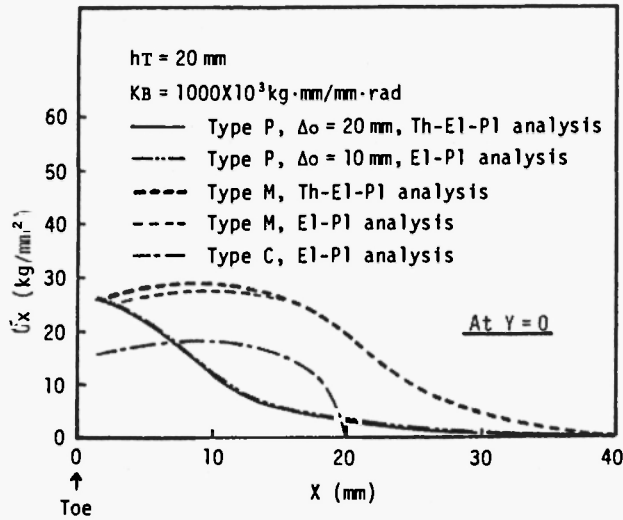
2.3.4 Multi-pass butt welded joint of thin and thick pipes (SUS 304, plate thickness: 5.5, 8.6 and 30.9mm) /25-27/

Residual stresses produced in SUS 304 steel pipes by circumferential multi-pass butt welding (V-groove) were theoretically analyzed. Sizes of the used pipes are 2B pipe (5.5mm thickness), 4B pipe (8.6mm) and 24B pipe (30.9mm), and the sequence of welding is shown in Fig.2-16. TIG welding method was applied to the initial passes and SMAW to the sequent passes. From the third layer, the heat-sink welding by which the inner surface of a weld zone is cooled by strong water-spraying during welding was applied in addition to the conventional welding by which a joint is naturally cooled. This heat-sink welding aims to produce compressive residual stresses on the inner surface of the weld zone in order to prevent stress corrosion cracking. 4B pipe was also used to investigate how the influence differs when heat input is increased and the number of passes is decreased. As the specimen is axisymmetrical, it was assumed for the analysis that the welding was applied axisymmetrically. That is, the deposited metal of each pass was assumed to be laid instantaneously and simultaneously for the whole circumference. Thus, the analysis becomes an axisymmetrical problem. Conse-

Fig.2-16   Dimensions and build-up sequences of pipes used in analysis
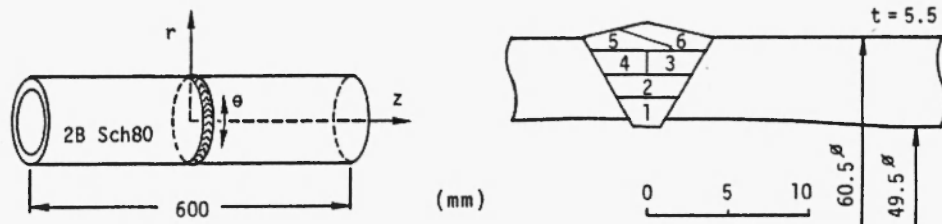
(a)   2-inch diameter pipe
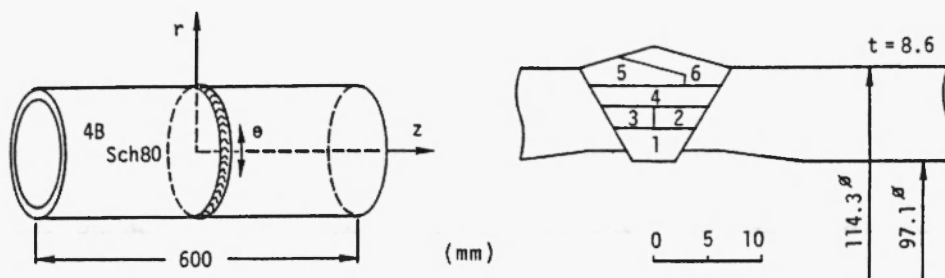
(b)   4-inch diameter pipe
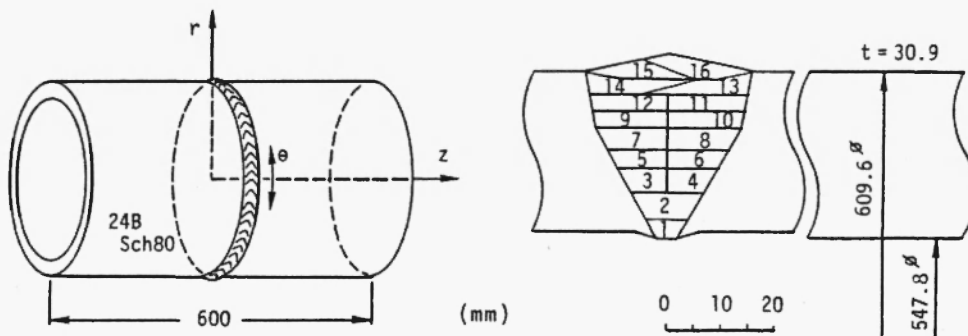
(c)   24-inch diameter pipe

quently, the welding thermal stress in the three-dimensional stress state could be obtained. Figure 2-17 is the mechanical properties of the material used in analysis. Analyzed residual stress distributions are shown in Figs.2-18 (heat input is increased to Q-14, Q-23, Q-45) and 2-19.

Since butt welded joints of pipes are axisymmetric, longitudinal bending

Fig.2-17   Mechanical properties used in thermal stress analysis
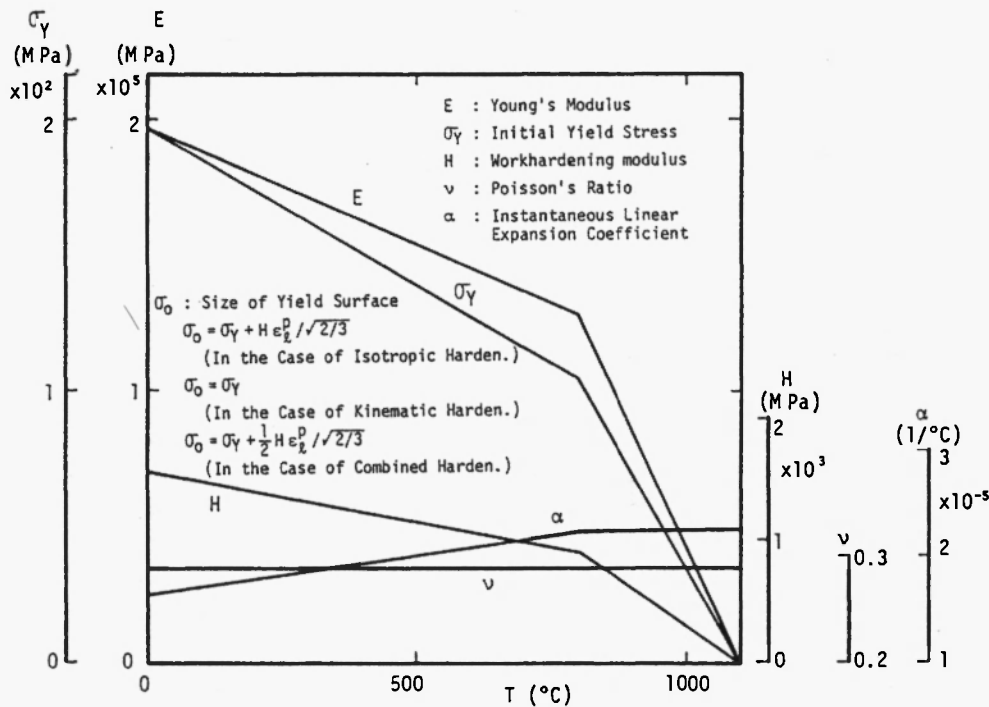
deformation due to welding is internally restrained, while angular distortion occurs to some degree. In case of 24B pipe (30.9mm thickness), stress distributions are similar to one produced under this restraint condition. That is, the distributions are between those produced under the two extreme restraint conditions of the butt joint of the first example.

If the heat-sink welding is used, the inner surface or the initially welded side is compulsorily cooled, so that a great temperature difference occurs in the plate thickness direction like the case of thick plates. Therefore, even in case of thin plates such as 2B pipe (5.5mm) and 4B pipe (8.6mm), residual stresses distribute similarly to those in the restraint condition B of the butt joint of thick plates of the first example, and compressive stresses remain on the inner surface of the weld zone. These compressive stresses prevent stress corrosion cracking.

Lastly, Fig.2-20 shows the effect of workhardening rule adopted in the
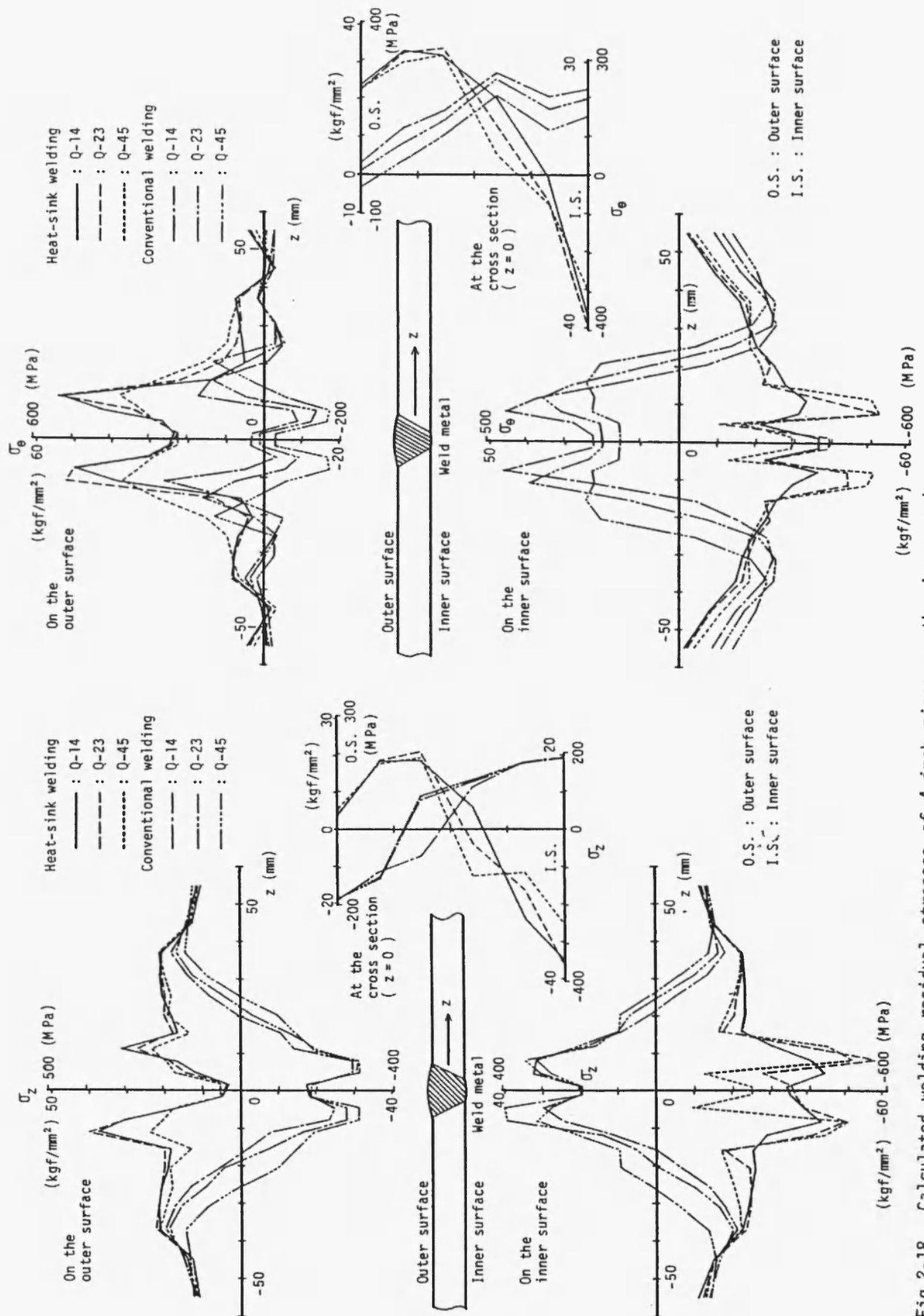
Fig.2-18　Calculated welding residual stresses of 4-inch pipes on the inner and outer surfaces and at the middle cross section
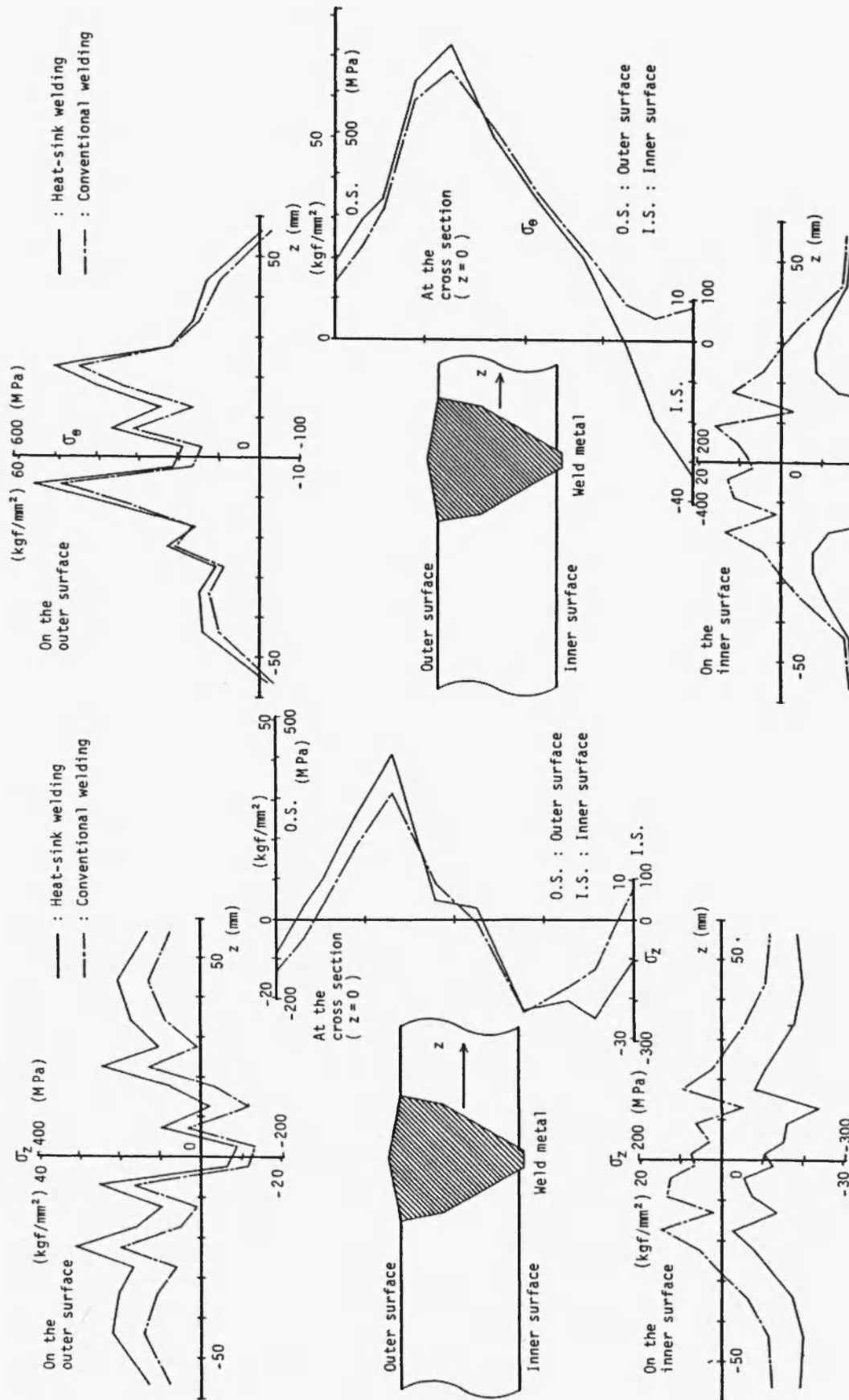
(a)　Axial stresses

Fig.2-19   Calculated welding residual stresses of 24-inch pipes on the inner and
outer surfaces and at the middle cross section

(a)   Axial stresses
(b)   .Circumferential stresses
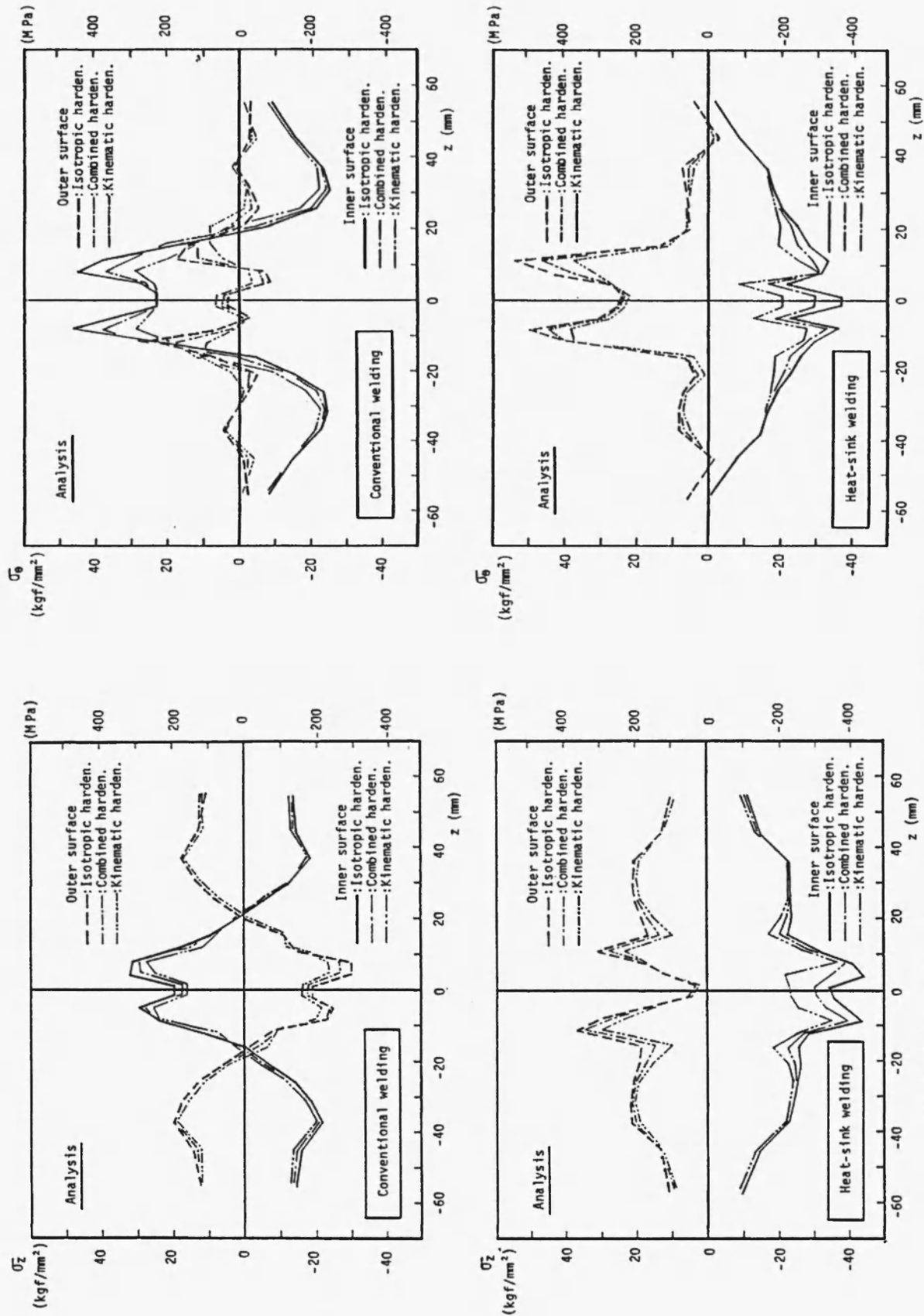
Fig. 2-20   Welding residual stresses of 4-inch pipe calculated adopting various workhardening rules

(a)   Axial stresses

(b)   Circumferential stresses

/20/
analysis on residual stresses obtained for 4B pipe. The absolute value of residual stresses analyzed using the isotropic workhardening rule and larger than the ones using the kinematic rule. This tendency is generally recognized in residual stresses of a specimen or a part of structure after cyclic loading between tension and compression.

3. Measurement of Three-Dimensional Residual Stresses Based on Theory of Inherent Strain

3.1 Introduction

In addition to the theoretical analysis, it is also very important to accumulate more accurate information about residual stresses in welded joints by measuring to clarify the mechanical aspect of weld cracking and to evaluate the strength of welded joints.

For this purpose, several measuring methods have been already proposed to estimate residual stresses, for example, Sachs' /6/, Mathar's /28/ and Rosenthal's /7/, the ring core and the hole drilling methods.

Any of these methods belongs to the same category as sectioning methods (Fig.3-1). By cutting a part of the object, a new surface is exposed and the forces acting on the surface before cutting are released. These forces are estimated from the changes of strains observed[*] on the surface. Therefore, the elastic response relation between changes of strains observed on the body surface

---

[*] In this paper, to observe implies to take a value of strain by some instrument and to measure is meant to obtain residual stresses by appropriate calculation using observed strains.

Fig.3-1   Released surface-force and its discretizaiton
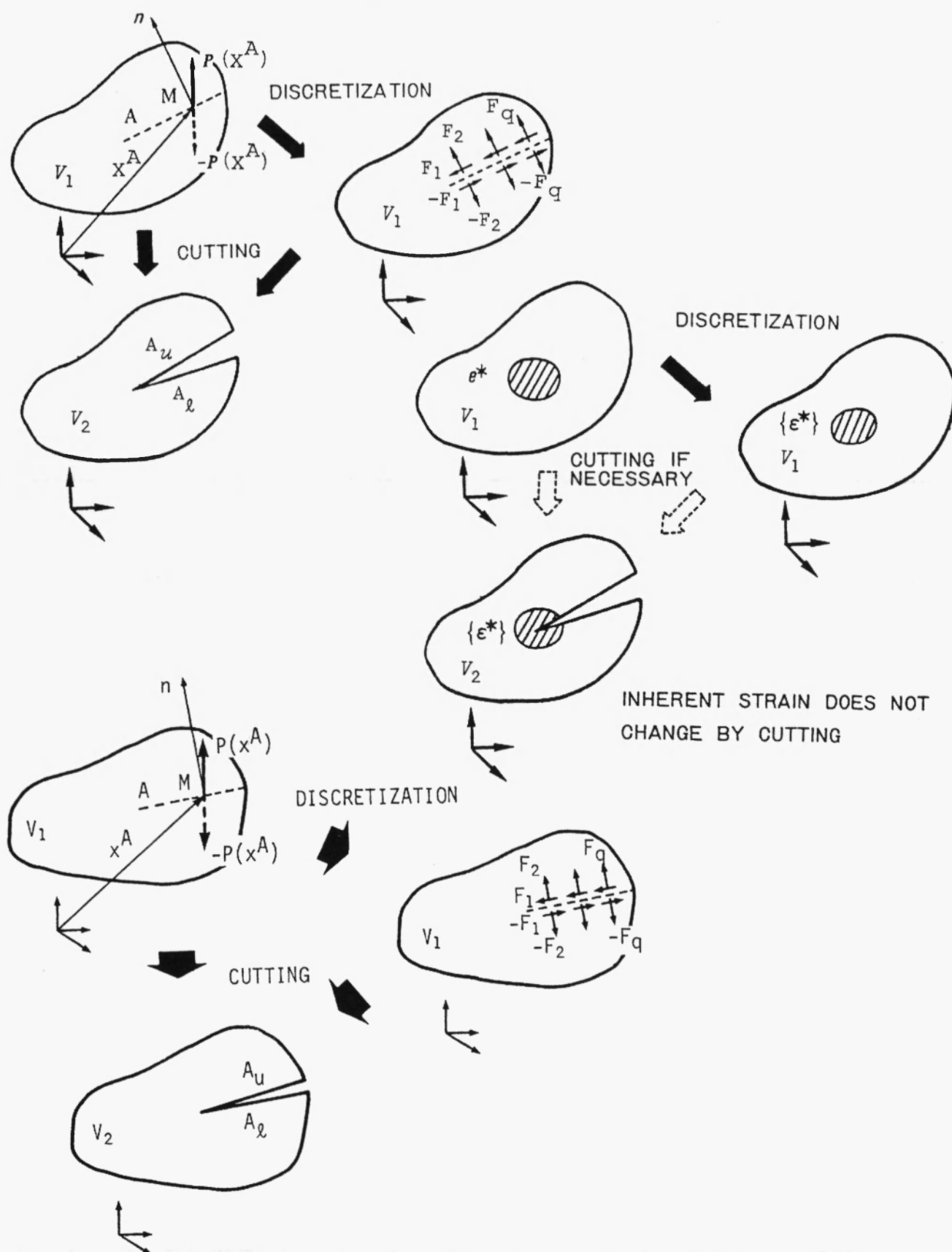
and released section forces by sectioning is necessary in advance. If this procedure is repeated until no more change of strains in a portion is observed, the residual stresses contained in the portion can be estimated as such stresses as produced by the total released section forces.

According to these existing methods which employ section forces as parameters, released strains are observed on the surface of the body and three-dimensional stresses are estimated indirectly with the aid of the elastic response relation. In this process, observation errors may influence greatly the result since the elastic response relation may magnify the error when the relation is used for two remote points. As long as this principle is based on, improvement of the elastic response relation is very difficult. So, it is necessary to discover a new measuring principle by which the elastic response relation can be easily improved.

In order to solve the above-mentioned fundamental problems, the authors have proposed for the first time a new approach in which sources of generation of residual stresses (inherent strains) are dealt as parameters of measurement (Fig. 3-1(b))/8/. According to this new measuring approach, it is clarified that improvement of the elastic response relation would be easy.

So, in this chapter, a general basic measuring theory of residual stresses is described using inherent strains as parameters. Secondly, the finite element method is introduced to obtain the general elastic response relation which can be applied to measure residual stresses in an arbitrary shaped body and the statistic theory is used to investigate reliability of estimated values of residual stresses. Thirdly, one of new measuring methods of three-dimensional residual stresses produced in a long welded joint /29,31/ will be introduced. The method was developed based on the new measuring approach, which was reduced to a simple method by taking advantage of the characteristics of the distribution of its inherent strains produced in this type of long welded joint. In these theories

described in this chapter, new and different notations from those in chapter 2, may be used since these notations are the same as those appearing in the related references to this chapter.

Lastly, applying this new method, the distributions of three-dimensional residual stresses in several multi-pass welded joints are measured These stresses are compared with stresses on the surfaces of the joints which are directly observed in order to demonstrate reliability and applicability of the new measuring method.

3.2 Measuring Method of Residual Stresses Using Inherent Strains as Parameters

3.2.1 Basic theory /8/

When residual stresses exist in the self-balanced object, these should be produced by plastic strains, thermal shrinkage strains in the weld metal, etc. which are generally called inherent strains.

Elastic strains (ϵ_{ij}) at an arbitrary point of the body are generally given by such a function that

$$\epsilon_{ij}(x) = R_{ij}^*(x; e^*, V) \tag{3-1}$$

where x : vector of position at an interior point of the object

   e^*: vector of inherent strains

   V : vector to express the body shape.

This equation expresses the relation of inherent strains to the consequent residual strains. The new measuring method is utilizing elastic response (change of strains) at arbitrary points, which is induced by changes of the shape of the body.

Inherent strain distribution is replaced by a finite series (or approximated by discretization) with q number of parameters $\{\epsilon^*\} = \{\epsilon_1^*, \epsilon_2^*, \cdots, \epsilon_q^*\}^T$.

$$e^*(x) = f^*(x; \epsilon_1^*, \epsilon_2^*, \cdots, \epsilon_q^*) \tag{3-2}$$

Substituting Eq.(3-2) into Eq.(3-1), it is seen that elastic strains are expressed by a function, h^*_{ij} , of the co-ordinates x , the parameters $\{\varepsilon^*\}$, the shape of the object, V. That is,

$$\epsilon_{ij}(x) = h^*_{ij}(x; \epsilon^*_1, \epsilon^*_2, \cdots, \epsilon^*_q, V) \tag{3-3}$$

When the relaxed strains of q number ($_m\varepsilon$) at positions where observation is possible are obtained, the simultaneous equations to decide the parameters $\{\varepsilon^*\}$ of the inherent strain distribution are constituted as follows;

$$_m\varepsilon_{IJ}(x_1) = h^*_{IJ}(x_1 ; \varepsilon^*_1, \varepsilon^*_2, \cdots\cdots, \varepsilon^*_q, V)$$

$$_m\varepsilon_{IJ}(x_2) = h^*_{IJ}(x_2 ; \varepsilon^*_1, \varepsilon^*_2, \cdots\cdots, \varepsilon^*_q, V)$$

$$- \tag{3-4}$$

$$_m\varepsilon_{IJ}(x_q) = h^*_{IJ}(x_q ; \varepsilon^*_1, \varepsilon^*_2, \cdots\cdots, \varepsilon^{\pm}_q, V)$$

The combination of (I,J) in above equations represents the particular component of strains at each observing point. If Eqs.(3-4) are composed of independent equations and the inverse function g^*_i of h^*_{ij} can be defined, the parameters $\{\varepsilon^*\}$ of the inherent strain distribution are determined as,

$$\varepsilon^*_i = g^*_i (_m\epsilon_{IJ}(x_1), {}_m\epsilon_{IJ}(x_2), \cdots, {}_m\epsilon_{IJ}(x_q); V) \qquad (i = 1 \sim q) \tag{3-5}$$

So, strains or stresses at arbitrary points are estimated by substituting Eq.(3-5) into Eq.(3-3).

There are two requirements in the process of the general formulation of the method. One is that continuous function e^* (Eq.(3-2)) must be replaced by a finite series (or approximated by discretization) to any desired degree of accuracy, which contain parameters $\{\varepsilon^*\}$. And the other is that response functions h^*_{ij} must be formulated based on Eq.(3-1). These functions depend on the shape of a body. Thus, it is impossible to find general analytical solutions except for special cases. Therefore, it is necessary to apply methods of numerical analysis such as the finite difference method, the finite element method, etc., to satisfy all of the preceding conditions. These numerical analyses are based on discretization of unknown functions and it is very convenient to use the

correspondency between the discretization and the finite number of measurement.

In this paper, the finite element method which is capable to satisfy the geometric shape is adopted and the general formulation will be shown in the following section.

3.2.2 Measuring theory based on F.E.M. /8/

(1) Basic equations (Observation equation)

When the finite element method is applied, the object is fictitiously divided into finite number of elements. When a finite element is subjected to initial strain (inherent strain) $\{\varepsilon^*\}^c$, the stiffness equation of the element can be expressed in the following from,

$$\{f_u\}^e = [K]^e\{u\}^e + \{f\}^e \tag{3-6}$$

where $\{f_u\}^e$: nodal forces of an element

$[K]^e$: stiffness matrix of an element

$\{u\}^e$: nodal displacements of an element

$\{f\}^e$: equivalent model forces of an element due to initial strain $\{\varepsilon^*\}^e$.

The parameters $\{\varepsilon^*\}$ of the inherent strains mentioned in section 3.2.1 correspond to components of inherent strains imposed in finite elements. The inherent strains $\{\varepsilon^*\}^c$ imposed in an element produce restraining nodal forces to keep it undeformed, which are usually called as equivalent nodal forces $\{f\}^e$. This relation is shown to be,

$$\{f\}^e = -\int_v [B]^{eT}[D]^e\{\varepsilon^*\}^e \, d(vol) = -[L]^e\{\varepsilon^*\}^e \tag{3-7}$$

where $[B]^e$: strain-displacement matrix of an element

$[D]^e$: elastic stress-strain matrix of an element

By collecting these forces and stiffness matrix of each element all over the object,

$$\{f\} = \Sigma\{f\}^e = -\Sigma[L]^e\{\varepsilon^*\}^e = -[L]\{\varepsilon^*\} \tag{3-8}$$

168

$$[K] = \Sigma [K]^e \qquad (3\text{-}9)$$

The nodal displacement $\{u\}$ is expressed in the following form,

$$\{O\} = [K]\{u\} + \{f\} \qquad (3\text{-}10)$$

$$\{u\} = -[K]^{-1}\{f\} = -[C]\{f\} = [C][L]\{\epsilon^*\} \qquad (3\text{-}11)$$

The relation between displacement and strain is given by Eq.(3-12) because the total strain of an element is the summation of elastic strains $\{\epsilon\}^e$ and inherent strains $\{\epsilon^*\}^e$.

$$\{\epsilon\}^e + \{\epsilon^*\}^e = [B]^e \{u\}^e = [B]^e[T]^e\{u\} = [B]^e[T]^e[C][L]\{\epsilon^*\} \qquad (3\text{-}12)$$

where $[T]^e$: transformation matrix of displacement, that is, $\{u\}^e = [T]^e\{u\}$

Matrix $[U]^e$ is defined as one to transform the inherent strains $\{\epsilon^*\}$ over the object into those $\{\epsilon^*\}^e$ of an element. Thus,

$$\{\epsilon^*\}^e = [U]^e\{\epsilon^*\} \qquad (3\text{-}13)$$

Therefore, Eq.(3-12) is transformed into the form,

$$\{\epsilon\}^e = [B]^e[T]^e[C][L]\{\epsilon^*\} - [U]^e\{\epsilon^*\}$$
$$= ([B]^e[T]^e[C][L] - [U]^e)\{\epsilon^*\} = [H^*]^e\{\epsilon^*\} \qquad (3\text{-}14)$$

And stresses in an element are evaluated as

$$\{\sigma\}^e = [D]^e\{\epsilon\}^e = [D]^e[H^*]^e\{\epsilon^*\}^e \qquad (3\text{-}15)$$

The elastic strains $\{\epsilon\}^e_A$, $\{\epsilon\}^e_B$, $\cdots$, the stresses $\{\sigma\}^e_A$, $\{\sigma\}^e_B$, $\cdots$ of elements A, B, ..., respectively are summarized over the object in the following forms,

$$\{\epsilon\} = \{\ \{\epsilon\}^e_A, \{\epsilon\}^e_B, \cdots \}^T = [H^{*\prime}]\{\epsilon^*\} \qquad (3\text{-}16)$$

$$\{\sigma\} = \{\{\sigma\}^e_A, \{\sigma\}^e_B, \cdots \}^T = [M']\{\epsilon^*\} \qquad (3\text{-}17)$$

Generally speaking, when the total number, q, of inherent strain components is equal to the total number, n, of the elastic strain components, the sizes of matrices $[H^{*\prime}]$, and $[M']$ are $(n \times n)$.

If special attention is paid to welding residual stresses, the portion where the inherent strains exist is limited in the vicinity of welded lines because the inherent strains are originated by thermal shrinkage of weld metal

and plastic deformation. Therefore, it is not difficult to presume such elements that apparently contain no inherent strains. Representing the inherent strain vector by the same notation, $\{\varepsilon^*\}$, which consist of only non-zero inherent strain components $q(<n)$, the above-mentioned matrices become matrices $[\overline{H^*}]$ and $[M]$ and their sizes are reduced to $(n \times q)$.

$$\{\epsilon_i\} = [H^*_{ij}] \{\epsilon^*_j\} \qquad (i = 1 \sim n, j = 1 \sim q) \qquad (3\text{-}18)$$

$$\{\sigma_i\} = [M_{ij}] \{\epsilon^*_j\} \qquad (i = 1 \sim n, j = 1 \sim q) \qquad (3\text{-}19)$$

For example, if m number of measurements of elastic strains can be done, the matrix $[\overline{H^*}] = (n \times q)$ is reduced to $[H^*] = (m \times q)$ and the observation equations are constituted as,

$$\{_m\epsilon_i\} = [H^*_{ij}] \{\epsilon^*_j\} \qquad (i = 1 \sim m, j = 1 \sim q) \qquad (3\text{-}20)$$

If the unknown inherent strains, $\{\varepsilon^*\}$, can be decided by these measured strains, $\{_m\varepsilon_i\}$, the residual strain and stress distributions can be calculated over the entire object.

The necessary condition to determined the parameters $\{\varepsilon^*\}$ by which residual stress distribution is estimated is to satisfy the inequality $m \geq q$. For example, if $m=q$, and $[H^*]^{-1}$ exist, the resulting stress distribution can be obtained uniquely. In contrast with this, if the number of equations included in Eq.(3-20) is not sufficient, that is $m < q$, the inherent strains $\{\varepsilon^*\}$, can not be determined. In this case, it is required to increase such relations as those in Eq.(3-20). These relations can be obtained simply by adding measuring points, if not, by producing a new self-balanced state by sectioning.

(2) Most probable value and its confidence interval

In case of $m > q$ in the observation equations, the number of equations is greater than the number of unknown parameters and consequently there should be (m-q) number of dependent equations. But these dependent equations do not exist apparently because errors contained in measured values change the dependency. So, for such cases where $m > q$ and errors are contained in the measured values,

the theory of statistics is introduced into the above-mentioned methods in order to decide the most probable values and these confidence intervals with the observation equations.

Here, the errors used are accidental ones and satisfy the three axioms of errors, and the process of evaluation of the most probable values and these confidence intervals are discussed.

(i) Most probable value

The relation between the true value $\{\varepsilon\}$ of the elastic strain and the true value $\{\varepsilon^*\}$ of the inherent strain is expressed by Eqs.(3-20), that is,

$$\{\varepsilon_i\} = [H^*_{ij}]\{\varepsilon^*_j\} \qquad (i=1\sim m, j=1\sim q) \tag{3-21}$$

Substituting measured values of strains, $\{_m\varepsilon\}$, into Eqs.(3-21) in place of $\{\varepsilon\}$, the errors $\{X\}$ are obtained in the following form.

$$\{_m\varepsilon\} - [H^*]\{\varepsilon^*\} = \{X\} \tag{3-22}$$

Furthermore, replacing $\{\varepsilon^*\}$ by the most probable value $\{\hat{\varepsilon}^*\}$ in Eq.(3-22), residuals $\{v\}$ are given as,

$$\{_m\varepsilon\} - [H^*]\{\hat{\varepsilon}^*\} = \{v\} \tag{3-23}$$

In the case where each measured value of strains is of the same precision, the sum of squares of the residuals, S, is

$$S = \{v\}^T\{v\} \tag{3-24}$$

According to the method of least squares, the most probable values $\{\hat{\varepsilon}^*\}$ are decided so as to minimize the sum of squares of the residuals, S. Thus, from the condition $\partial S/\partial\{\hat{\varepsilon}^*\} = 0$,

$$[H^*]^T\{_m\varepsilon\} = [H^*]^T[H^*]\{\hat{\varepsilon}^*\} \tag{3-25}$$

The above equation which was normalized is called normal equations and $[H^*]^T[H^*]$ is a square matrix of a size $(q \times q)$. So, if the square matrix is regular, its inverse matrix can be obtained and the most probable values are given as follows,

$$\{\hat{\varepsilon}^*\} = ([H^*]^T[H^*])^{-1}[H^*]^T\{_m\varepsilon\} \equiv [G^*]\{_m\varepsilon\} \tag{3-26}$$

By using this result and Eq.(3-19), the residual stress distribution over the

171

object is estimated.

$$\{\hat{\sigma}\} = [M] \{\hat{\epsilon}*\} = [M][G*] \{_m\epsilon\} \equiv [N] \{_m\epsilon\} \tag{3-27}$$

(ii) Confidence interval

(a)   Accuracy of most probable value

The relation among measurement variance s^2 of unit weight, inherent strain variances $\{s*^2\}$ and these weights $\{p*\}$ is represented as follows.

$$p*_i s*_i^2 = s^2 \qquad (i = 1 \sim q) \tag{3-28}$$

The unbiased estimate $\hat{s}^2$ of the measurement variance is given as,

$$\hat{s}^2 = \{v\}^T \{v\} / (m-q) = S / (m-q) \tag{3-29}$$

And with components $g*_{ij}$ of the matrix $[G*]$, the weights of Eq.(3-28) can be evaluated.

$$p*_i = 1 / \sum_{j=1}^{m} g*_{ij}^2 \qquad (i = 1 \sim q) \tag{3-30}$$

By substituting Eqs.(3-29) and (3-30) into Eq.(3-28), the unbiased estimate of population variance of the most probable value $\{\hat{\epsilon}*\}$ can be determined.

Otherwise, the unbiased variance $\hat{s}_{\sigma i}^2$ of the most probable value $\{\hat{\sigma}\}$ of residual stresses is expressed in the following equation if the components of the matrix $[N]$ are n_{ij}.

$$\hat{s}_{\sigma i}^2 = (\sum_{j=1}^{m} n_{ij}^2) \cdot \hat{s}^2 \qquad (i = 1 \sim n) \tag{3-31}$$

(b)   Confidence interval

Stochastic variable $(\hat{\epsilon}*_i - \epsilon*_i)/s*_i$ which is dimensionlessly normalized $\{\epsilon*\}$ of the inherent strains obeys the standard normal distribution N(0,1). A variable S/s^2 obeys χ^2-distribution with degree of freedom $\phi = m-q$. So, a variable t in the following expression depends upon Student's t-distribution with ϕ degree of freedom.

$$t = (\hat{\epsilon}*_i - \epsilon*_i) / s*_i / \sqrt{S / s^2 / \phi} = (\hat{\epsilon}*_i - \epsilon*_i) / \hat{s}*_i \tag{3-32}$$

So, the relation between confidence coefficient $(1-\alpha)$ and t-value is represented as follows.

$$1 - \alpha = 2 \int_{0}^{t} \frac{\Gamma\{(\phi + 1)/2\}}{\sqrt{\phi\pi}\ \Gamma(\phi/2)} (1 + \frac{x^2}{\phi})^{-\frac{\phi + 1}{2}} dx$$

(3-33)

where Γ : gamma function

If the confidence coefficient is given, t-value is decided by Eq.(3-33) and the confidence intervals are obtained in the following forms.

$$\left.\begin{array}{l} \hat{\epsilon}^{*}_{i} - t\hat{s}^{*}_{i} \leqq \epsilon^{*}_{i} \leqq \hat{\epsilon}^{*}_{i} + t\hat{s}^{*}_{i} \\ \hat{\sigma}_{i} - t\hat{s}_{\sigma i} \leqq \sigma_{i} \leqq \hat{\sigma}_{i} + t\hat{s}_{\sigma i} \end{array}\right\} \text{(confidence coef. } 1 - \alpha)$$

(3-34)

These intervals do not contain errors in the process of the discretization, which are inevitable in the finite element method but contain round-off errors in the calculation.

3.2.3 Measuring method for three-dimensional residual stresses in long

       multi-pass welded joint, L_z method /29,31/

The authors have developed several new measuring methods from the basic theory presented in section 3.2.2 for each individual problem. One of them is named "L_z method", and will be shown here.

When the general measuring theory is applied to measure three-dimensional residual stresses in the middle of the weld line of a multi-pass welded joint as shown in Fig.3-2, the theory can be simplified by taking advantage of the characteristics of the distribution of inherent strains induced in the welded joint.

In general, inherent strains in a welded joint are produced by the result of thermal elastic-plastic behavior due to non-steady temperature distribution and restraint for the welded joint. In such a case as this specimen, restraining conditions and temperature distributions of the welded joint are nearly uniform and quasi-steady states except in the vicinities of both ends of the weld line. Then, when the weld line is very long, the inherent strain distribution can be considered to be uniform along the weld line except in the vicinities of both ends. And it is well known that welding residual stresses are almost symmetric

173

with respect to a cross section at the middle. This implies that the components γ_{xy}^* and γ_{zx}^* of the inherent strains which produce non-symmetric residual stress with respect to that cross section can be ignored.

Here, the following assumptions may be introduced for the measurement of the three-dimensional welding residual stresses.

1)   Strains in the specimen change elastically due to cutting.

2)   The remaining stresses in sliced thin plates are in the state of plane stress (to be sliced thin enough).

3)   Each component of inherent strains do not change along the weld line (x-axis) and the components ε_x^* , ε_y^* , ε_z^* , γ_{yz}^* are functions of y and z co-ordinates.

The assumption 3) is only for simplification of the measuring theory based on the characteristics of the inherent strain distribution in a long welded joint and not indispensable to the measuring theory.

(1)   Separation of components of three-dimensional inherent strains

As the cutting lines are shown in Fig.3-2, Specimen T and Specimens $L_1 \sim L_m$ are taken out of the original welded joint which is named as Specimen R. The same magnitude of inherent strains as exist in Specimen R remain in Specimens T and L because the inherent strains do not change without production of plastic strains by these slicings. These plates are sliced so thin that the inherent strains in the normal direction to the surfaces of these plates do not contribute to the remaining stress distribution of the plates. Then, the remaining stresses in Specimen T are produced only by the inherent strains (ε_y^*, ε_z^* , γ_{yz}^*) in the cross section and the remaining stresses in Specimens L only by the longitudinal inherent strain (ε_x^*) (ε_y^* does not contribute to these stresses in Specimen L_i because it is constant along x-axis).

As a result, three-dimensional inherent strains can be divided into the

Fig.3-2   Experimental   model   and   procedure   of   slicing   Specimens   T   and L_i (L_z Method)
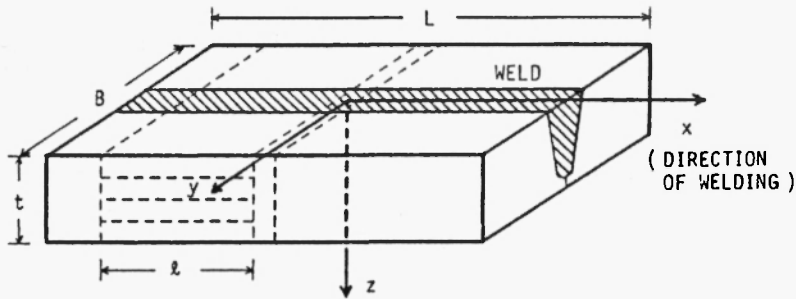
(a)   Experimental model of multi-pass welded joint (Specimen R)
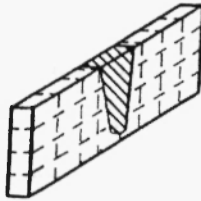
(b)   Sliced cross section in the weld line (Specimen T)
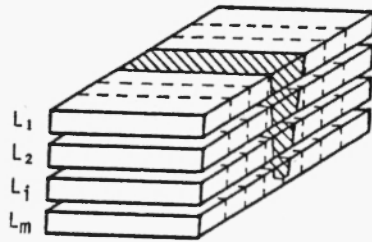
(c)   Sliced plates, parallel to XY-plane (Specimen L_i)

inherent strains in the cross section and the inherent strains in the longitudinal direction.   The three-dimensional residual stresses $\{\sigma\}$ of Specimen R can be expressed by the sum of the stresses $\{\sigma^A\}$ which are produced in Specimen R only by the inherent strains in the cross section, and the stresses $\{\sigma^B\}$ which are produced in Specimen R only by the inherent strain in the longitudinal direction, that is,

$$\{\sigma\} = \{\sigma^A\} + \{\sigma^B\} \qquad\qquad (3\text{-}35)$$

175

(2) Stresses $\{\sigma^{\stackrel{\wedge}{A}}\}$ produced by the inherent strains $\{\varepsilon_{\stackrel{*}{y}}, \varepsilon_z^*, \gamma_{yz}^*\}$ in the cross section

The residual stresses $\{\sigma^{Ao}\} = \{0, \sigma_y^{Ao}, \sigma_z^{Ao}, \tau_{yz}^{Ao}, 0, 0\}^T$ in Specimen T are in the state of plane stress and can be observed directly. Then, the inherent strains (ε_y^* , ε_z^* , γ_{yz}^*) in the cross section can be estimated by the observed strains and the three-dimensional stresses $\{\sigma^{\wedge}\}$ in Specimen R may be calculated by these resulting inherent strains. On the other hand, there is a clear relation between $\{\sigma^{\wedge o}\}$ and $\{\sigma^{\wedge}\}$, which makes determination of the stresses $\{\sigma^A\}$ simplified by the stresses $\{\sigma^{Ao}\}$.

As the inherent strains (ε_y^* , ε_z^* , γ_{yz}^*) in the cross section are uniform along the weld line, it can be considered that the cross sections of Specimen R remain plane (so called plane deformation) in the middle portion which are away approximately by its thickness from the ends of weld line. Further, as the stresses in the plane of Specimen T and in the state of plane strain, which are produced by these inherent strains are balanced in the cross section (yz-plane), the stresses perpendicular to its cross section (in the direction of x-axis) which are produced by constraining the deformation in its direction are also self-balanced in the cross section. As a result, the state of the above-mentioned plane deformation is equivalent to that of plane strain (The detail proof is shown in Appendices of Ref.29).

In such a case, the stresses $\{\sigma^{\wedge}\}$ can be determined by the observed values $\{\sigma^{Ao}$ in the state of plane stress, using the relation between plane strain and plane stress without knowing the inherent strains in the cross section.

$$\sigma_x^{A} = \nu \, (\sigma_y^{Ao} + \sigma_z^{Ao})/(1 - \nu^2)$$

$$\sigma_y^A = \sigma_y^{Ao}/(1 - \nu^2), \sigma_z^A = \sigma_z^{Ao}/(1 - \nu^2)$$

$$\tau_{yz}^A = \tau_{yz}^{Ao}/(1 - \nu^2), \tau_{xy}^A = \tau_{zx}^A = 0 \qquad\qquad (3\text{-}36)$$

where ν : Poisson's ratio

Judging from this fact, it is evident that the longitudinal elastic strain ε_x of Specimen R at a certain distance (approximately its thickness) away from the ends of weld line is produced only by the inherent strains ε_x^* in its direction because the inherent strains in the plane of a cross section make the state of plane strain and does not produce any longitudinal elastic strain but stresses.

In connection to $\{\sigma^{Ao}\}$, there are many reports /10,4,21-24/ on the results of measurement of residual stresses remained in the planes of thin plates which are sliced in the perpendicular direction to the weld line. According to the above-mentioned fact, these measurements can be considered nearly to measure the stresses due to the inherent strains in the cross section.

(3) Stresses $\{\sigma^B\}$ produced by the longitudinal inherent strains ε_x^*

For the measurement of $\{\sigma^B\}$, Specimens L is cut out from Specimen R. Depending upon the relative proportion of the length ℓ of Specimens L to the thickness t of Specimen R, ℓ/t, two measuring methods were developed.

(i) In case of $\ell \geq 2t$

If ε_x^* is imposed onto a long stress-free Specimen R uniformly along the longitudinal axis, plane deformation is observed in its middle portion.

When Specimen L_i is taken out from this portion, the specimen is regarded as one thin plate being kept straight at the middle cross section.

As for strains (stresses) in the middle surface of the specimen, the total strain $\varepsilon_x^T(y)$ is expressed as the sum of the elastic strain $\varepsilon_x(y)$ and the inherent strain $\varepsilon_x^*(y)$, such as,

$$\varepsilon_x^T(y) = \varepsilon_x(y) + \varepsilon_x^*(y) \tag{3-37}$$

As the plane deformation is assumed, $\varepsilon_x^T(y)$ may be expressed as a linear function of the y-coordinate,

$$\varepsilon_x^T(y) = a + by \tag{3-38}$$

where a and b are coefficients (b=0 if the specimen is perfectly symmetric with respect to x-axis).

From the above two equations, $\varepsilon_X^*(y)$ is obtained as,

$$\varepsilon_X^*(y) = \varepsilon_X(y) - (a+by) \tag{3-39}$$

If $\varepsilon_X^*(y)$ is imposed onto Specimen L_i, the second term of the above equation does not produce any stress but translation and rotation of the cross section so as to satisfy the self-equilibrating condition. Therefore, $\varepsilon_X(y)$ is simply taken as $\varepsilon_X^*(y)$, that is,

$$\varepsilon_X^*(y) = \varepsilon_X(y) \tag{3-40}$$

Elastic strains $\varepsilon_X(y)$ in Specimen L_i can be determined from the relaxed strains $_m\varepsilon_X(y)$ which are observed by strain gages when cutting the specimen into narrow strips or bars as depicted by the broken lines in Fig.3-2(c), as,

$$\varepsilon_X(y) = -_m\varepsilon_X(y) \tag{3-41}$$

Thus determined inherent strains can reproduce the same residual stresses as in the respective Specimen L_i, which are not necessarily the same ones as $\{\sigma^B\}$ at the corresponding location of Specimen L_i in Specimen R, since some portion of the residual stresses in Specimen R are released when it is sliced into Specimen L_i.

In order to calculate $\{\sigma^B\}$ in Specimen R, the inherent strains in the entire cross section are imposed to the stress-free Specimen R. These inherent strains are composed of the respective ones in each Specimen L_i, but are not simply the summation of these. They should be modified by adjusting the coefficients a and b in Eq.(3-39) in order to compensate the released stresses. These coefficients may be determined by assuming the inherent strains at both sides of each Specimen L_i to be zero, since the actual inherent strains away from the welded portion should be zero. These coefficients a and b cause additional inherent strains which are effective for Specimen R, but non-effective for each Specimen L_i.

By imposing these inherent strains $\varepsilon_X^*(y,z)$ onto Specimen R under the condi-

tion of the plane deformation, three-dimensional residual stresses $\{\sigma^D\}$ may be calculated by the finite element method.

(ii) In case of $\ell < 2t$

In this case, the above simplification can not be adopted. The axial inherent strain ε_X^* should be estimated with the aid of the finite element method as described in section 3.2.2..

3.3 Results of Measurement and Discussion

According to the proposed measuring theory, several experiments were conducted to measure three-dimensional residual stresses, mainly in a multi-pass welded joint and demonstrate the effectiveness of the method. Followings are the examples.

3.3.1 Multi-pass butt welded joint of thick plane plate (SS 41, plate thickness:
   50mm, measured by L_z method) /29/

In experiment, residual stresses of a multi-pass butt welded joint (Fig.3-2) of a mild steel (SS 41) plate were measured. The size of the used specimen is as follows: weld length L=200mm, plate width B=200mm and plate thickness t=50mm. 14-passes of weld metal was applied to the U-groove of the specimen by submerged arc welding. No restraint was provided to welding deformation such as longitudinal bending deformation or angular distortion. In measurement, L_z method /29,31/ was applied.

Residual stress distributions of σ_X (longitudinal direction) and σ_y (plate width direction) measured on the top and bottom surfaces and in the cross sections in the middle of the weld line are shown in Figs.3-3 and 3-4. In the same figure, the direct measurements of the surface stresses are indicated in order to compare with the estimated values. These directly measured values are not used for estimation of the three-dimensional residual stresses by the present

Fig.3-3 Measured welding residual stresses on the surfaces in the middle of the weld line

(kg/mm²)

ON TOP SURFACE   —— : THIS METHOD
O ● : DIRECT MEAS-
UREMENT

σ_x

σ_y

(a)   On the top surface

(kg/mm²)

ON BOTTOM SURFACE   —— : THIS METHOD
O ● : DIRECT MEAS-
UREMENT

σ_y

σ_x

(b)   On the bottom surface
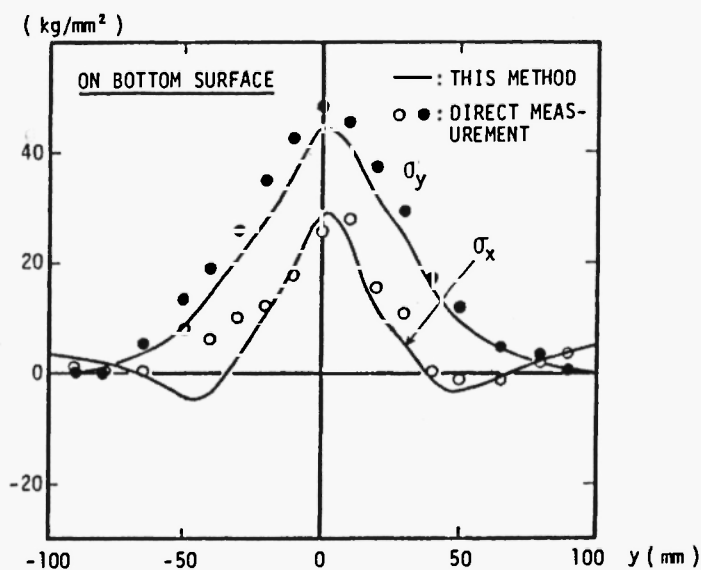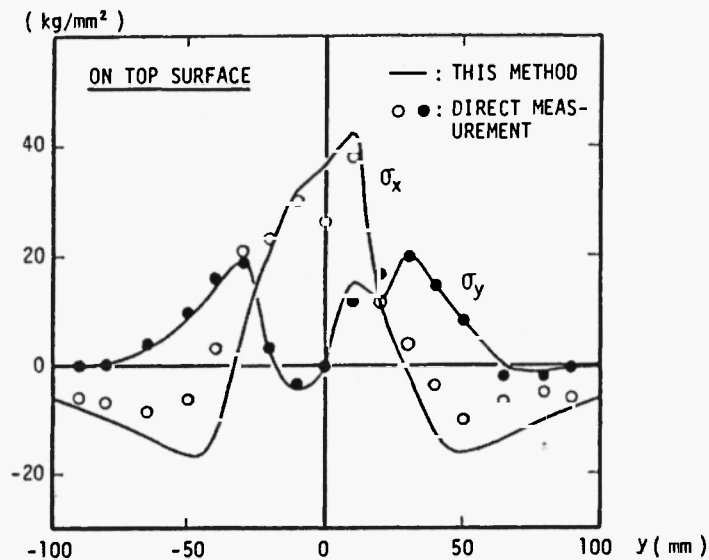
method.   Then it can be considered that the estimated residual stresses show

good coincidence with the directly measured stresses on its surfaces.   Especial-

ly, the accuracy of the estimated transverse stresses σ_y is very high.   B

Fig.3-4 Measured welding residual stresses at the cross sections in the middle
        of the weld line
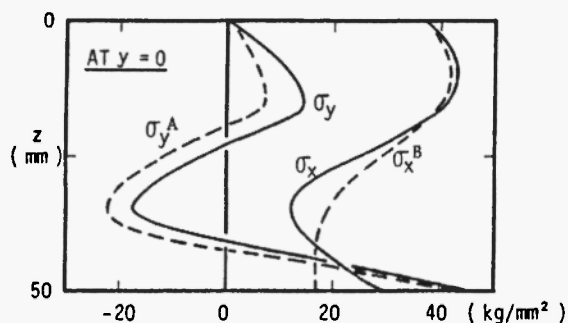
(a)   At y=0
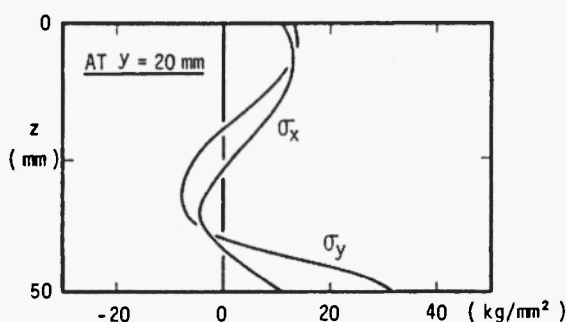
(b)   At y=20mm

there is some difference in some portions between the estimated and directly

measured values of the longitudinal stress σ_X . The reasons for these differ-

ences is described in Ref.29.

Their distribution patterns are quite the same as those under the restraint

condition A of the joint of the first example (Section 2.3.1), in which no exter-

nal restraint is added. That is to say, large tensile stresses are produced not

only immediately below the finishing bead but also at the bottom surface owing to

the great influence of longitudinal bending deformation and angular distortion.

This is one of the typical characteristics of the residual stress distributions.

Accordingly, root crack may occur in this case.

3.3.2 Multi-pass butt longitudinal and circumferential welded joints in a

penstock (HT 80, plate thickness: 50mm , measured by L_y and $L_{\theta z}$ methods) /30/

Using a large size penstock model of 80 kgf/mm^2 class high tensile strength steel plate, three-dimensional residual stresses produced in a tubular shell plate by (1) cold bending, (2) longitudinal welding of a joint and (3) circumferential welding of a joint were measured respectively. The penstock model and the location of each specimen taken out are shown in Fig.3-5. The plate thickness of the model is 50mm. Submerged arc welding was applied first to the inner side and then to the outer side of the X-grooves. For measurement of residual stresses due to cold bending $L_{\theta z}$ method was applied, and for welding residual stresses L_y method was applied. They are the similar methods to L_z method, and are presented in Refs.30 and 31.

Distributions of three-dimensional residual stresses produced in the shell plate by cold bending are shown in Fig.3-6. Residual stresses in the axial direction of the model, σ_z^M , and those in the circumferential direction, σ_θ^M , are almost point-symmetric with respect to the center of the plate thickness.

Fig.3-5   Model of penstock
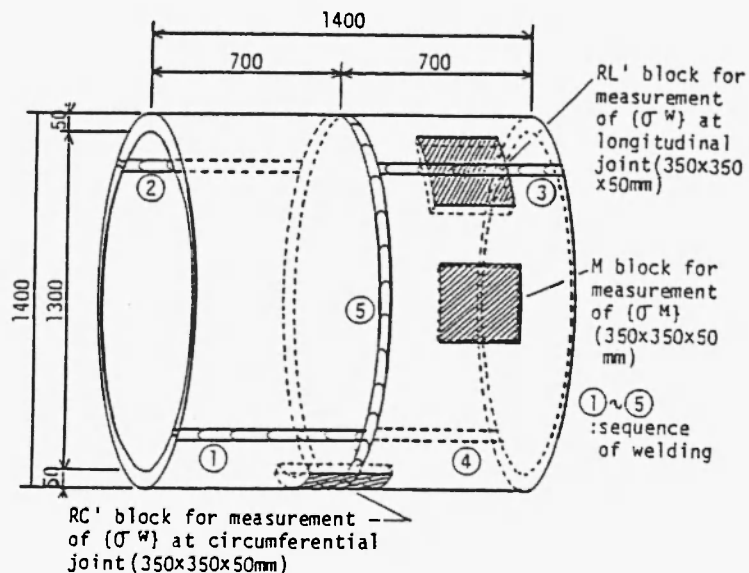
Fig.3-6   Measured residual stresses due to cold bending in shell plate
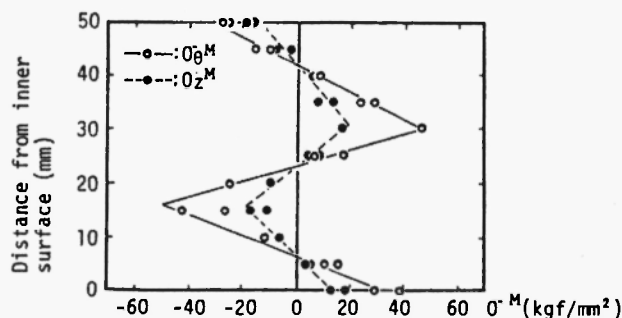
σ_z^M is approximately $30 \sim 50\%$ of σ_θ^M in magnitude. It is considered that these are the typical characteristics of residual stress distributions by this type of cold bending.

Welding residual stress distributions in the longitudinal joint are shown in Figs.3-7 and 3-8. Distributions in Fig.3-7 are complicated since welding residual stresses distribute on and near the weld metal, and combined residual

Fig.3-7   Measured welding residual stresses on the surfaces (longitudinal joint)
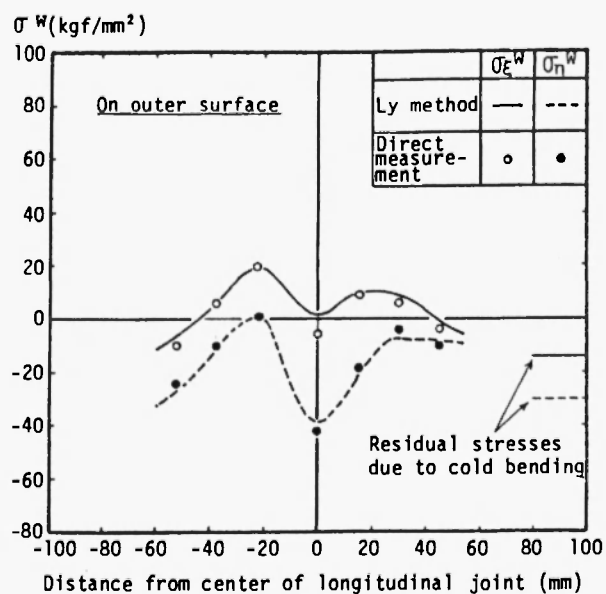
(a)   On the outer surface
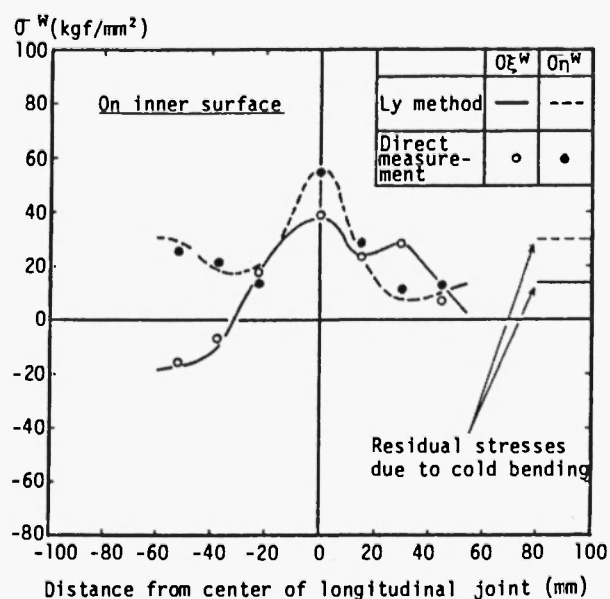
(b)   On the inner surface

stresses by cold bending and the subsequent weldings on the base plate near the weld line. The above residual stresses distributed in the plate thickness direction are shown in Fig.3-8. Figure 3-8(a) shows welding residual stresses in the weld zone and (b) residual stresses by cold bending and the subsequent weldings in the base plate. From these distributions, especially Fig.3-8(a), in reference to the first example of section 2.3.1, welding deformation behavior of this joint is predicted as follows: Angular distortion occurs easily in longitudinal joints as is evident from the distribution of σ_η^W (circumferential stress) in Fig.3-8 (a). While longitudinal bending deformation, which is considered to occur hardly, is known to considerably occur from the distribution of σ_ξ^W (axial stress, along the weld line here) in the same figure. This may be explained by

Fig.3-8 Measured welding residual stresses at the cross sections (longitudinal joint)
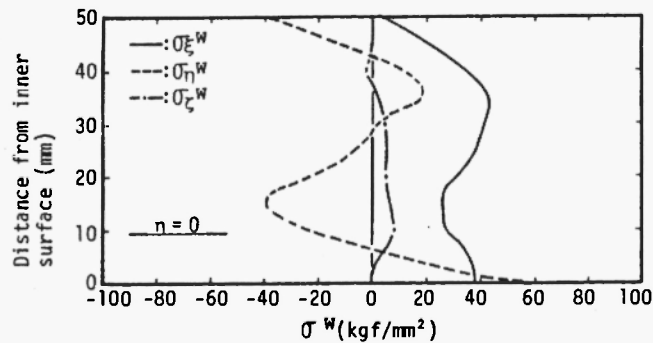
(a)   At $\eta=0$
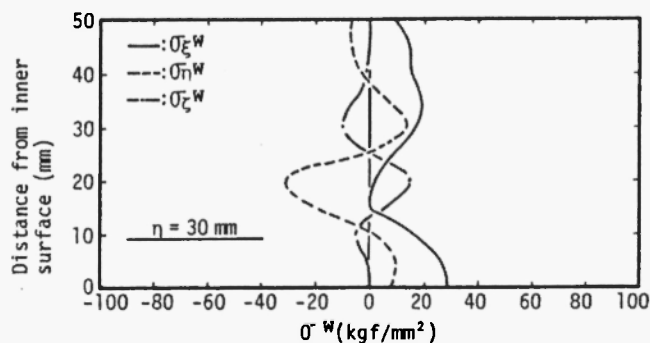
(b)   At $\eta=30mm$

the fact that the length of the model at the longitudinal welding is shorter in comparison to the radius.

Distributions of welding residual stresses in a circumferential joint are shown in Figs.3-9 and 3-10. It is seen from the residual stress distributions in

Fig.3-9 Measured welding residual stresses on the surfaces (circumferential joint)
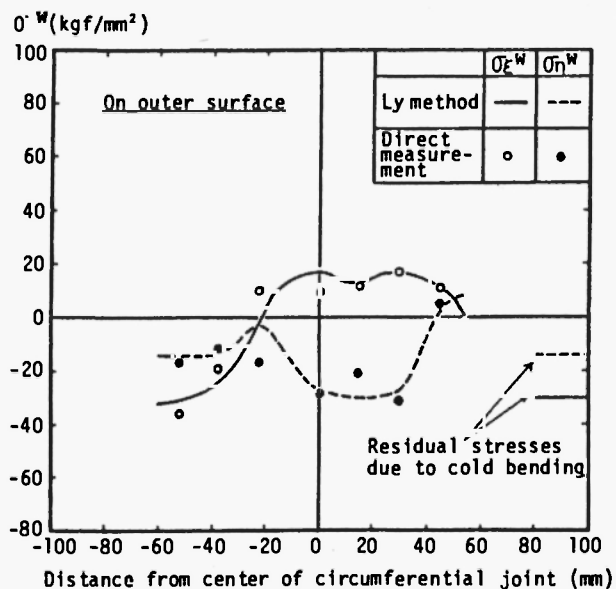
(a)   On the outer surface
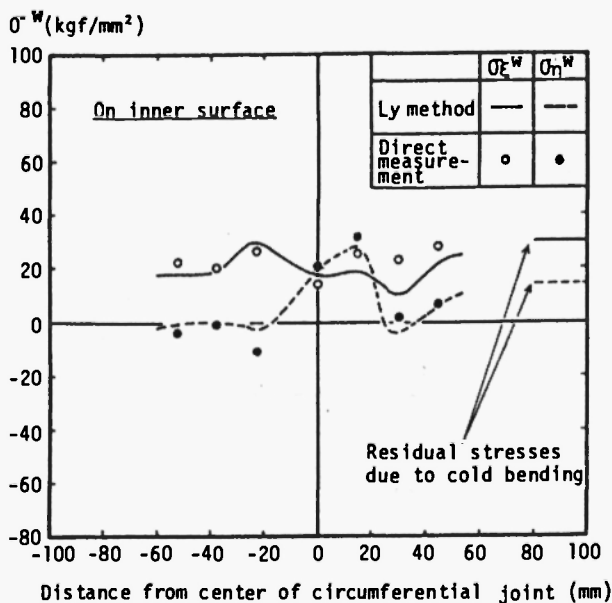
(b)   On the inner surface

Fig.3-10 Measured welding residual stresses at the cross sections (circumferen-
        tial joint)

(a)   At η=0
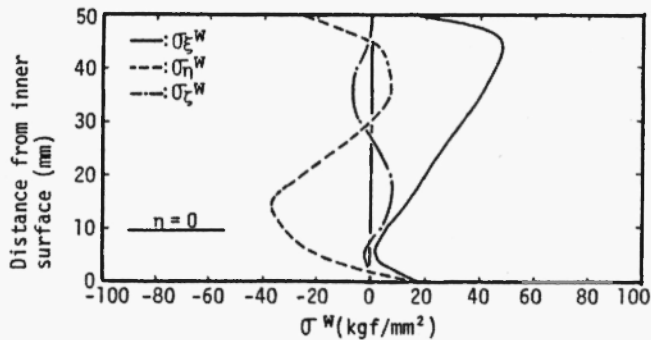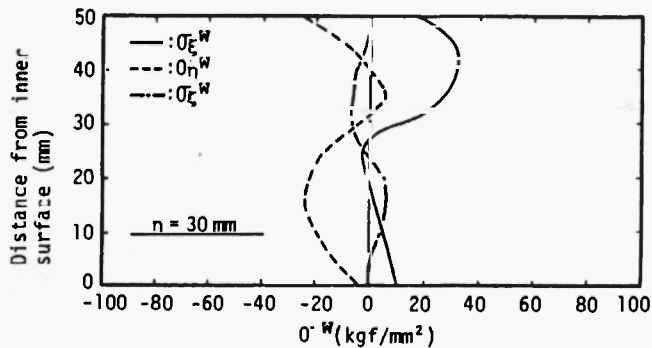
(b)   At η=30mm

the plate thickness direction of the weld zone shown in Fig.3-10(a) that distri-
butions of circumferential (along the weld line) stresses σ_ξ^W and axial stresses
σ_η^W are similar to those in the circumferential butt joint of 24B pipe already
described in Section 2.3.4. Especially, σ_ζ^W shows a close resemblance to those
in 24B pipe. Naturally, their production mechanisms are the same. It is consid-
ered that angular distortion occurs to some extent and longitudinal bending
deformation little.

3.3.3 Butt welded joint of very thick plate by electroslag welding (SM 50, plate
      thickness: 100mm, measured by L_y method) /31/
      Residual stresses of a butt welded joint of SM 50 steel of 100mm plate

Fig.3-11   Test joint of electroslag welding
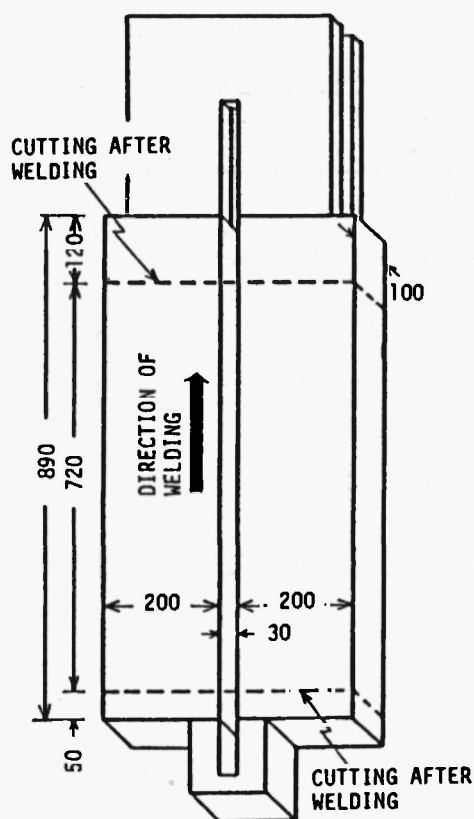
thickness by electroslag welding (Fig.3-11) were measured by applying L_y method /30,31/. Electroslag welding takes quite a different welding process from the conventional multi-pass welding which has been treated in this study. Residual stresses by electroslag welding deserve attention as those produced by applying large heat input (2094 KJ/cm) for the single pass.

Welding residual stresses at the middle cross section of the weld line produced by this welding method are shown in Figs.3-12 and 3-13. Figure 3-12(a) shows the distributions of residual stresses in the plate width direction (y-direction) on the surface, Fig.3-12(b) those along the center of the plate thickness, and Fig.3-13 the distributions of residual stresses in the plate thickness direction. The residual stress along the weld line, σ_x, shown in Fig.3-12(b) is comparatively similar to that produced in a one-pass butt welded joint made of a thin steel plate in which phase transformation occurs at a low temperature /32/.

Fig.3-12 Measured welding residual stresses at the middle cross section of the weld line

σ (kg/mm²)
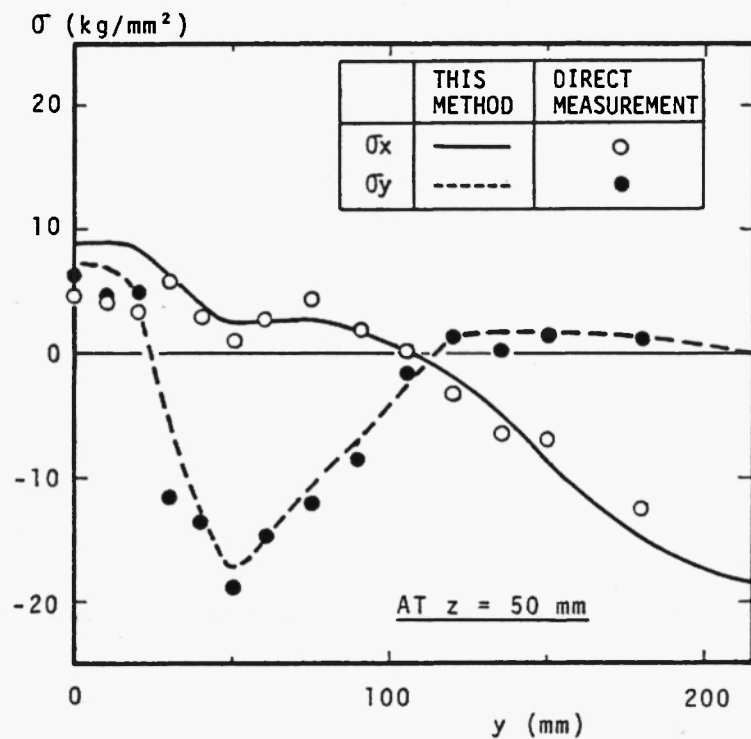
(a)   On the surface (at z=50mm)

σ (kg/mm²)
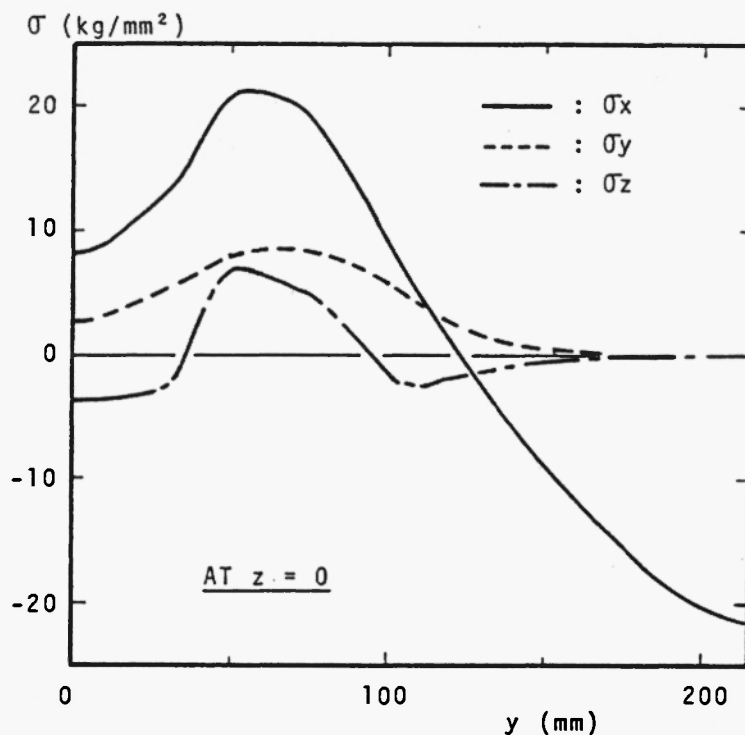
(b)   Along the center of the plate thickness (at z=0)

That is to say, of the distribution in the plate width direction, large tensile stresses are produced in the HAZ and small tensile stresses in the weld metal. The maximum tensile stresses are produced at the center of the plate thickness as seen from the distributions in the plate thickness direction at the HAZ (y=50mm) shown in Fig.3-13(b). The reason may be that the specimen is made of very thick plates so that the center of the plate thickness cools more slowly than any other portions.

4.   Characteristics of Residual Stress Distributions in Multi-pass Welded Joints of Thick Plates and Influential Factors /33/

Characteristics of residual stress distributions in several kinds of multi-pass welded joints of thick plates described in this research are summarized in the following.

Conceivable influential factors on the residual stress distributions are the followings:

(i) material properties (physical and mechanical properties), (ii) welding condition (especially heat input), (iii) groove shape, (iv) build-up sequence, (v) restraint condition of a joint, etc..

Materials used for the joint models were;

(a) SM 50, (b) 2 1/4 Cr-1Mo, (c) SUS 304, (d) SS 41 and (e) HT 80.

Their mechanical properties, the afore-mentioned (i), such as yield stress, instantaneous linear expansion coefficient, etc., and their changes during phase transformation are greatly different from one another. So are (ii) the welding condition, (iii) the groove shape and (iv) the build-up sequence of the respective joints. These factors influence the welding residual stresses quantitatively. For example, in the joints made of HT 80 described in section 3.3.2, the maximum residual stresses do not reach the yield stress. This is due to the

phase transformation expansion at low temperature (400∼500°C), which reduces the

maximum tensile residual stresses greatly. However, as having already mentioned
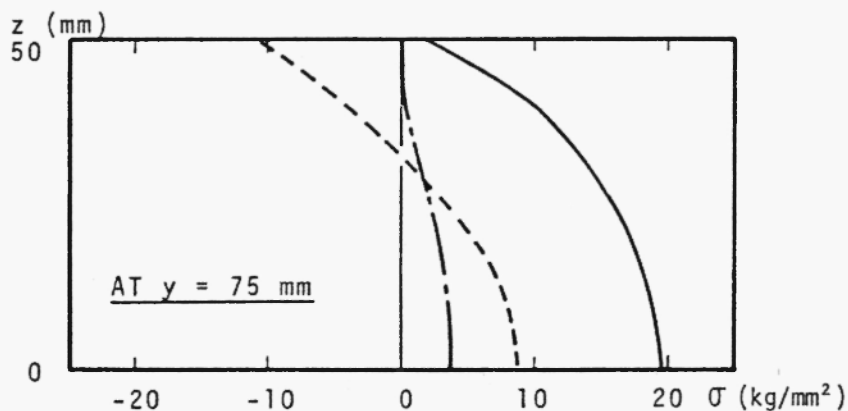
Fig.3-13 Measured welding residual stresses at the middle cross section of the
         weld line (Distributions in the plate thickness direction)
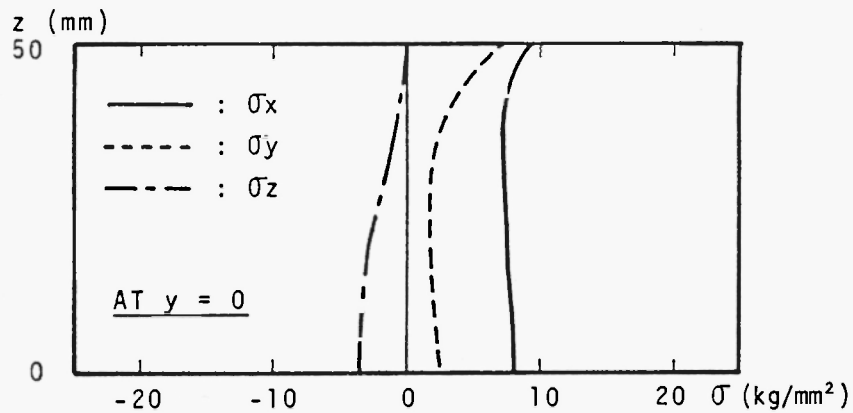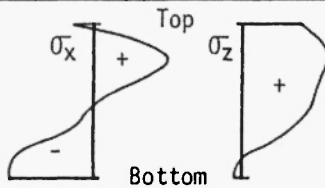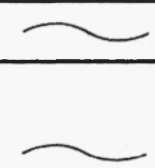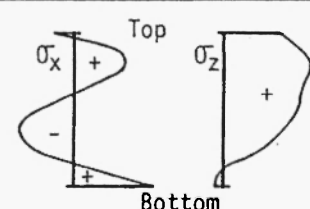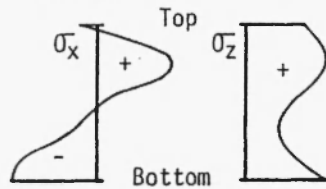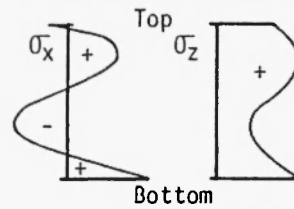
(a)   At y=0
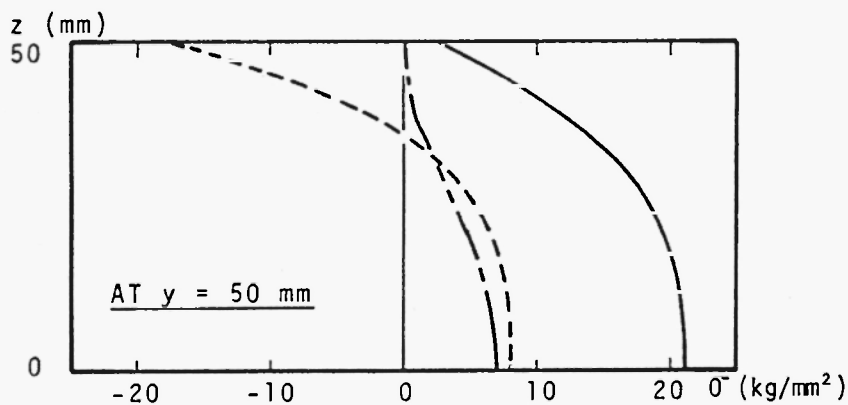
(b)   At y=50mm

(b)   At y=75mm

hereinbefore, the patterns of residual stress distributions are influenced a little by (i) material properties, (ii) the welding condition, (iii) the groove shape and (iv) the build-up sequence, while they are greatly influenced by and dependent on (v) the restraint condition of a joint. Therefore, such characteristics of residual stress distributions were arranged with respect to the restraint condition of a joint as shown in Table 4-1.

Correlations of the restraint condition of a joint with residual stress

Table 4-1 Classification of welding residual stress distributions according to the restraint condition

σ_x : Transverse Welding Residual Stress, $\bar{\sigma_z}$: Longitudinal Welding Residual Stress

distributions and welding cracks may be simply stated as follows: "Irrespective of severity of the restraint condition of a joint, longitudinal and transverse (in the directions of the weld line and the plate width) large tensile stresses are produced in the surrounding portion of the finishing bead. These tensile stresses may cause underbead crack, longitudinal crack or transverse crack. If the restraints against longitudinal bending deformation and angular distortion are weak, large tensile residual stresses are produced near the initially welded bottom surface and may cause root crack."

As a result, the characteristics of residual stress distributions can be read qualitatively in this Table, provided that the restraint condition of a joint is estimated.

5.   Conclusion

In this paper, the theories of thermal elastic-plastic-creep analysis and measurement of residual stresses were described, which had been presented by the authors. These theories enable us to obtain information on elastic-plastic behavior of joints during and after welding and stress-relief annealing (PWHT). Several examples, mainly on multi-pass welding of thick plate, demonstrated the effectiveness and reliability of the methods of analysis and experimental measurement of residual stresses, which were developed based on their theories. For each welded joint, characteristics of residual stress distribution, their production mechanisms, influencial factors on them and their relations with cold cracks were discussed, being compared with a basic example.

Lastly, calculated and measured welding residual stress distributions were analyzed, and it was emphasized that the most important influencial factor upon the pattern of the distribution is the restraint condition of a joint.

References

1) Y. Ueda and T. Yamakawa: Analysis of Thermal Elastic-plastic Stress and Strain during Welding by Finite Element Method, Trans. of JWS (The Japan Welding Society), Vol.2, No.2, 1971, pp.90-100, and IIW (International Institute of Welding) Doc.X-616-71, 1971, and J. of JWS, Vol.42, No.6, 1973, pp.567-577 (in Japanese).

2) Y. Ueda and K. Nakacho: Theory of Thermal Elastic-plastic Analysis with a More General Workhardening Rule, Trans. of JWRI (Welding Research Institute of Osaka Univ., Japan), Vol.9, No.1, 1980, pp.107-114, and IIW Doc.X-989-81, 1981.

3) Y. Ueda and K. Fukuda: Analysis of Welding Stress Relieving by Annealing based on Finite Element Method, Trans. of JWRI, Vol.4, No.1, 1975, pp.39-45, and J. of JWS, Vol.44, No.11, 1975, pp.902-908 (in Japanese).

4) Y. Ueda et al.: Multipass Welding Stresses in Very Thick Plates and Their Reduction from Stress Relief Annealing, IIW Doc.X-850-76, 1976, and Trans. of JWRI, Vol.5, No.2, 1976, pp.179-189, and Proc. of Third Int. Conf. on Pressure Vessel Technology (ASME), Part II, 1977, pp.925-933, and J. of JWS, Vol.47, No.8, 1978, pp.500-506 (in Japanese).

5) Y. Ueda and K. Nakacho: Constitutive Equation for Thermal Elastic-plastic Creep State, Trans. of JWRI, Vol.10, No.1, 1981, pp.89-94.

6) G. Sachs: Evidence of Residual Stresses in Rods and Tubes, Zeitschrift für Metallkunde, Vol.19, 1927, pp.352-357.

7) D. Rosenthal and J.T. Norton: A Method of Measuring Triaxial Residual Stress in Plates, Welding J., Vol.24, No.5, 1945, pp.295s-307s.

8) Y. Ueda et al.: A New Measuring Method of Residual Stresses with the Aid of Finite Element Method and Reliability of Estimated Values, J. of SNAJ (The Society of Naval Architects of Japan), Vol.138, 1975, pp.499-507 (in

Japanese), and Trans. of JWRI, Vol.4, No.2, 1975, pp.123-131, IIW Doc.X-810-76, 1976, and THEORETICAL AND APPLIED MECHANICS, University of Tokyo Press, Vol.25, 1977, pp.539-554.

9) Y. Ueda et al.: Analysis of Thermal Elastic-plastic Stresses and Strains due to Welding —Multi-layer Welds—, Proc. of 7th National symp. of Matrix Methods of Structural Analysis and Design (The Society of Steel Construction of Japan), 1973, pp.419-426 (in Japanese).

10) Y. Ueda et al.: Transient and Residual Stresses in Multi-pass Welds, IIW Doc.X-698-73, 1973, Trans. of JWRI, Vol.3, No.1, 1974, pp.59-67, and J. of JWS, Vol.44, No.6, 1975, pp.464-474 (in Japanese).

11) Y. Ueda, K. Fukuda and K. Nakacho: Basic Procedures in Analysis and Measurement of Welding Residual Stresses by the Finite Element Method, Proc. of Int. Conf. on Residual Stresses in Welded Construction and Their Effects (The Welding Institute, England), 1977, pp.27-37.

12) Y. Ueda and K. Nakacho: Simplifying Methods for Analysis of Transient and Residual Stresses and Deformation due to Multi-pass Welding, Trans. of JWRI, Vol.11, No.1, 1982, pp.95-103, and Quart. J. of JWS, Vol.2, No.1, 1984, pp.75-82 (in Japanese).

13) R. Hill: The Mathematical Theory of Plasticity, Clarendon Press (Oxford), 1950.

14) For example, W. Prager: The Theory of Plasticity, A Survey of Recent Achievements (James Clayton Lecture), Proc. Instn. Mech. Engrs., 169, 1955, pp.41-57.

15) H. Ziegler: A Modification of Prager's Hardening Rule, Quart. Appl. Math., Vol.17, 1959, p.55.

16) T. Inoue et al.: Foundations of Solid Mechanics, Nikkan Kogyo-Shinbunsha (Tokyo), 1981, Chapter 7 (in Japanese).

17) R.W. Bailey: J. of Institute of Metals, Vol.35, 1926, p.27.

18) E. Orowan: J. of the West Scotland Iron and Steel Institute, Vol.54, 1946, p.45.

19) Y. Ueda, K. Nakacho and K. Fukuda: Constitutive Equations for Thermal Elastic-plastic Creep Analysis, Proc. of Int. Conf. on Welding Research in the 1980's (JWRI), 1980, Poster Session P-14, pp.77-82.

20) K. Nakacho: D. Eng. Dissertation, Osaka University, January, 1985, Section 3.5 (in Japanese).

21) Y. Ueda et al.: Dynamical Characteristics of Weld Cracking in Multipass Welded Corner Joint, Trans. of JWS, Vol.8, No.2, 1977, pp.138-142 and J. of JWS, Vol.48, No.1, 1979, pp.34-39 (in Japanese).

22) Y. Ueda et al.: Preventions of Lamellar Tearing in Multipass Welded Corner Joint, Trans. of JWS, Vol.9, No.2, 1978, pp.128-133 and J. of JWS, Vol.48, No.7, 1979, pp.525-531 (in Japanese).

23) Y. Ueda et al.: Weld Cracking in Multipass Welded Corner Joint —Comparison of Submerged Arc Welding with Covered Arc Welding—, J. of JWS, Vol.50, No.4, 1981, pp.421-427 (in Japanese), IIW Doc.IX-1236-82 and IIW Doc.X-1010-82,1982.

24) Y. Ueda et al.: Cracking in Welded Corner Joints, Metal Constr., Vol.16, No.1, 1984, pp.30-34.

25) Y. Ueda et al.: Residual Stresses at Circumferential Weld of Austenitic Strainless Steel Pipe by Heat-sink Welding, J. of JWS, Vol.49, No.1, 1980, pp.61-66 (in Japanese).

26) Y. Ueda et al.: Residual Stresses and Their Mechanisms of Production at Circumferential Weld by Heat-sink Welding, J. of JWS, Vol.52, No.2, 1983, pp.90-97 (in Japanese).

27) Y. Ueda, K. Nakacho and T. Shimizu: Improvement of Residual Stresses of Circumferential Joint of Pipe by Heat-sink Welding for IGSCC, 1984 Pressure Vessel and Piping Conference (ASME), 84-PVP-10,. 1984 and J. of Pressure

Vessel Technology (ASME), Vol.108, No.1, 1986, pp.14-23.

28) J. Mathar: Determination of Initial Stresses by Measuring the Deformations Around Drilled Holes, Welding J., July 1934, pp.24-29.

29) Y. Ueda, K. Fukuda and M. Tanigawa: New Measuring Method of 3-dimensional Residual Stresses Based on Theory of Inherent Strain, J. of SNAJ, Vol.145, 1979, pp.203-211 (in Japanese), and Trans. of JWRI, Vol.8, No.2, 1979, pp.249-256, and IIW Doc.X-987-81, 1981.

30) Y. Ueda et al.: Three Dimensional Cold Bending and Welding Residual Stresses in Penstock of 80kgf/mm^2 Class High Strength Steel Plate, J. of JWS, Vol.51, No.7, 1982, pp.570-577 (in Japanese), and Trans. of JWRI, Vol.12, No.2, 1983, pp.117-126, and IIW Doc.X-1064-84, 1984.

31) Y. Ueda, K. Fukuda and M. Fukuda: A Measuring Theory of Three Dimensional Residual Stresses in Long Welded Joints, J. of JWS, Vol.49, No.12, 1980, pp.845-853 (in Japanese), and Trans. of JWRI, Vol.12, No.1, 1983, pp.113-122, and IIW Doc.X-1066-84, 1984.

32) K. Satoh and T. Terasaki: Effect of Transformation Expansion on Welding Residual Stresses Distributions and Welding Deformations, J. of JWS, Vol.45, No.7, 1976, pp.560-566 (in Japanese).

33) Y. Ueda and K. Nakacho: Three-dimensional Welding Residual Stresses Calculated and Measured, Proc. of Int. Conf. on The Effects of Fabrication Related Stresses on Product Manufacture and Performance (The Welding Institute, England), 1985, P32, and Trans. of JWRI, Vol.15, No.1, 1986, pp.113-124.